Utilization of lignin to obtain olefin and aromatic compounds through hydrogenation and subsequent fast pyrolysis processes

By
ZHANG Lijuan

DISSERTATION

For the Degree of
Doctor of Chemical Systems Engineering
Doctor of Engineering

GRADUATE SCHOOL OF ENGINEERING
NAGOYA UNIVERSITY

Approved by the Faculty Council: July 2022

DECLARATION

To the best of my knowledge and belief, this thesis contains no material previously published by any other person except where due acknowledgment has been made.

This thesis contains no material which has been accepted for the award of any other degree or diploma in any university.

Signature : 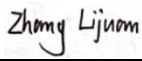

Date : 2022.07.21

ABSTRACT

Major global issues such as greenhouse gas emissions and the excessive exploration of petroleum dictate the importance of looking for clean renewable sources to replace fossil fuels. Lignocellulosic biomass is one of the most prospective resources for sustainable carbon-based energy. Based on that, the production of petroleum-based green fuels, chemicals, and solvents from biomass-derived products has garnered much attention in the recent past. The study of hydrogenation on biomass or biomass derivatives has proved that it improves the efficiency of generating high-value chemicals and provides much-needed insights into the primary reaction mechanism for the effective utilization of raw biomass and its components. Lignin, one of the three major components in lignocellulosic biomass, is internally rich in phenolic units and has significant research potential, which would greatly improve the utilization of biomass if it can be effectively converted. Therefore, this study focused on the pretreatment of lignin through the hydrogenation process, so that the hydrogenated lignin is expected to have greater pyrolytic properties and produce more olefins and aromatic hydrocarbons in fast pyrolysis. Thermal catalytic hydrogenation (TCH) of lignin has been extensively discussed, while hydrogenolysis or depolymerization of lignin was mainly achieved under severe conditions and an energy-intensive process. A cleaner alternative conversion technology, like electrochemical conversion and photocatalytic conversion, is required, which can be integrated directly with other technologies and operate at ambient temperatures or under more moderate conditions. Hence, electrochemical hydrogenation (ECH) used as an alternative pretreatment technology for lignin was checked in this work, and the pyrolytic property of hydrogenated lignin in fast pyrolysis was investigated. In this work, the hydrogenation of lignin through the TCH and ECH processes was compared, including the effect of catalyst types and reaction conditions on hydrogenation efficiency, pyrolysis reactivity, product selectivity, and technical limitations. The advantages and disadvantages of the two technologies for lignin utilization have also been compared, which provides a more favourable knowledge base and theoretical basis for the subsequent research work. Besides, techno-economic analysis of this two-stage process (hydrogenation coupled with fast pyrolysis) was also checked based on experimental data. In order to verify the feasibility of this two-stage process, ASPEN Plus software was used to conduct process simulations for plant scale. A comprehensive economic assessment of the process was performed, including a

comparative analysis of the impact of both the feedstock and hydrogenation methods on overall profitability. It is expected to make some contribution to the utilization of lignin as well as to promote the industrialization process by providing some data support.

Keywords

Lignin, olefins, aromatic hydrocarbons, thermal catalytic hydrogenation, electrochemical hydrogenation

ACKNOWLEDGMENTS

After completing my thesis, I felt a million emotions. My research was built on the help of many people, and I could not have completed it successfully without their assistance.

First of all, I would like to express my special appreciation and deepest gratitude to Prof. Koyo Norinaga for giving me the opportunity to pursue a doctoral degree under his supervision. His encouragement, expert guidance, and concerns were invaluable. Without his continuous support, this thesis could not have been realized. I would also like to thank Prof. Hiroshi Machida, for his contributions and assistance in characterization as well as equipment construction and maintenance.

My sincere thanks also go to Dr. Cheolyong Choi for his helpful discussions, suggestions, instruction, and assistance over the course of my research. He helped me to set up my experimental system and gave me a lot of advice and help in thermal hydrogenation experiments and fast pyrolysis operations at the beginning. I also extend my appreciation to Dr. Suchada Sirisomboonchai for helping me until I transferred to the electrochemical reaction field. She has much experience with electrochemical reactions and gave me a lot of advice about the electrochemical hydrogenation of lignin, including catalytic preparation, experiment setup, and so on. Their encouragement and suggestions were invaluable for my research work.

I would also like to sincerely thank all the staff and students in our lab for always being very warm and friendly to me. I also made a lot of foreign friends, including THUPPATI Upender Rao, Suchada Sirisommboonchai, Tobe Etsuko, and TRAN Viet bao khuyen, and had a great time with them during my Ph.D. period. I also extend my sincere thanks to other Ph.D. members of Nori lab Tong san, Park san, Dai san, and especially Li Qiao san for his assistance in Aspen Plus simulations.

I was honoured to join a China-Japanese collaborative project called Japan Science and Technology Agency Strategic International Collaborative Research Program (JST SICORP, grant number JPMJSC18H1) and my research was funded by the Japanese side (Nagoya University) of this project. I returned to China in January 2020 to participate in the symposium of the project, but since then, due to the Coronavirus pandemic, the annual symposium has been held online. Besides that, I will give my most sincere thanks to the financial support provided by my home country. The Chinese government provided financial support for me through the China Scholarships Council (Grant Number: 201906730062),

which is very helpful and supportive for my life and study. I can say that it is the biggest motivation that supports me to be able to study abroad and further my studies.

Finally, I would like to thank my parents, who have always respected my choice and supported my decision, and it is because of their understanding that I can persist in my dream of studying abroad. I regret that I have not been able to go home to visit my family because of the COVID-19 pandemic. Finally, I would like to thank my friends and my boyfriend for their constant support and encouragement that allowed me to be braver.

LIST OF PUBLICATIONS

(1) L. Zhang, C. Choi, H. Machida, K. Norinaga, Production of light hydrocarbons from organosolv lignin through catalytic hydrogenation and subsequent fast pyrolysis, J. Anal. Appl. Pyrolysis. 156 (2021) 105096. https://doi.org/https://doi.org/10.1016/j.jaap.2021.105096.

(2) L. Zhang, C. Choi, H. Machida, Z. Huo, K. Norinaga, Catalytic hydrotreatment of alkaline lignin and its consequent influences on fast pyrolysis, Carbon Resour. Convers. 4 (2021) 219–229. https://doi.org/https://doi.org/10.1016/j.crcon.2021.09.001.

(3) L. Zhang, U.R. Thuppati, J. Wang, D. Ren, and et al., A review of thermal catalytic and electrochemical hydrogenation approaches for converting biomass-derived compounds to high-value chemicals and fuels, Fuel Process. Technol. 226 (2022) 107097. https://doi.org/10.1016/j.fuproc.2021.107097.

(4) L. Zhang, S. Sirisomboonchai, C. Choi, H. Machida, K. Norinaga, Pretreatment of lignin by electrochemical hydrogenation to enhance the olefins and aromatic products during rapid pyrolysis, J. Anal. Appl. Pyrolysis. 166 (2022) 105625. https://doi.org/10.1016/j.jaap.2022.105625

LIST OF FIGURES

LIST OF TABLES

Contents

Chapter 1 Introduction

1.1 Research background

In response to the target of the Paris Agreement, numerous countries/nations have pledged “Carbon neutrality” as of October 2021. Among them, Japan has announced their plans to reach carbon neutrality by 2050, and China also has planned to reach carbon neutrality by 2060. There are two strategies to achieve the equilibrium between greenhouse gas emissions and absorption: (1) Using carbon offsets to balance carbon dioxide emissions; (2) Using low-carbon energy sources instead of fossil fuels. This work is based on this world hotspot to explore new and effective technologies to maximize the use of biomass resources and to realize the carbon resource cycle.

According to the data of IEA (International Energy Agency) in 2019, biofuel and waste energy account for 9.4% of the World's Total Primary Energy Supply. The supply of biomass energy is the first among the renewable energy, but the utilization of biomass is still mainly through the traditional way. In China, the biomass industry has a massive source of raw materials, including agricultural waste, forestry production waste, Chinese medicine residues, coffee grounds, energy crops, etc. The annual capacity potential of crop straw, forestry residues, and woodland biomass can reach more than 700 million tons of standard coal, of which straw and woody raw materials account for 40% and 60%, respectively, rich in farmland and woodland. Furthermore, the Renewable Energy Institute (REI) provided data on solid biomass consumption in Japan to show the overall picture of solid biomass fuel deployment. In 2020, 25.3 million dry-ton of solid biomass was consumed, with 10.3 million dry-ton of black liquor and 4.17 million dry-ton of waste wood included. The utilization of photosynthesis to absorb carbon dioxide, on the one hand, and reaching the carbon resource cycle through the use of biomass waste, on the other hand, both play a part in lessening the greenhouse effect. In addition to being used for direct-fired power generation, biomass resources can be converted into a variety of ways and products, such as mixed-fired power generation, cracking gasification, or liquefaction, and it is best to have diversified development, which have no absolute advantages and disadvantages. However, nowadays, with varying resource statuses and technical sophistication, multiple ways of exploitation

should be used to better utilize biomass resources.

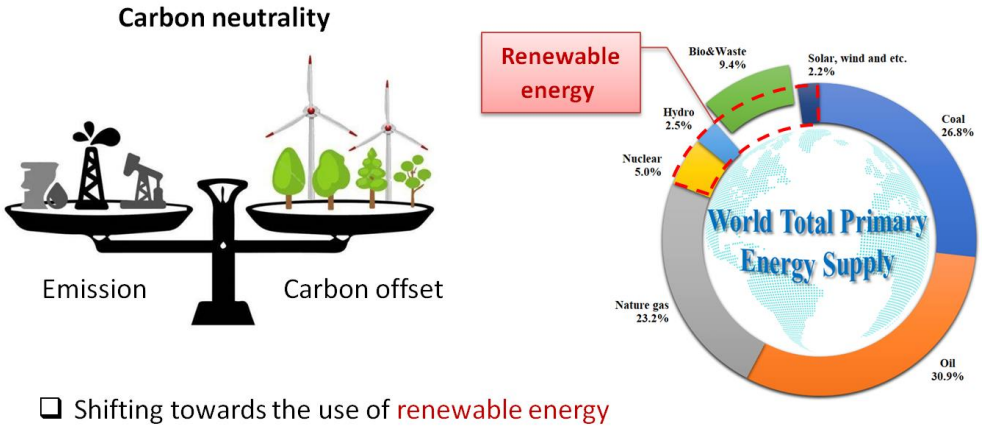

Fig. 1- 1 The balance of carbon neutrality and the world total primary energy supply in 2019 by IEA.

Lignocellulosic biomass belongs to a broad category of biomass sources, containing three main components: cellulose, hemicellulose, and lignin like Fig. 1-2. The abundant carbon-neutral and renewable organic carbon resource makes it a part of alternative fossil materials, showing good application prospects. Lignocellulosic biomass, including a large number of crops, wood, agricultural residue, grass, and so on, appears to be one of the most promising candidates in industrial utilization[1], like power plants for electricity, combustion for heating energy, pulp and paper industry for paper products, bio-oil products, and production of valuable chemicals. Therefore, it is very necessary and essential to study how to utilize such a large amount of lignocellulosic biomass source in an effective and environmentally friendly way. Hierarchically utilizing or studying must be one way to use or study lignocellulosic biomass sources. In lignocellulosic biomass, the cellulose and hemicellulose fractions are polysaccharides made up of glucose, D-pentose, and xylose sugar monomers, which are used to make platform chemicals such levulinic acid (LVA), 5-hydroxymethylfuran (HMF), and furfural. Apart from these, lignin accounts for 15-30%[2], has received less attention and generally been regarded as a low-valued waste in the pulp and paper industry. The cross-linked lignols and 3D stubborn structure are the main reasons to restrict lignin's utilization. However, the abundance of phenolic units in lignin polymers makes it very promising for the production of high-value compounds, like hydrocarbons and

aromatics.

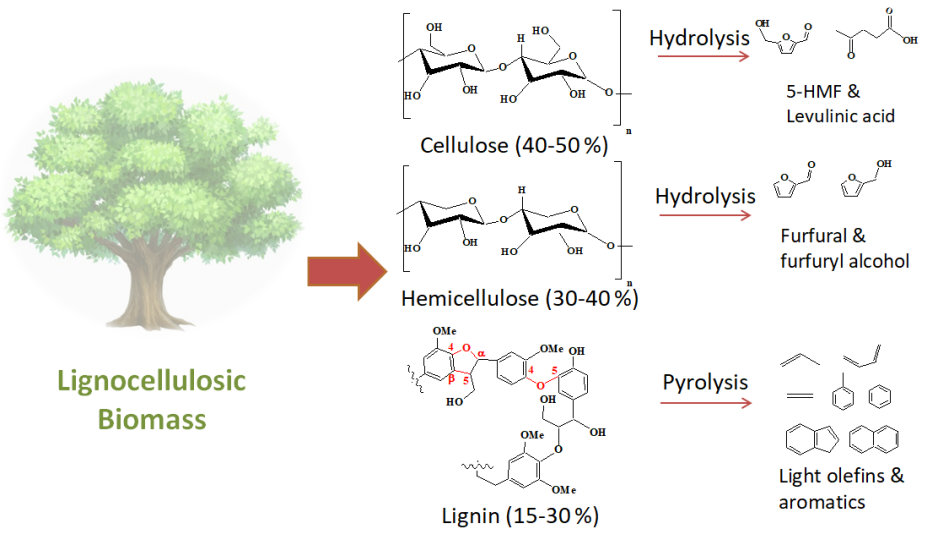

Fig. 1- 2 The distribution of the lignocellulosic biomass components and conversion.

1.2 Lignin composition and properties

Lignin, as an undervalued resource, was chosen as the subject of this study. Finding ways to effectively utilize lignin is beneficial for (1). improving the utilization of lignocellulosic biomass; (2). utilizing lignin in a hierarchically manner, and the products would be more selective; (3). exploring the properties of lignin to provide directions for biomass utilization; and (4). Waste source utilization (especially for the waste in the pulp and paper industry). The typical structure of the lignin polymers is shown in Fig. 1-3. Lignin has a cross-linked 3D irregular structure, which constitutes three main phenolic units, including guaiacyl (G), syringyl (S), and p-hydroxyphenyl (H) units[3], which is the largest renewable source of aromatics on earth. Generally speaking, the source of lignocellulosic biomass results in the ratio of precursor units, hardwoods are rich in G- and S- units, and softwoods are rich in G units[4]. The macromolecular weight of lignin exceeds 10000 u, while the polymerization degree is difficult to measure due to its heterogeneous property. The internal units are connected randomly by C–O linkage bond (β-O-4, α-O-4, 4-O-5) or C–C bond (β-5, β-1, β-β, 5-5)[5]. The β-O-4 bond is the most abundant bond (especially in hardwood) due to its labile nature[5]. Some researchers stated that lignin consists of 69 % of β-O-4 ether bonds, which could theoretically yield a maximum of 36 % of monomers[6]. Through pyrolysis of lignin

model compounds, Drage et al. concluded that the C-O bond of β-aryl ether type being cleaved is prior to the side of aryl methoxyl groups[7]. Therefore, ether bond is a key reason for the liquefaction of lignin. However, the amorphous structural, compositional features of lignin and different types of lignins are dominant factors affecting the degradation process. The industrial applications of lignin are limited severely due to its complex nature and chemical structure, further research is needed.

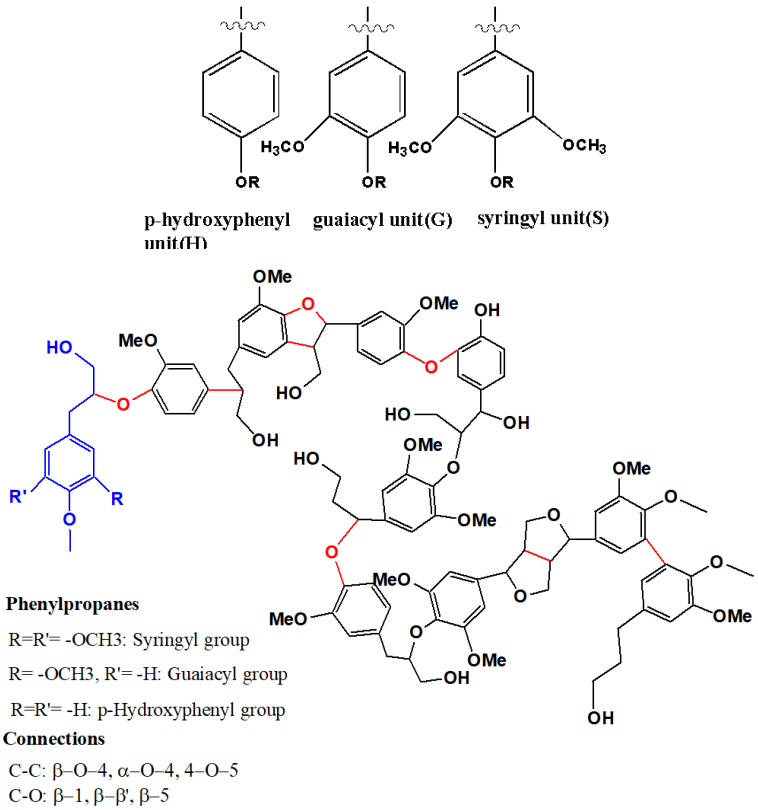

Fig. 1- 3 Typical structure of the lignin polymers and its three main lignols (Syringyl, Guaiacyl, p-Hydroxyphenyl units) inside.

1.3 Lignin types and comparison

The lignin feature partially depends on the type of biomass. Table 1-1 lists the major lignocellulosic biomass sources, and the components distribution of the various biomasses summarized from the literature survey. Because diverse temperatures and production choices exist in different regions and countries, the distribution of lignocellulosic biomass resources varies widely. For example, China mainly produces waste such as Chinese herbal medicine

residue, sugarcane bagasse, walnut shells, and other waste, and wheat straw and corn stover also occupy a large proportion of agricultural production. For Japan, cedar and spruce are very rich wood resources, and the prevalence of coffee also leads to the use of coffee grounds as a biomass resource. Other trees, including pine, oak, eucalyptus, beech, and bamboo, which are found in different temperate zones around the world, are the most discussed and researched woody biomass in the literature. Despite the fact that they all contain three main substances: cellulose, hemicellulose, and lignin, the proportions and properties vary by species.

Lignocellulosic biomass sources are broadly classified as softwood, hardwood, and grass, the order of lignin percentage generally is grass< hardwood<softwood. And it is worth mentioning that lignin constitutes 25–35% of softwood sources, 18-25% of hardwood sources, and around 19% of grass[8]. Softwood lignin is primarily formed by guaiacylpropane units (around 90-95%), whereas hardwood lignin possesses almost equal amounts of guaiacyl and syringyl units with less amount of condensed units[8]. Having a larger proportion of β-O-4 structural units, and C-C bonds (β-1 and β-β) are also typical features of hardwood lignin. Grass lignin comprises guaiacyl and syringyl units, the former being the major component, which is chemically bound to the lignin core, mostly by ether bonds. Some p-hydroxyphenylpropane units are also incorporated in the grass-type of lignin, and the amounts are a little higher than that in woody lignin[9].

Table 1- 1 Primary organic components in the typical lignocellulosic biomass feedstocks.

Lignocellulosic biomass type	**Cellulose (%)**	**Hemicellulose (%)**	**Lignin (%)**	**Reference**
Softwood				
Pine sawdust	44	26	30	[10]
Japanese cedar	-	-	32	[11]
Spruce wood	47.11	21.31	31.58	[12]
Hardwood				
Oak	36.7-46.6	36.5	17.6-25.3	[13]
Walnut shell	36	25.43	38	[14]
Eucalyptus	49	21	18	[9]
Beech	46.27	31.86	21.87	[12]

Grasses				
Bamboo	40-60	20-30	20-30	[15]
Corn stover	38	29	15	[12]
Wheat straw	38	29	19	[12]
Waste				
Herbal residue	36.5	18.5	24.2	[16]
Coffee Grounds	12.4	39.1	23.9	[17]
Bagasse	45-55	20-25	18-24	[9]

Different types of lignin have been described depending on the means of isolation, such as organic, enzymatic, kraft, milled wood lignin, lignosulfonate, and soda process. Generally, lignin's content and chemical structure depend on the type of biomass on the one hand, and on the other hand the extraction process can have a noticeable effect. Many strategies for recovering lignin from biomass have been proposed (seen in Table 1-2). In the large-scale pulp and paper industry, the Kraft process (hydrolysis of lignin with Na_2S) is employed for making paper products by using biomass or wood as raw material, in which lignin residue including sulfur (~2 wt.%) is disposed of as waste[18]. Acidic solutions allow recovering lignin from the kraft process due to unusual liquid-liquid phase behaviour, called kraft lignin. Alkaline lignin (or soda lignin) is also a typical type of technical lignins, which is also extracted from the waste of the paper industry, Zhao et al. have revealed the exact differences in the structure of Alkaline lignin and kraft lignin[19]. In a lignosulfonate method, lignin is isolated by the sulphite coking process, which employs sulphite precursors of calcium and magnesium. Lignosulfonate lignin is isolated from woody biomass with a molecular weight range from 5000 to 60000 Da[20]. Milled wood lignin (MWL) is isolated by solvent and purified finely with a ground wood meal, which can be thought of as the best lignin to represent the lignin component in the wood. Moreover, enzymatic mild acidolysis can isolate an even higher yield of lignin, and enzymatic mild acidolysis lignin (EMAL) has higher purity than that of MWL. Other methods, such as the organic process provide lignin with a relatively simple structure, named organosolv lignin, while an organic solvent and catalyst such as dilute acid are required. The general extraction of organosolv lignin is conducted at 443-493 K with 1-2 h treatment time to generate small molecular weight lignin that is between 1000-3000 Da[21]. Notably, due to its sulfur-free and less-condensed structure,

organosolv lignin is one of the most potential types of technical lignin for further investigation and valorization[8].

Table 1- 2 Property of various types of lignin through different isolation methods.

Lignin type	Number average molecular weight (g/mol)	Dispersity (M_w/M_n)	Features	Ref.
Organosolv lignin	1249	2.8	High unsaturation degree and molecular weight. Mild conditions result in more unaltered lignin	[21]
EMAL (enzymatic mild acidolysis lignin)	~1900	~3	Higher yield and purity than those of MWL.	[22]
Kraft lignin	1000-3000	2-4	Highly modified, partially fragmented.	[23]
MWL (milled wood lignin)	2800-14200	3.7-12.9	Most similar to the native structure	[24]
Lignosulfonated lignin (hardwood)	5000-60000	1.3-3.5	Lignosulphonate lignin exhibits a higher molecular weight. Moreover, lignosulphonate lignin has high impurities, accounts for 30%.	[25]
Dealkaline lignin	60000	-	Demethylation of lignosulphonate lignin	[26]
Alkaline/soda lignin	11646±1972	4.33±0.54	Adjusting the PH value of dealkaline lignin in the range of PH 8.0-10.0	[27]

1.4 Lignin utilization

The research on lignin utilization technology has been investigated over the years. Thermochemical conversion of biomass into biofuel is one of the recognized and up-and-coming technologies, which consists of two main utilization methods, the first one is depolymerization of lignin, including the conversion of lignin into bio-oil by pyrolysis technology, and liquefying lignin by hydrogenation or hydrogenolysis; the second one is the conversion of biomass into biogas by gasification or fermentation technology. Among them, bio-oil is considered as a renewable energy source that can be alternative petroleum. Therefore, the technology for depolymerization of biomass or biomass components has been

researched and developed for decades.

While due to lignin's 3D recalcitrant property and cross-linked structure, lignin has usually been considered as a low-value by-product in the pulp and paper industry. That is the main reason to restrict biomass utilization. Due to its inherent physical properties, lignin is often considered a good additive in products such as concrete, asphalt, protective coatings and foams. Lignin can increase its compressive strength and makes concrete stronger as admixtures. For asphalts, lignin can improve the viscosity, hardness, and high-temperature stability of modified asphalts[28]. And protective coating modified by lignin shows excellent anti-corrosion, anti-bacterial, anti-icing, and UV-shielding properties[29]. Lignin-based foam can be used as an insulation material[30]. Besides being a material additive, lignin has been investigated more on the laboratory scale in terms of chemical conversion. Lignin pyrolysis was first investigated as a means of better understanding biomass pyrolysis processes by examining the pyrolytic capabilities of the three key components of biomass independently[31]. Then some scholars started to study catalytic pyrolysis of lignin, especially zeolite-based catalysts, aiming at the selective production of olefins and aromatic hydrocarbons from lignin[32][33][34]. Besides, hydrogenolysis is one of the means to obtain high-value bio-oil by liquefying lignin polymers, which is now the mainstream technology for lignin treatment. By providing an external hydrogen donor, lignin polymers are depolymerized and hydrogenated under high temperature and pressure to obtain phenolic monomer compounds such as guaiacol, phenol, and so on[35][36][37]. In addition, some people used the hydrogenation process on bio-oil to improve its H/C ratio and increase its availability[38]. Other techniques, such as lignin oxidation and gasification, have also been supported in the literature. Oxygenated compounds such as phenolics, vanillin, ketones, and acids can be obtained from lignin oxidation[39], while syngas can be obtained from the gasification of lignin[40].

Based on the analysis of the internal unit composition and structure of lignin, the authors concluded that its richness in aromatic resources needed to be better utilized. And if high-value chemicals like olefins and aromatic hydrocarbons could be obtained from lignin instead of fossil fuel energy that would be very meaningful. It is well known that olefins and aromatics are the most common petrochemicals, and are essential sources for industrial chemicals and products. It is known that the production capacity of ethylene and market volume of benzene has been on an upward trend over the years. By 2025, Statista forecasts

the production capacity of ethylene to reach around 300 million metric tons and the market volume of benzene reach to 67 million metric tons. So, olefins and aromatic hydrocarbons will be the target products in this work. The author focuses on the technology for transferring lignin into olefins and aromatic hydrocarbons.

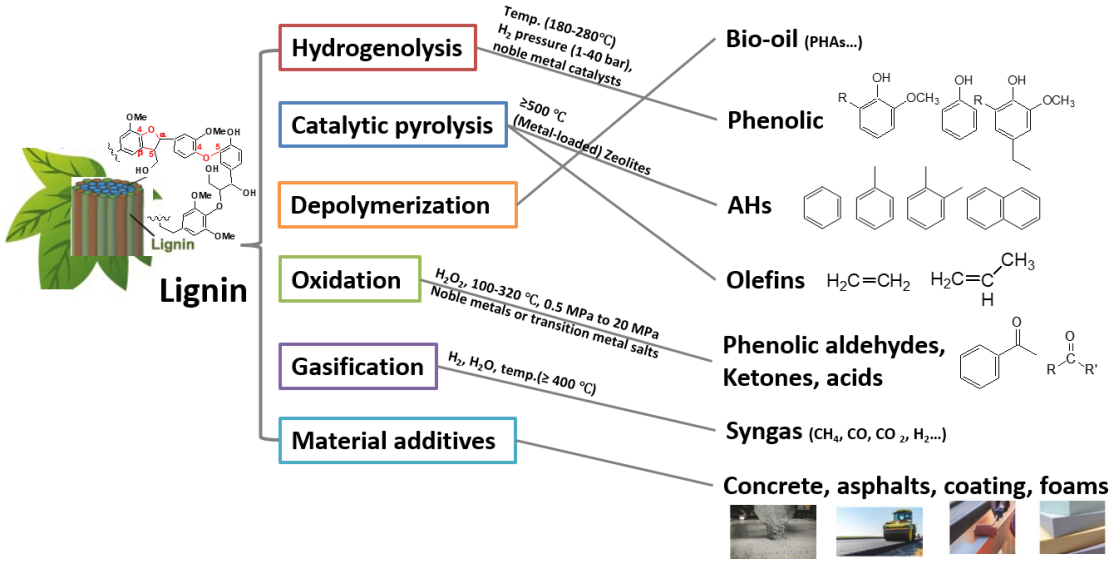

Fig. 1- 4 The various technologies for lignin utilization.

1.5 Reference

[1] W. Den, V.K. Sharma, M. Lee, G. Nadadur, R.S. Varma, Lignocellulosic biomass transformations via greener oxidative pretreatment processes: Access to energy and value added chemicals, Front. Chem. 6 (2018). https://doi.org/10.3389/fchem.2018.00141.

[2] E. Ahmad, K.K. Pant, Chapter 14 - Lignin Conversion: A Key to the Concept of Lignocellulosic Biomass-Based Integrated Biorefinery, in: T. Bhaskar, A. Pandey, S.V. Mohan, D.-J. Lee, S.K.B.T.-W.B. Khanal (Eds.), Elsevier, 2018: pp. 409–444. https://doi.org/https://doi.org/10.1016/B978-0-444-63992-9.00014-8.

[3] J.K. Weng, X. Li, N.D. Bonawitz, C. Chapple, Emerging strategies of lignin engineering and degradation for cellulosic biofuel production, Curr. Opin. Biotechnol. 19 (2008) 166–172. https://doi.org/10.1016/j.copbio.2008.02.014.

[4] W. Boerjan, J. Ralph, M. Baucher, Lignin Biosynthesis, Annu. Rev. Plant Biol. 54 (2003) 519–546. https://doi.org/10.1146/annurev.arplant.54.031902.134938.

[5] J. Zakzeski, P.C.A. Bruijnincx, A.L. Jongerius, B.M. Weckhuysen, The catalytic valorization of lignin for the production of renewable chemicals, Chem. Rev. 110 (2010) 3552–3599. https://doi.org/10.1021/cr900354u.

[6] E.M. Anderson, M.L. Stone, R. Katahira, M. Reed, W. Muchero, K.J. Ramirez, G.T. Beckham, Y. Román-Leshkov, Differences in S/G ratio in natural poplar variants do not predict catalytic depolymerization monomer yields, Nat. Commun. 10 (2019). https://doi.org/10.1038/s41467-019-09986-1.

[7] T.C. Drage, C.H. Vane, G.D. Abbott, The closed system pyrolysis of β-O-4 lignin substructure model compounds, Org. Geochem. 33 (2002) 1523–1531. https://doi.org/https://doi.org/10.1016/S0146-6380(02)00119-5.

[8] P. Azadi, O.R. Inderwildi, R. Farnood, D.A. King, Liquid fuels, hydrogen and chemicals from lignin: A critical review, Renew. Sustain. Energy Rev. 21 (2013) 506–523. https://doi.org/10.1016/j.rser.2012.12.022.

[9] G. Brunow, Methods to Reveal the Structure of Lignin, Biopolym. Online. (2005). https://doi.org/https://doi.org/10.1002/3527600035.bpol1003.

[10] A. Rusanen, K. Lappalainen, J. Kärkkäinen, T. Tuuttila, M. Mikola, U. Lassi, Selective

hemicellulose hydrolysis of Scots pine sawdust, Biomass Convers. Biorefinery. 9 (2019) 283–291. https://doi.org/10.1007/s13399-018-0357-z.

[11] M. Takada, S. Saka, Characterization of lignin-derived products from Japanese cedar as treated by semi-flow hot-compressed water, J. Wood Sci. 61 (2015) 299–307. https://doi.org/10.1007/s10086-015-1464-0.

[12] A. Demirbaş, Relationships between lignin contents and heating values of biomass, Energy Convers. Manag. 42 (2001) 183–188. https://doi.org/10.1016/S0196-8904(00)00050-9.

[13] A. Geffert, E. Výbohová, J. Geffertová, Changes in the chemical composition of oak wood due to steaming, Acta Fac. Xylologiae Zvolen. 61 (2019) 19–29. https://doi.org/10.17423/afx.2019.61.1.02.

[14] F. Safari, M. Salimi, A. Tavasoli, A. Ataei, Non-catalytic conversion of wheat straw, walnut shell and almond shell into hydrogen rich gas in supercritical water media, Chinese J. Chem. Eng. 24 (2016) 1097–1103. https://doi.org/10.1016/j.cjche.2016.03.002.

[15] F. Rusch, A.D. Wastowski, T.S. de Lira, K.C.C.S.R. Moreira, D. de Moraes Lúcio, Description of the component properties of species of bamboo: a review, Biomass Convers. Biorefinery. (2021). https://doi.org/10.1007/s13399-021-01359-3.

[16] H.L. Wei, J. Bu, S.S. Zhou, M.C. Deng, M.J. Zhu, A facile ionic liquid and p-toluenesulfonic acid pretreatment of herb residues: Enzymatic hydrolysis and lignin valorization, Chem. Eng. J. 419 (2021). https://doi.org/10.1016/j.cej.2021.129616.

[17] L.F. Ballesteros, J.A. Teixeira, S.I. Mussatto, Chemical, Functional, and Structural Properties of Spent Coffee Grounds and Coffee Silverskin, Food Bioprocess Technol. 7 (2014) 3493–3503. https://doi.org/10.1007/s11947-014-1349-z.

[18] T. Li, S. Takkellapati, The current and emerging sources of technical lignins and their applications, Biofuels, Bioprod. Biorefining. 12 (2018) 756–787. https://doi.org/https://doi.org/10.1002/bbb.1913.

[19] C. Zhao, J. Huang, L. Yang, F. Yue, F. Lu, Revealing Structural Differences between Alkaline and Kraft Lignins by HSQC NMR, Ind. Eng. Chem. Res. 58 (2019) 5707–5714. https://doi.org/10.1021/acs.iecr.9b00499.

[20] N.E. El Mansouri, J. Salvadó, Structural characterization of technical lignins for the

production of adhesives: Application to lignosulfonate, kraft, soda-anthraquinone, organosolv and ethanol process lignins, Ind. Crops Prod. 24 (2006) 8–16. https://doi.org/10.1016/j.indcrop.2005.10.002.

[21] S.K. Singh, P.L. Dhepe, Isolation of lignin by organosolv process from different varieties of rice husk: Understanding their physical and chemical properties, Bioresour. Technol. 221 (2016) 310–317. https://doi.org/10.1016/j.biortech.2016.09.042.

[22] A. Guerra, I. Filpponen, L.A. Lucia, C. Saquing, S. Baumberger, D.S. Argyropoulos, Toward a Better Understanding of the Lignin Isolation Process from Wood, J. Agric. Food Chem. 54 (2006) 5939–5947. https://doi.org/10.1021/jf060722v.

[23] G. Anderson, M. Régis, F. André, L. Fachuang, R. John, Structural Characterization of Lignin during Pinus taeda Wood Treatment with Ceriporiopsis subvermispora, Appl. Environ. Microbiol. 70 (2004) 4073–4078. https://doi.org/10.1128/AEM.70.7.4073-4078.2004.

[24] B. Xiao, X.F. Sun, R. Sun, Chemical, structural, and thermal characterizations of alkali-soluble lignins and hemicelluloses, and cellulose from maize stems, rye straw, and rice straw, Polym. Degrad. Stab. 74 (2001) 307–319. https://doi.org/https://doi.org/10.1016/S0141-3910(01)00163-X.

[25] G.E. Fredheim, S.M. Braaten, B.E. Christensen, Molecular weight determination of lignosulfonates by size-exclusion chromatography and multi-angle laser light scattering, J. Chromatogr. A. 942 (2002) 191–199. https://doi.org/10.1016/S0021-9673(01)01377-2.

[26] A.K. Deepa, P.L. Dhepe, Lignin Depolymerization into Aromatic Monomers over Solid Acid Catalysts, ACS Catal. 5 (2015) 365–379. https://doi.org/10.1021/cs501371q.

[27] A. Ang, Z. Ashaari, E.S. Bakar, N.A. Ibrahim, Characterisation of sequential solvent fractionation and base-catalysed depolymerisation of treated alkali lignin, BioResources. 10 (2015) 4137–4151. https://doi.org/10.15376/biores.10.3.4137-4151.

[28] H. Yao, Y. Wang, J. Liu, M. Xu, P. Ma, J. Ji, Z. You, Review on Applications of Lignin in Pavement Engineering: A Recent Survey, Front. Mater. 8 (2022). https://doi.org/10.3389/fmats.2021.803524.

[29] J. Carlos de Haro, L. Magagnin, S. Turri, G. Griffini, Lignin-Based Anticorrosion

Coatings for the Protection of Aluminum Surfaces, ACS Sustain. Chem. Eng. 7 (2019) 6213–6222. https://doi.org/10.1021/acssuschemeng.8b06568.

[30] V. Mimini, V. Kabrelian, K. Fackler, H. Hettegger, A. Potthast, T. Rosenau, Lignin-based foams as insulation materials: a review, Holzforschung. 73 (2019) 117–130. https://doi.org/doi:10.1515/hf-2018-0111.

[31] H. Yang, R. Yan, H. Chen, C. Zheng, D.H. Lee, D.T. Liang, In-Depth Investigation of Biomass Pyrolysis Based on Three Major Components: Hemicellulose, Cellulose and Lignin, Energy & Fuels. 20 (2006) 388–393. https://doi.org/10.1021/ef0580117.

[32] H. Zhang, J. Zheng, R. Xiao, Catalytic pyrolysis of willow wood with Me/ZSM-5 (Me = Mg, K, Fe, Ga, Ni) to produce aromatics and olefins, BioResources. 8 (2013) 5612–5621. https://doi.org/10.15376/biores.8.4.5612-5621.

[33] X. Li, L. Su, Y. Wang, Y. Yu, C. Wang, X. Li, Z. Wang, Catalytic fast pyrolysis of Kraft lignin with HZSM-5 zeolite for producing aromatic hydrocarbons, Front. Environ. Sci. Eng. China. 6 (2012) 295–303. https://doi.org/10.1007/s11783-012-0410-2.

[34] M. Yang, J. Shao, Z. Yang, H. Yang, X. Wang, Z. Wu, H. Chen, Conversion of lignin into light olefins and aromatics over Fe/ZSM-5 catalytic fast pyrolysis: Significance of Fe contents and temperature, J. Anal. Appl. Pyrolysis. 137 (2019) 259–265. https://doi.org/10.1016/j.jaap.2018.12.003.

[35] A. Bjelić, M. Grilc, M. Hu\vs, B. Likozar, Hydrogenation and hydrodeoxygenation of aromatic lignin monomers over Cu/C, Ni/C, Pd/C, Pt/C, Rh/C and Ru/C catalysts: Mechanisms, reaction micro-kinetic modelling and quantitative structure-activity relationships, Chem. Eng. J. (2019).

[36] R. Shu, Y. Xu, P. Chen, L. Ma, Q. Zhang, L. Zhou, C. Wang, Mild Hydrogenation of Lignin Depolymerization Products over Ni/SiO2 Catalyst, Energy and Fuels. 31 (2017) 7208–7213. https://doi.org/10.1021/acs.energyfuels.7b00934.

[37] H. Wu, J. Song, C. Xie, C. Wu, C. Chen, B. Han, Efficient and Mild Transfer Hydrogenolytic Cleavage of Aromatic Ether Bonds in Lignin-Derived Compounds over Ru/C, ACS Sustain. Chem. Eng. 6 (2018) 2872–2877. https://doi.org/10.1021/acssuschemeng.7b02993.

[38] X. Zhang, K. Wang, J. Chen, L. Zhu, S. Wang, Mild hydrogenation of bio-oil and its derived phenolic monomers over Pt–Ni bimetal-based catalysts, Appl. Energy. 275

(2020) 115154. https://doi.org/https://doi.org/10.1016/j.apenergy.2020.115154.

[39] V.E. Tarabanko, N. Tarabanko, Catalytic Oxidation of Lignins into the Aromatic Aldehydes: General Process Trends and Development Prospects, Int. J. Mol. Sci. 18 (2017) 2421. https://doi.org/10.3390/ijms18112421.

[40] E.T. Liakakou, B.J. Vreugdenhil, N. Cerone, F. Zimbardi, F. Pinto, R. André, P. Marques, R. Mata, F. Girio, Gasification of lignin-rich residues for the production of biofuels via syngas fermentation: Comparison of gasification technologies, Fuel. 251 (2019) 580–592. https://doi.org/10.1016/j.fuel.2019.04.081.

Chapter 2 Literature survey and research strategy

2.1 Hydrogenation of lignin

Hydrogenation (or hydrogenolysis, hydrodeoxygenation) is one of the depolymerization technologies for lignin sources, in which hydrogen as a reductant yields phenolic monomers with high stability[1]. The process is generally performed under severe conditions affording a high liquefaction rate. In 1938, the catalytic hydrogenation reaction was conducted on hardwood lignin by Harris and co-workers[2]. The lignin was reported to react with hydrogen gas with copper-chromium oxide as a catalyst. After that, the catalytic hydrogenation process is used to tailor the functional groups, improve lignin's property, and control the product's distribution[3–5]. K. Kashima et al. also started to work on lignin liquefaction and discovering catalysts in 1964. After the hydrogenolysis process, they found a mixture of C6-C9 mono-phenolic products that can reach as high as 40% of yield and published on Canadian Patents. A co-catalyst of iron sulfide with another metal sulfide (like Cu, Co, Ni, Zn, or Mo) was used on bio-oil and phenolics, which was conducted at 523-723 K with an initial hydrogen pressure of 15.2-45.6 MPa. Around 21% yield of lignin-derived phenol was obtained. This demonstrates the variant of such research direction, and the reproducibility of the experimental results was not well achieved because the composition of lignin was too complex and inconsistent[6].

The conversion of lignin to unfunctionalized aromatic hydrocarbons deserves more attention, especially compounds such as BTX (benzene, toluene, xylene), which can theoretically produce 60% of the aromatic compounds from lignin[7,8]. The hydrogenation reaction is a very promising option, and the hydrogenation process for lignin is mainly divided into two major parts in terms of products to produce high-value chemicals and bio-oil refining. And there are two types of hydrogenation technologies, thermal catalytic hydrogenation (TCH) and electrochemical hydrogenation (ECH) with the catalysts. Here a literature summary of these two different hydrogenation techniques studied on lignin and lignin model compounds was presented in this section.

2.1.1 Thermal catalytic hydrogenation

The summary of thermal catalytic hydrogenation (TCH) on different types of lignin is presented in Table 2-1. For the catalytic hydrogenation of lignin by heterogeneous catalysts, there are several main types of catalysts, like non-metallic catalysts, nickel-based catalysts, noble-metal catalysts, metal oxides, and multi-metal composite catalysts. The researchers mainly focus on the liquefaction rate and depolymerized compounds of lignin, pursuing higher conversion rates and more bio-oil or phenolic products via using different catalysts. Lignin liquefaction yields, calculated by the difference of recovered lignin residue, are generally above 50% (seen in Table 2-1). Ni-based catalysts as the most popular catalysts have been used in integrated hydroprocessing of lignin[9], which is efficient for the hydrogenolysis reaction with high conversion rates[10]. Noble metal catalysts (Ru, Rh, Pt, and Pd) also demonstrated substantial catalytic reactivity in the hydrogenolysis of C-O ether bonds[11,12] and the hydrogenation of aromatic rings in the liquid products (Table 2-1, entry 7&8). Pepper et al. studied and compared several common catalysts (Raney Ni, Pd/C, Rh/C, Rh/Al_2O_3, Ru/C, Ru/Al_2O_3) for the hydrogenation of lignin. A significant amount of raw lignin was converted into monomeric products, like 4-propylguaiacol and dihydroconiferyl alcohol, among them Rh/C showed a maximum yield[13]. The Pd/C yielded 24% of dihydroconiferyl alcohol, whereas Rh/C resulted in producing 4-propylguaiacol and dihydroconiferyl alcohol accounting for 34% of raw lignin. Noble metal catalysts have better selectivity for specific hydrogenated products, but the economics limit their industrial application. In the absence of a catalyst, the lignin macromolecules were thermally depolymerized due to internal bonds breaking, which limited the hydrogenation or hydrogenolysis reaction to some extent (Table 2-1, entry 10).

In fact, the temperature has a significant effect on the hydrogenation process as well as the catalyst. High temperatures and pressures are more favourable for heterogeneous hydrogenation reactions, which are usually carried out at 200-400 ℃ and an initial hydrogen pressure of 3-10 MPa[14][15]. Kumar et al.[16] performed the depolymerization of Kraft lignin via NiMo and CoMo catalysts at 350 ℃ for 4 h with 100 bar initial H_2 pressure, 87% of lignin can be converted, and 26.4 wt.% of monomers were obtained. However, severe conditions also lead to the formation of coke which is the main obstacle to hydrogenolysis. It was reported that the formation of coke and oligomers was caused by the repolymerization and condensation of intermediates followed by dehydration under the thermal effect[14][17].

Table 2- 1 Thermal catalytic hydrogenation of various lignin.

Entry	Lignin feedstock	Catalysts	Reaction conditions	Products	Conv. rate	Ref.
1	Lignosulfonate	Ni/AC	200 ℃, 5 MPa H_2, ethylene glycol	4-ethyl-guaiacol, 4-propyl-guaiacol, and amount of dimers	68 %	[18]
2	Kraft lignin	Ni/HZSM-5	220 ℃, 0.1 MPa Ar, 7 h, MeOH/H_2O, 1.7 mmol of NaOH	Alkyl substituted phenols and oligomers	96.9 %	[19]
3	Birch sawdust	Ni/C	200 ℃, 1 atm Ar, 6 h, MeOH	Propylguaiacol, propylsyringol, dimers	54 %	[20]
4	Poplar lignin	Nb_2-Ni_1/ZnO-Al_2O_3	225 ℃, 2 MPa H_2, MeOH	2-methoxy-4-propylphenol, 2,6-dimethoxy-4-propylphenol, and 4-(3-hydroxypropyl)-2,6-dimethoxyphenol	83.6 %	[21]
5	Organosolv lignin	$Ni_{85}Pd_{15}$	130 ℃, 1 MPa H_2, 12 h, H_2O	4-(3-Hydroxypropyl)-2-dimethoxyphenol, 4-(3-Hydroxypropyl)-2,6-dimethoxyphenol	56 %	[22]
6	Alkaline lignin	Nitrogen-doped solvothermal carbon	N_2, DI water, 250 °C, 3 h	Phenolic monomers (phenol, o-guaiacol, catechol, 4-ethyl guaiacol, vanillin) yield (7.52 %),	55.2 %	[23]
7	Organosolv lignin	5 % Ru/C	260 ℃, 2 MPa H_2, 1 h, 0.025 mol NaOH, 70 % isopropanol/ water mixtures	44.6 % of water-soluble product and 26.5 % of oil-soluble product, 6.4 % of char	75.7 %	[24]
8	Organosolv lignin	5 % Pd/C	260 °C, 2 MPa H_2, 1 h. 0.025 mol NaOH, 70 % i-PrOH/water mixtures	73.8 % of water-soluble product and 13.3 % of oil-soluble product, 17.2 % of char	67 %	[24]
9	Pine lignin	MgO	THF, 250 ℃, 0.5 h	13.2 % yield of useful phenolic monomers (Phenol, guaiacol, syringol)	59 %	[25]

10	Alkaline lignin	Non-catalyst	N_2, DI water, 250 °C, 3 h	Phenolic monomers yield (2.5 %), residue lignin yield (60.70 %), char yield (25.8 %)	39.3 %	[23]

Note: MeOH: methanol; DI water: deionized water; i-PrOH: isopropanol.

2.1.2 Electrochemical hydrogenation

Electrochemical has been regarded as a low-cost and environmentally friendly approach, and can be carried out under mild reaction conditions. Electrochemical hydrogenation (ECH) has been intensively studied on lignin model compounds in the recent past. Formally, electrochemical hydrogenation consists of integrating the reduction of protons and the hydrogenation of organic compounds in the cathodic electrolyte. Moreover, other oxidation reactions of water occur and oxygen is formed at the anode[26][27]. Table 2-2 lists the electrochemical hydrogenation pathways of common lignin model compounds that can cover the most typical functional groups and linkage bonds of lignin. As seen in Table 2-2, ECH occurred selectively on the aromatic ring without destroying other functional groups (like hydroxyl, methyl, and methoxyl). Even for dimers, electrochemical hydrogenation can very effectively happen on diphenyl ether (Table 2-2, entry 8). The electrochemical hydrogenation reaction can mainly occur on the aromatic rings and generate di-cyclohexyl and cyclohexyl phenyl ether. The ester bonds were also partially broken at the same time, resulting in a minor amount of cyclohexanone and cyclohexanol.

Table 2- 2 Electrochemical hydrogenation reaction of common lignin model compounds.

Entry	Model compounds	Reaction process	Ref.
1	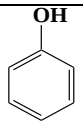 Phenol	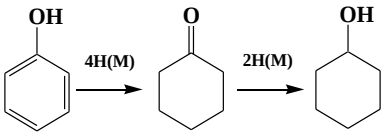	[28]
2	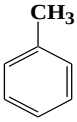 Toluene	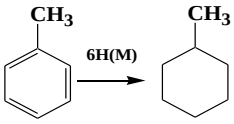	[29]
3	 Benzene		[30]

4	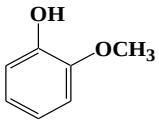 Guaiacol	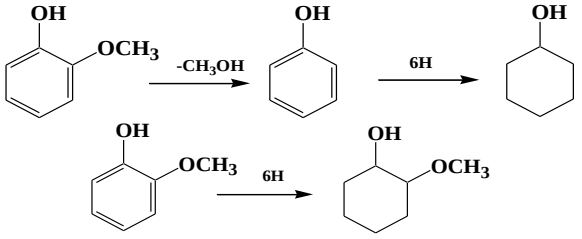	[31]
5	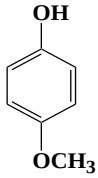 4-methoxyl phenol	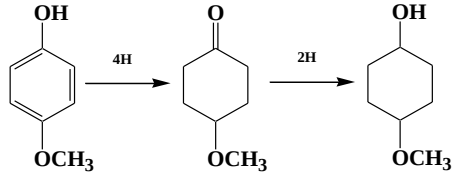	[26]
6	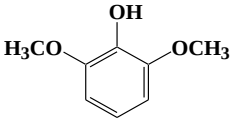 Syringol	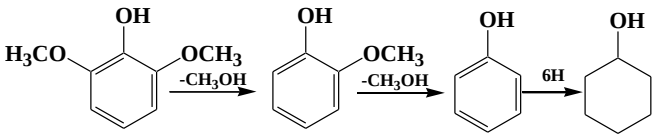	[31]
7	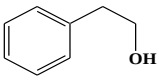 2-phenyl ethanol	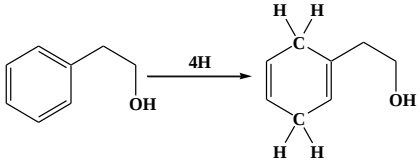	[32]
8	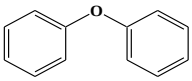 Diphenyl ether	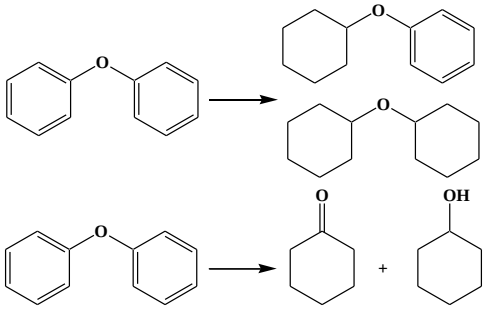	[26]

Table 2-3 summarizes studies on model compounds that can be successfully converted to cycloalkanes with high conversion rates in the presence of catalysts utilizing electrocatalytic hydrogenation. Anna et al. have investigated various electrodes for electro-reduction of phenol, and the order of catalytic activity is Ru/Ni > Pt/Pt > Rh/Ni. 92% of cyclohexanol product was obtained with 11% current efficiency under a current density of 10 mA/cm^2 and NaCl as the supporting electrolyte at 60 ℃[28]. Song et al. also tested the electrochemical hydrogenation of phenol with Pt/C, Pd/C, and Rh/C. The reaction pathway from phenol to cyclohexanone was proposed, then further hydrogenated to cyclohexanol (like Entry 1)[33]. In their work, Rh/C led to the highest conversion rate of phenol (50-66%) under different electrolytes, followed by Pt/C and Pd/C. Furthermore, the conversion rate increases with temperature up to 50 ℃ under exploring Pt/C with −40 mA of current. The noble metal

catalysts have also been explored in Peng's work[34]. PtRhAu, PtRh, and Pt deposited on carbon felt were prepared as electrocatalysts and compared the affection on the electrochemical hydrogenation of guaiacol. The ternary PtRhAu (additional incorporation of Au) catalyst produced 2MC (2-methoxycyclohexanol) more selectively than the PtRh catalyst and prevented the generation of deoxygenated by-products (like methoxyl-cyclohexane, cyclohexanone, and cyclohexanol). PtRhAu catalyst was proposed to convert 91% of the guaiacol with a 74% selectivity of 2MC. Moreover, PtRhAu catalyst maintained over 40% of FE[31]. The performance of this electrocatalytic hydrogenation system on lignin-derived bio-oil was also checked in Li's work[31]. The bio-oil from wood was further electro-reduced in 0.2 M $HClO_4$, and after 3 hours reaction, 92% of conversion rate and 68% of selectivity for the 2-methoxy-4-propylcyclohexanol were achieved.

The purpose of investigating the behaviour of lignin derivatives or model compounds under different variables is to gain a better understanding of the electrochemical mechanism, and to allow a visual comparison with conventional thermal catalytic hydrogenation techniques. The model compounds, however, are unable to totally replace the obstinate and more complex structure of raw lignin. Therefore, the behaviour of raw lignin in the electrochemical hydrogenation process still needs further observation for industrial application. A further summary of the electrochemical reactions in raw feedstock will be presented below.

Table 2- 3 Various catalysts for electrocatalytic hydrogenation of lignin model compounds.

Substrate	WE/CE/RE	Catalyst/membrane	Electrolyte	Conditions	Products	Ref.
Phenol (Conc.=8.5* 10^{-3} M)	Ru3.5%-Ni / Glassy C plate / non	Ru dispose on WE / Nafion 324	0.1 M H_2SO_4 aqueous solution	Temp.: RT; Current density: 1 mA/cm^2; Time: 12 F/mol	Cyclohexanol (100%); Conv. rate: 92%	[28]
Phenol (2 mL)	Reticulated vitreous carbon (RVC) / Pt wire /	Rh/C, Pt/C, Pd/C / Nafion 117	Anolyte: 0.1 M of H_2SO_4; Catholyte: acetic acid, H_3PO_4,	Current: -40, -60 mA; Time: 2 h; Temp.: 5-80 °C;	Cyclohexanol, cyclohexanone; Conv. rate: 26-63%	[33]

	Ag|AgCl		H_2SO_4	Stirring: 500 rpm		
4-methoxyphenol (16 mM)	Carbon felt connected to graphite rod / Pt wire / Ag|AgCl	Rh/C (50 mg) / Nafion 117	Acetate buffer	Temp.: 23 ℃; Current: 40 mA; Time: 30 min.	Methoxy cyclohexanone (40% around), methoxy cyclohexanol; Conv. rate: 80% around	[26]
Benzene	Rh–Pt / not mention / non	Rh–Pt / Nafion, Du Pont	Water	Surface area: 7.07 cm^2; Atmosphere: H_2 with atmospheric pressure	Cyclohexane (16%)	[30]
Guaiacol	Ru|ACC / Pt wire / non	3-CE-NH_3 / Nafion-117	Catholyte: 0.2 M HCl; Anolyte: 0.2 M phosphate buffer	100 mA, 80 ℃, 2 h	2-methoxycyclohexanol (47%), cyclohexanol (53%); Conv. Rate: 75%	[31]
Guaiacol	PtRhAu-C felt / Pt / RHE reference	PtRhAu deposited on carbon felt / Nafion-117	0.2 M $HClO_4$	Current density: 60 mA/cm^2 Time: 1 h Stirring: 1000 rpm. Surface area: 1 cm^2	96% of conversion rate; 2-methoxy-4-propylcyclohexanol (68% of selectivity)	[34]
Syringol	Ru|ACC / Pt wire / non	1.5-CE-NH_3 / Nafion-117	Catholyte: 0.2 M HCl; Anolyte: 0.2 M phosphate buffer	Current: 100 mA; Temp.: 80 ℃; Time: 2 h	2-methoxycyclohexanol (36%), cyclohexanol (35%), guaiacol (15%) Conv. rate: 58%	[31]

Notes: WE: working electrode; CE: counter electrode; RE: reference electrode; Conc.: concentration; M: mol; Conv. rate: conversion rate.

The electrochemical reactions have also been utilized on raw lignin, summarized in Table 2-4. Although the primary lignin model compounds and bio-oils both use electrochemical hydrogenation to obtain high-quality chemicals, the electrochemical hydrogenation of raw lignin has been rarely studied. The current focus of electrochemical lignin is on electrochemical oxidation reactions to depolymerize the lignin macromolecular structure for valuable chemicals.

To date, from previous research on lignin electrochemical reactions, we can know the alkaline solution was used commonly as electrolyte solutions. Moreover, ILs and DESs were also used as electrolytes due to their excellent conductivity and recyclability. Besides, the electrode is an important factor to improve reaction rate as (1) various substrate materials supported the catalyst during the reaction; (2) the conductivity of the electrode substrate; (3) the interaction effect between the loading of the catalyst and the substrate, all these factors have a significant influence on the electrochemical depolymerization reaction. Electrode structure was investigated by Stiefel and his group[35]. They found that the large porosities of electrode material as fleece> wire> foam> plate and explained the porosities were not related to mass transport coefficients due to mass transport limitation from the bulk molecule to the catalyst surface, which was effectively limiting the reaction rates. Other factors, like current density and reaction temperature in the electrochemical reactions of lignin also have a significant effect on the products. It was proposed that the current density affected the reaction efficiency and the products, higher current density resulted in more organic products, like aldehydes and ketones[36]. The electrochemical oxidation of lignin with a higher current density was proposed to generate more monomeric compounds such as anisole, vanillin, and acids. Meanwhile, higher temperatures favoured more aqueous products, like phenolics and acids, with oxygen species associated with hydrophilic groups. Wang et al. observed that increasing the temperature could enhance the yield of anisole[37].

In another study, Cai et al. investigated both the electrochemical oxidation and electrocatalytic hydrogenation of lignin in alkaline electrolytes[38]. They have tested the CV (cyclic voltammetry) curve and AP (anodic polarization) curves under different lignin concentration (10-60 g lignin/L), reaction time (0.5-2.5 h), and NaOH concentration (0.8-1.2 M) electrolyte. The electrochemical oxidation of lignin on Pb/PbO_2 has been observed in CV curves that the oxidation potential of Pb/PbO_2 in 1 M sodium hydroxide solution was higher than that in other concentrations of NaOH. Furthermore, oxidation potential also rose when

the concentration of lignin increased from 10 to 40 g lignin/L. The high oxidation potential provides better lignin degradation efficiency and a lower degree of side reactions. For the reaction time, the over-potential increased with increasing of the reaction time, and promoted oxidation efficiency. Hydrogenation performance on Cu/Ni-Mo-Co was also investigated in Cai's group[38]. The hydrogenation ability was proportional to NaOH concentration, reaction time and reached a peak at a concentration of 50 g-lignin/L. Lignin compounds and hydrogen molecules from water were chemisorbed on the cathode electrocatalyst, and then hydrogenation occurred. At the same time, hydrogen gas was competitively formed as a side reaction, which has a negative effect on electrochemical hydrogenation efficiency.

Table 2- 4 The summary of electrochemical depolymerization of lignin-derived bio-oil and raw lignin.

Feedstock	**Anode /Cathode/ RE**	**Catalysts**	**Electrolyte**	**Conditions**	**Products**	**Ref.**
Rice husk lignin-derived oligomers	Platinum wire / platinum foil / non	-	Substrate, 0.1 M LiCl as the supporting electrolyte	Constant potential: 10 V; Time: 0-12 h	Saturated compounds and less aromatics	[39]
Hydrogenolyzed lignin-derived oil	Pt / PtRhAu-C felt / RHE reference	PtRhAu deposited on carbon felt	0.2 M $HClO_4$	Current density: 60 mA/cm^2; Time: 1-3 h; Stirring: 1000 rpm. Surface area: 1 cm^2	96% of conversion rate; Oxygenated 2-methoxy-4-propylcyclohexanol (68 % selectivity)	[34]
Kraft lignin	Nickel (plate, wire, foam, fleece) / Nickel (plate, wire, foam, fleece) /	-	1 M NaOH	Current: 2-8 A Time: 0-4 h; Temp.: RT Pressure: ambient pressure.	The molecular weight is reduced by 96% The small yield of vanillin, apocynin, and syringaldehyde	[35]

	non					
Enzymatic lignin	RuO_2–IrO_2|Ti mesh / porous graphite felt / non	RuO_2-IrO_2 as electrocatalyst doped on anode	1 M NaOH	Current density: 2-10 mA/cm^2; Temp.: 20-80 ℃ Time: 0-10 h	Aldehydes and ketones (18-23%); phenols and acids (10-48%)	[36]
Aspen lignin	Pb/PbO_2 / stainless steelwire mesh / non	-	1 M NaOH	Current density: 20–90 mA/cm^2; Temp.: 30–90 °C; Time: 0–8 h	4-methylanisole (64.9 g/kg), vanillin (31.8 g/kg), syringaldehyde (11.9 g/kg)	[37]
Sodium lignosulphonate lignin	Ti|Sb-SnO_2 / Ti|PbO_2	Sb-SnO_2 as electrocatalyst doped on anode	0.5 M Na_2SO_4	Current density: 10-60 mA/cm^2 Temp.: 25-50 ℃ Time: 1-7 h; Stirring: 200 rpm.	Low-chain carboxylic acid	[40]
DDQ polar lignin	Pt wire / RVC / non	-	PH 8 phosphate buffer / isopropanol (2 : 1, v/v), addition of 2,2'-dithiodiethanol, $LiBF_4$, and radical inhibitor (BHT)	Current density: 10 mA /cm^2; Time: 6 h; Temp.: RT	38–54 wt.% of insoluble residue; 24-36 wt.% of ethyl acetate soluble; 22-26 wt.% of aqueous soluble	[41]
Alkalin lignin	Titaniumb (Ti) foil / Pt / mercury| mercury oxide (Hg|HgO)	Nickel (Ni), cobalt (Co) and Ni-Co bimetallic	1 M NaOH	Temp.: RT; Time: 16 h; Voltage: 0.6 V vs. SHE	Vanillin (10.8-31.6 g/kg/h); 3-Methylbenzaldehyde (4.9-22.6 g/kg/h); Apocynin (2.1-4.2 g/kg/h)	[42]
Kraft	Ni / Ni /	Ni as	DES	Potential:	Guaiacol (34-37%),	[43]

Lignin	Ag|AgCl	electrocatalyst	(Choline chloride-urea; Choline chloride-ethylene glycol)	0.5 V, 1.0 V; Temp.: RT; Time: 7, 24 h	vanillin (30-38%), acetovanillone (9%) and syringaldeyhde (12%)	
Rice straw lignin	Ti|SnO_2–Sb_2O_3|α-PbO_2|β-PbO_2 / Ti-based / non	Ti/Fe, Ti/Cu and Ti/Cu/Sn as electrocatalysts	1 M NaOH	Current density: 10-60 mA/cm^2 Temp.: 25-65 ℃ Time: 1-5 h	Aromatic ketone (4.09 g/kg); aromatic aldehyde (1.53 g/kg); aromatic acid (23.92 g/kg)	[44]
Corn stover lignin	Pb|PbO_2 / Cu|Ni-Mo-Co / non	Ni-Mo-Co alloy coatings on the copper plate	1 M NaOH	Current density: 10-45 mA/cm^2; Temp.: 20-70 ℃ Time: 0-4 h	Trans-ferulic acid, vanillin, 3-hydroxy-4-methoxy phenyl-ethanone, syringaldehyde, acetosyringone and 4-methoxy-3-methyl-phenol (22.40, 11.09, 2.37, 10.04, 6.95 and 38.83 g/kg, respectively)	[38]

Note: RT means room temperature; g/kg all based on raw lignin; Temp.: temperature.

2.2 Fast pyrolysis of lignin

As a traditional process, pyrolysis has a wide range of applications in energy utilization and conversion[45][46], which is one of the conventional technologies to decompose lignin and produce valuable chemicals, especially aromatics and light hydrocarbons[47][48]. In Fast pyrolysis, when the temperature is in the range of 200 to 400 °C, C-O ether linkages (β-O-4 and α-O-4) are severed while ensues the cleavage of oxygenated compounds as by-products and keeps aliphatic groups at 300 °C. At temperatures between 550 and 650 °C, pyrolysis resulted in 40 wt.% of bio-oil and 20 wt.% of phenolic products[49]. The current challenges with lignin pyrolysis are the high yield of carbon-rich char, low conversion rate, and low selectivity of hydrocarbons like aromatics and olefins[50]. Compared with polysaccharides-containing cellulose and hemicellulose, the folded 3D structure and complicated substrates of lignin limit its further decomposition to light volatiles. The biomass type and isolation methods of lignin are the main factors influencing the pyrolysis behaviour. Alkaline lignin or Kraft lignin has been highly modified in the extraction process[51], the char yield from pyrolysis of alkaline lignin even up to half of the feeding amount, and particularly low olefins can be produced[50]. In contrast, the low molecular weight properties of organosolv lignin lead it to suffer from thermal depolymerization susceptibly[52].

Generally, catalytic pyrolysis is one of the strategies for increasing the selectivity of hydrocarbons and aromatic products. Zeolite catalysts loaded on metal particles have been proved that it can in-situ promote more hydrocarbon products and enhance the reformation of aromatics. Yang et al. performed the pyrolysis of alkaline lignin with a 3.0 wt.% Fe/ZSM-5 catalyst. The maximum carbon yield of light olefins plus aromatic compounds was 12.8 C-mol.%, in which around 3.0 C-mol.% olefins were obtained[53]. Huang et al. have investigated the production of olefins under a La-modified HZSM-5

catalyst. 5.3 wt.% of light olefins can be recovered at 600 ℃, while a trace amount of olefins can be obtained without catalysts[54]. Nevertheless, providing hydrogen atoms during pyrolysis can promote thermal decomposition better, showing efficiency and performance[55]. Avni et al. studied the effect of different gaseous environments, including 30 vol.% of H_2 in N_2[56]. Kawamoto et al. proposed that hydrogen from cellulose-derived products can stabilize internal mediate radicals and suppress the rearrangement of the methoxyl group[57]. The hydrogen transfer from tetralin to lignin inferred that the hydrocarbons and aromatics increased due to the synergistic function of hydrogen atoms and acidic zeolites[58]. Therefore, in addition to the role of the catalyst, the selectivity of the pyrolysis products can be improved by changing the structural properties of the lignin, or by using active gases to facilitate the pyrolysis reaction. These are worth further investigating.

2.3 Proposed process for utilizing lignin

Exploring lignin utilization technologies is a way to make more efficient use of biomass resources. The internal characteristics of lignin make it difficult to utilize. However, after an extensive literature survey, a novel process was proposed that using hydrogenation as a pretreatment process for lignin and combined with fast pyrolysis in this work to obtain olefins (C2-C4) and aromatics (BTXs and naphthalene). Lignin is expected to be modified through the hydrogenation reaction, including the reduction of aromatic rings and the saturation. The modified lignin was named hydrogenated lignin. Hydrogenated lignin was thought to be a candidate feedstock to get more aimed products in the fast pyrolysis process. In this study, the author tried not only traditional thermal catalytic hydrogenation (TCH) to treat lignin, but also electrochemical hydrogenation (ECH). TCH requires high-temperature and high-pressure conditions, while ECH can occur more selectively, and mild reaction conditions can avoid thermal

decomposition of lignin[59].

Hydroprocess not only includes hydrogenolysis but hydrogenation and hydrodeoxygenation, in which hydrogenation can saturate lignin macromolecule through reduction and limit the recombination of internal free radicals and formation of more stubborn coke[60][15]. There are limited research groups focusing on the solid residue from lignin hydrogenation, while most of the studies give more attention to increasing the yield of oil products[61][62]. Noble metal (Pt, Pd, Ru, & Rh) supported catalysts show a significant catalytic activity for hydrogenolysis and hydrogenation of lignin, especially on lignin model compounds[60][11][12]. Most of the hydrogenation research was conducted on model compounds of lignin such as phenol, o-cresol, guaiacol, dimer compounds, etc.[63][64][65][66]. So, the author also believes that for hydrogenation reaction can have the same effect on lignin depolymerization and reduction. Shen et al. reported that the partly degraded lignin containing abundant aliphatic C-H bonds, and thermal decomposition started to occur even in the low-temperature range (200-280 ℃)[24]. Long et al. investigated the properties of recovered lignin after catalytic decomposition with the synergic function of NaOH and Ru/C. The recovered lignin possessed a lower molecular weight and lower degree of unsaturation[17].

Besides, electrochemical conversion has been reported that it may afford better control over the conversion and require mild reaction conditions than traditional thermochemical conversion. Lan et al. have studied electrochemically catalytic conversion on cornstalk lignin, including anodic oxidation to form lignin fragments and cathodic hydrogenation on the lignin fragments[68]. Fang et al. have performed electrocatalytic reduction on both lignin β-O-4 models and lignin, while the product distribution from lignin was shown in the literature[41]. Meanwhile, Zhang et al. have investigated the effect of technological factors on the electrochemical hydrogenation of lignin[69]. They found that obtained hydrogenated lignin showed hydrogen content and

H/C ratio increased by 1.7% and 0.04, respectively. These suggest that electrochemical hydrogenation is also a potential technology for treating lignin in the current context of low carbon and emission reduction. However, the exploration of electrochemical hydrogenation on lignin is still at an early stage and its implementation in the large-scale industry requires further investigation[70].

Thus, this study aims to contribute to this growing area of research by exploring pretreatment technology for lignin to modify the structure and improve the selectivity of pyrolyzed products, as shown in Fig. 2-1.

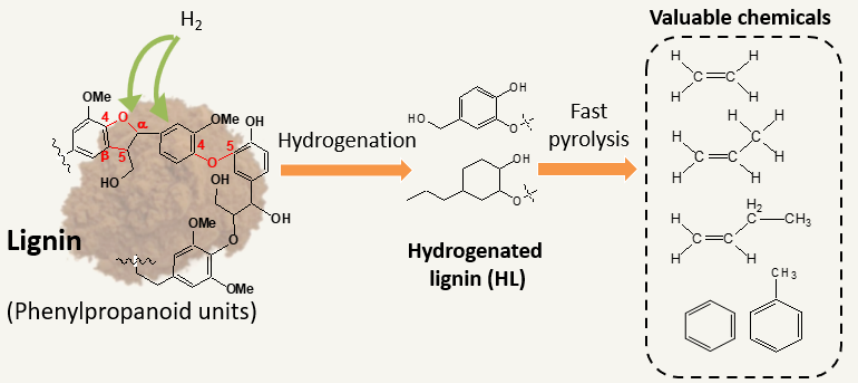

Fig. 2- 1 The rough flow sheet of the processes proposed in this work.

This work investigated the performance of ECH and traditional thermal catalytic hydrogenation (TCH) on lignin. In the past few years, TCH has been studied extensively in almost all possible directions, including supportive donors or environments, unconventional catalytic routes, and optimized conditions regarding affecting reaction parameters. In this regard, enormous progress has been registered. Most importantly, thermodynamic studies and kinetic parameter evaluation are essential to understand the reaction progress, and have been in an advanced state for TCH. However, the interest has been shifted to ECH lately, keeping from the limitations of TCH such as energy-intensive processes, high temperature, and pressure conditions. Through the review of TCH processes, we can identify the metals that readily reduce

the functional groups of organics at elevated conditions, which could also be highly active for the ECH process subjected to the suitable electrolyte. Hence, a comparison of the two technologies is clearly required to make progress on the ECH.

In addition, the hydrogenation capabilities of the two techniques on the model compounds have been compared by Song et al.[26]. In Table 2-5, the comparison of phenolic compounds and diaryl ether conversion via ECH and TCH has been shown. For the hydrogenation of aromatic hydrocarbons (saturated benzene ring), the functional group has a significant influence on the reactivity, and the conversion rate is increased as follows: diphenyl ether < benzyl phenyl ether < 4-methoxy phenol < 4-methyl phenol < phenol. When the conversion rates of the two hydrogenation procedures were compared, TCH conversion rates were consistently higher than electrochemical hydrogenation conversion rates (Table 2-5). However, it should be noted that the concentration conditions in the two technologies are not identical, so differences in hydrogen coverage as shown might be the reason. From all the model compounds listed here, the TOF under catalytic thermochemical conversion is higher than that under electrochemical conversion, probably because a thermal catalytic conversion has higher reaction efficiency and requires a shorter reaction time. It is noteworthy that the conversion of phenolic compounds was higher than that of di-aryl ether (diphenyl ether, benzyl phenyl ether). There are three reaction pathways for di-aryl ethers: hydrogenation (yielding hydrogenated ethers), hydrogenolysis, and hydrolysis (yielding monomers). Under the thermochemical conversion, hydrogenolysis and hydrolysis reactions are all more violent, leading to a decrease in the selectivity of the reaction, especially for reactants containing ether bonds.

Table 2- 5 The comparison of standard lignin model compounds conversion via electrocatalytic hydrogenation and thermal catalytic hydrogenation.

Compounds	**Phenol**	**Diphenyl**	**4-methyl**	**4-methoxy**	**Benzyl**

			ether	phenol	phenol	phenyl ether
Electrochemical hydrogenation	Conv. Rate	16	3.2	8.1	7.4	4.7
	FE	68	25	31	35	36
	TOF	296	60	151	138	88
Thermal catalytic hydrogenation	Conv. Rate	20	4.5	10	11	8.2
	TOF	374	85	191	212	155

Note: Conv. rate: conversion rate ($*10^{-5}$ $mol \cdot s^{-1} \cdot g^{-1}$); FE: faradaic efficiency (%); TOF: turnover frequency (h^{-1}); Conditions: solvent/electrolyte: isopropanol; Catalyst: Rh/C.

This work examined the hydrogenation technology on lignin, which has evident advantages and disadvantages for thermal catalytic hydrogenation (TCH) and electrochemical hydrogenation (ECH), as seen in Fig. 2-2. TCH is a non-homogeneous reaction, which requires the transfer of gaseous hydrogen into the liquid phase reactants. Moreover, heterogeneous catalysts were used, so the reaction must be carried out at moderate to high temperatures and pressure. It also has a severe impact on the reactor and operating conditions. However, unlike traditional TCH, ECH performs the chemical transfer reaction more gently based on consuming electrical energy. It can control the reaction effectively by applying current or voltage externally. Using electrocatalysts can make the reaction more efficient and selective, which does not need to consider high-temperature deactivation, but only their corrosion resistance in acidic and alkaline environments. Of course, more intensive research using organic electrolytes such as ILs and DESs has been progressing, which will make ECH greener and more environmentally friendly.

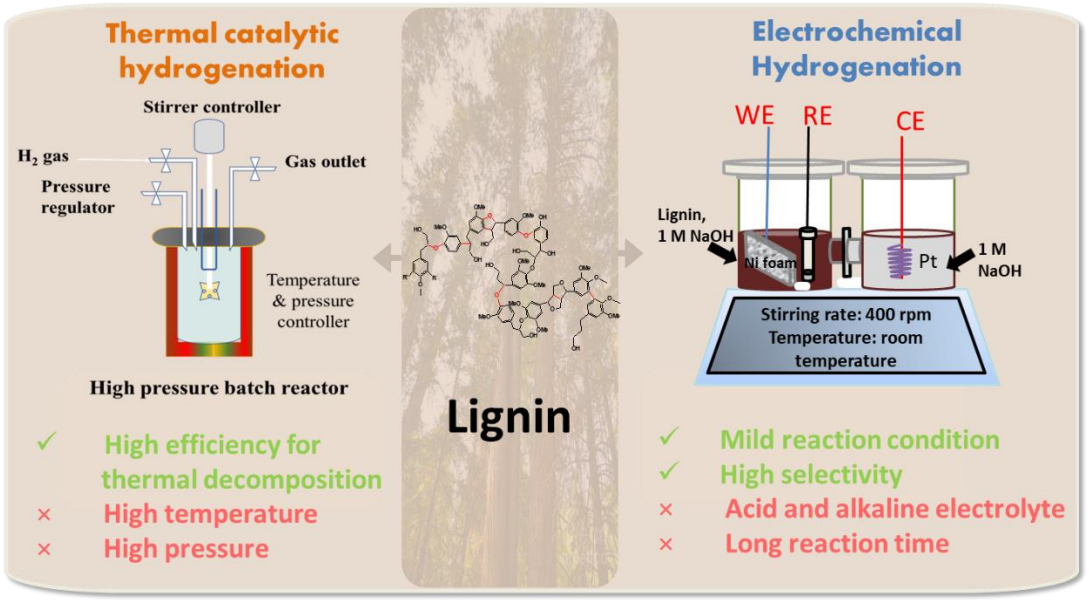

Fig. 2- 2 Hydrogenation technologies (including thermal catalytic hydrogenation and electrochemical hydrogenation) for lignin pretreatment.

2.4 Reference

[1] C. Li, X. Zhao, A. Wang, G.W. Huber, T. Zhang, Catalytic Transformation of Lignin for the Production of Chemicals and Fuels, Chem. Rev. 115 (2015) 11559–11624. https://doi.org/10.1021/acs.chemrev.5b00155.

[2] E.E. Harris, J. D'Ianni, H. Adkins, Reaction of Hardwood Lignin with Hydrogen, J. Am. Chem. Soc. 60 (1938) 1467–1470. https://doi.org/10.1021/ja01273a056.

[3] K.M. Torr, D.J. van de Pas, E. Cazeils, I.D. Suckling, Mild hydrogenolysis of in-situ and isolated Pinus radiata lignins, Bioresour. Technol. 102 (2011) 7608–7611. https://doi.org/https://doi.org/10.1016/j.biortech.2011.05.040.

[4] W. Xu, S.J. Miller, P.K. Agrawal, C.W. Jones, Depolymerization and hydrodeoxygenation of switchgrass lignin with formic acid, ChemSusChem. 5 (2012) 667–675. https://doi.org/10.1002/cssc.201100695.

[5] K. Barta, G.R. Warner, E.S. Beach, P.T. Anastas, Depolymerization of organosolv lignin to aromatic compounds over Cu-doped porous metal oxides, Green Chem. 16 (2014) 191–196. https://doi.org/10.1039/c3gc41184b.

[6] A. Jongerius, Catalytic Conversion of Lignin for the Production of Aromatics., 2013.

[7] L. Axelsson, M. Franzén, M. Ostwald, G. Berndes, G. Lakshmi, N.H. Ravindranath, Perspective: Jatropha cultivation in southern India: Assessing farmers' experiences, Biofuels, Bioprod. Biorefining. 6 (2012) 246–256. https://doi.org/10.1002/bbb.

[8] X. Zeng, R. Shao, F. Wang, P. Dong, J. Yu, G. Xu, Industrial demonstration plant for the gasification of herb residue by fluidized bed two-stage process, Bioresour. Technol. 206 (2016) 93–98. https://doi.org/10.1016/j.biortech.2016.01.075.

[9] S.C. Qi, J.I. Hayashi, S. Kudo, L. Zhang, Catalytic hydrogenolysis of kraft lignin to monomers at high yield in alkaline water, Green Chem. 19 (2017) 2636–2645. https://doi.org/10.1039/c7gc01121k.

[10] Q. Song, J. Cai, J. Zhang, W. Yu, F. Wang, J. Xu, Hydrogenation and cleavage of the C-O bonds in the lignin model compound phenethyl phenyl ether over a nickel-based catalyst, Cuihua Xuebao/Chinese J. Catal. 34 (2013) 651–658. https://doi.org/10.1016/s1872-2067(12)60535-x.

[11] A. Bjelić, M. Grilc, M. Huš, B. Likozar, Hydrogenation and hydrodeoxygenation of aromatic lignin monomers over Cu/C, Ni/C, Pd/C, Pt/C, Rh/C and Ru/C catalysts: Mechanisms, reaction micro-kinetic modelling and quantitative structure-activity relationships, Chem. Eng. J. 359 (2019) 305–320. https://doi.org/10.1016/j.cej.2018.11.107.

[12] I. Hita, P.J. Deuss, G. Bonura, F. Frusteri, H.J. Heeres, Biobased chemicals from the catalytic depolymerization of Kraft lignin using supported noble metal-based catalysts, Fuel Process. Technol. 179 (2018) 143–153. https://doi.org/10.1016/j.fuproc.2018.06.018.

[13] J.M. Pepper, Y.M. Lee, Lignin and related compounds., Can. J. Chem. 47 (1969) 723–727.

[14] J.M. Lavoie, W. Baré, M. Bilodeau, Depolymerization of steam-treated lignin for the production of green chemicals, Bioresour. Technol. 102 (2011) 4917–4920. https://doi.org/10.1016/j.biortech.2011.01.010.

[15] R. Shu, Y. Xu, P. Chen, L. Ma, Q. Zhang, L. Zhou, C. Wang, Mild Hydrogenation of Lignin Depolymerization Products over Ni/SiO2 Catalyst, Energy and Fuels. 31 (2017) 7208–7213. https://doi.org/10.1021/acs.energyfuels.7b00934.

[16] C.R. Kumar, N. Anand, A. Kloekhorst, C. Cannilla, G. Bonura, F. Frusteri, K.

Barta, H.J. Heeres, Solvent free depolymerization of Kraft lignin to alkyl-phenolics using supported NiMo and CoMo catalysts, Green Chem. 17 (2015) 4921–4930. https://doi.org/10.1039/c5gc01641j.

[17] J. Long, Y. Xu, T. Wang, Z. Yuan, R. Shu, Q. Zhang, L. Ma, Efficient base-catalyzed decomposition and in situ hydrogenolysis process for lignin depolymerization and char elimination, Appl. Energy. 141 (2015) 70–79. https://doi.org/10.1016/j.apenergy.2014.12.025.

[18] Q. Song, F. Wang, J. Xu, Hydrogenolysis of lignosulfonate into phenols over heterogeneous nickel catalysts, Chem. Commun. 48 (2012) 7019–7021. https://doi.org/10.1039/c2cc31414b.

[19] S.K. Singh, J.D. Ekhe, Towards effective lignin conversion: HZSM-5 catalyzed one-pot solvolytic depolymerization/hydrodeoxygenation of lignin into value added compounds, RSC Adv. 4 (2014) 27971–27978. https://doi.org/10.1039/c4ra02968b.

[20] Q. Song, F. Wang, J. Cai, Y. Wang, J. Zhang, W. Yu, J. Xu, Lignin depolymerization (LDP) in alcohol over nickel-based catalysts via a fragmentation-hydrogenolysis process, Energy Environ. Sci. 6 (2013) 994–1007. https://doi.org/10.1039/c2ee23741e.

[21] Y. Wang, D. Wang, X. Li, G. Li, Z. Wang, M. Li, X. Li, Investigation on the Catalytic Hydrogenolysis of Lignin over NbOx-Ni/ZnO-Al2O3, Ind. Eng. Chem. Res. 58 (2019) 7866–7875. https://doi.org/10.1021/acs.iecr.9b00376.

[22] J. Zhang, J. Teo, X. Chen, H. Asakura, T. Tanaka, K. Teramura, N. Yan, A series of NiM (M = Ru, Rh, and Pd) bimetallic catalysts for effective lignin hydrogenolysis in water, ACS Catal. 4 (2014) 1574–1583. https://doi.org/10.1021/cs401199f.

[23] S. Totong, P. Daorattanachai, A.T. Quitain, T. Kida, N. Laosiripojana, Catalytic

Depolymerization of Alkaline Lignin into Phenolic-Based Compounds over Metal-Free Carbon-Based Catalysts, Ind. Eng. Chem. Res. 58 (2019) 13041–13052. https://doi.org/10.1021/acs.iecr.9b01973.

[24] X.-J. Shen, P.-L. Huang, J.-L. Wen, R.-C. Sun, A facile method for char elimination during base-catalyzed depolymerization and hydrogenolysis of lignin, Fuel Process. Technol. 167 (2017) 491–501. https://doi.org/https://doi.org/10.1016/j.fuproc.2017.08.002.

[25] J. Long, Q. Zhang, T. Wang, X. Zhang, Y. Xu, L. Ma, An efficient and economical process for lignin depolymerization in biomass-derived solvent tetrahydrofuran, Bioresour. Technol. 154 (2014) 10–17. https://doi.org/https://doi.org/10.1016/j.biortech.2013.12.020.

[26] Y. Song, S.H. Chia, U. Sanyal, O.Y. Gutiérrez, J.A. Lercher, Integrated catalytic and electrocatalytic conversion of substituted phenols and diaryl ethers, J. Catal. 344 (2016) 263–272. https://doi.org/10.1016/j.jcat.2016.09.030.

[27] B. Zhao, Q. Guo, Y. Fu, Electrocatalytic hydrogenation of lignin-derived phenol into alkanes by using platinum supported on graphite, Electrochemistry. 82 (2014) 954–959. https://doi.org/10.5796/electrochemistry.82.954.

[28] A. Martel, B. Mahdavi, J. Lessard, H. Ménard, L. Brossard, Electrocatalytic hydrogenation of phenol on various electrode materials, Can. J. Chem. 75 (1997) 1862–1867. https://doi.org/10.1139/v97-619.

[29] M. Wakisaka, M. Kunitake, Direct electrochemical hydrogenation of toluene at Pt electrodes in a microemulsion electrolyte solution, Electrochem. Commun. 64 (2016) 5–8. https://doi.org/10.1016/j.elecom.2016.01.001.

[30] N. Itoh, W.C. Xu, S. Hara, K. Sakaki, Electrochemical coupling of benzene hydrogenation and water electrolysis, Catal. Today. 56 (2000) 307–314. https://doi.org/10.1016/S0920-5861(99)00288-6.

[31] Z. Li, M. Garedew, C.H. Lam, J.E. Jackson, D.J. Miller, C.M. Saffron, Mild electrocatalytic hydrogenation and hydrodeoxygenation of bio-oil derived phenolic compounds using ruthenium supported on activated carbon cloth, Green Chem. 14 (2012) 2540–2549. https://doi.org/10.1039/c2gc35552c.

[32] B.K. Peters, K.X. Rodriguez, S.H. Reisberg, S.B. Beil, D.P. Hickey, Y. Kawamata, M. Collins, J. Starr, L. Chen, S. Udyavara, K. Klunder, T.J. Gorey, S.L. Anderson, M. Neurock, S.D. Minteer, P.S. Baran, Scalable and safe synthetic organic electroreduction inspired by Li-ion battery chemistry, Science (80-.). 363 (2019) 838–845. https://doi.org/10.1126/science.aav5606.

[33] Y. Song, O.Y. Gutiérrez, J. Herranz, J.A. Lercher, Aqueous phase electrocatalysis and thermal catalysis for the hydrogenation of phenol at mild conditions, Appl. Catal. B Environ. 182 (2016) 236–246. https://doi.org/https://doi.org/10.1016/j.apcatb.2015.09.027.

[34] G. Dick, J. Wicks, M. Wang, X. Wang, Selective electrocatalytic hydrogenation of bio-oil to oxygenated chemicals via suppression of deoxygenation, (n.d.) 1–22.

[35] S. Stiefel, A. Schmitz, J. Peters, D. Di Marino, M. Wessling, An integrated electrochemical process to convert lignin to value-added products under mild conditions, Green Chem. 18 (2016) 4999–5007. https://doi.org/10.1039/c6gc00878j.

[36] H. Zhu, L. Wang, Y. Chen, G. Li, H. Li, Y. Tang, P. Wan, Electrochemical depolymerization of lignin into renewable aromatic compounds in a non-diaphragm electrolytic cell, RSC Adv. 4 (2014) 29917–29924. https://doi.org/10.1039/c4ra03793f.

[37] Y. sheng Wang, F. Yang, Z. hua Liu, L. Yuan, G. Li, Electrocatalytic degradation of aspen lignin over Pb/PbO2 electrode in alkali solution, Catal. Commun. 67 (2015) 49–53. https://doi.org/10.1016/j.catcom.2015.03.033.

[38] P. Cai, H. Fan, S. Cao, J. Qi, S. Zhang, G. Li, Electrochemical conversion of corn stover lignin to biomass-based chemicals between Cu/Ni–Mo–Co cathode and Pb/PbO2 anode in alkali solution, Electrochim. Acta. 264 (2018) 128–139. https://doi.org/10.1016/j.electacta.2018.01.111.

[39] W. Deng, K. Xu, Z. Xiong, W. Chaiwat, X. Wang, S. Su, S. Hu, J. Qiu, Y. Wang, J. Xiang, Evolution of Aromatic Structures during the Low-Temperature Electrochemical Upgrading of Bio-oil, Energy and Fuels. 33 (2019) 11292–11301. https://doi.org/10.1021/acs.energyfuels.9b03099.

[40] T.S.A. Sno, T. Pbo, D. Shao, J. Liang, X. Cui, H. Xu, W. Yan, Electrochemical oxidation of lignin by two typical electrodes :, 244 (2014) 288–295.

[41] Z. Fang, M.G. Flynn, J.E. Jackson, E.L. Hegg, Thio-assisted reductive electrolytic cleavage of lignin β-O-4 models and authentic lignin, Green Chem. 23 (2021) 412–421. https://doi.org/10.1039/d0gc03597a.

[42] R. Ghahremani, J.A. Staser, Electrochemical oxidation of lignin for the production of value-Added chemicals on Ni-Co bimetallic electrocatalysts, Holzforschung. 72 (2018) 951–960. https://doi.org/10.1515/hf-2018-0041.

[43] D. Di Marino, D. Stöckmann, S. Kriescher, S. Stiefel, M. Wessling, Electrochemical depolymerisation of lignin in a deep eutectic solvent, Green Chem. 18 (2016) 6021–6028. https://doi.org/10.1039/c6gc01353h.

[44] Y. Jia, Y. Wen, X. Han, J. Qi, Z. Liu, S. Zhang, G. Li, Electrocatalytic degradation of rice straw lignin in alkaline solution through oxidation on a Ti/SnO2-Sb2O3/α-PbO2/β-PbO2 anode and reduction on an iron or tin doped titanium cathode, Catal. Sci. Technol. 8 (2018) 4665–4677. https://doi.org/10.1039/c8cy00307f.

[45] C. Zhang, R. Wu, E. Hu, S. Liu, G. Xu, Coal pyrolysis for high-quality tar and gas in 100 kg fixed bed enhanced with internals, Energy and Fuels. 28 (2014)

7294–7302. https://doi.org/10.1021/ef501923f.

[46] X. Zeng, Y. Wang, J. Yu, S. Wu, J. Han, S. Xu, G. Xu, Gas upgrading in a downdraft fixed-bed reactor downstream of a fluidized-bed coal pyrolyzer, Energy and Fuels. 25 (2011) 5242–5249. https://doi.org/10.1021/ef2012276.

[47] Damayanti, H.S. Wu, Pyrolysis kinetic of alkaline and dealkaline lignin using catalyst, J. Polym. Res. 25 (2018). https://doi.org/10.1007/s10965-017-1401-6.

[48] P.R. Patwardhan, R.C. Brown, B.H. Shanks, Understanding the fast pyrolysis of lignin, ChemSusChem. 4 (2011) 1629–1636. https://doi.org/10.1002/cssc.201100133.

[49] J. Rajesh Banu, S. Kavitha, R. Yukesh Kannah, T. Poornima Devi, M. Gunasekaran, S.-H. Kim, G. Kumar, A review on biopolymer production via lignin valorization, Bioresour. Technol. 290 (2019) 121790. https://doi.org/https://doi.org/10.1016/j.biortech.2019.121790.

[50] H. Yang, K. Norinaga, J. Li, W. Zhu, H. Wang, Effects of HZSM-5 on volatile products obtained from the fast pyrolysis of lignin and model compounds, Fuel Process. Technol. 181 (2018) 207–214. https://doi.org/10.1016/j.fuproc.2018.09.022.

[51] H. Lange, S. Decina, C. Crestini, Oxidative upgrade of lignin - Recent routes reviewed, Eur. Polym. J. 49 (2013) 1151–1173. https://doi.org/10.1016/j.eurpolymj.2013.03.002.

[52] H. Yang, K. Norinaga, J. Li, W. Zhu, H. Wang, Effects of HZSM-5 on volatile products obtained from the fast pyrolysis of lignin and model compounds, Fuel Process. Technol. 181 (2018) 207–214. https://doi.org/10.1016/j.fuproc.2018.09.022.

[53] M. Yang, J. Shao, Z. Yang, H. Yang, X. Wang, Z. Wu, H. Chen, Conversion of lignin into light olefins and aromatics over Fe/ZSM-5 catalytic fast pyrolysis:

Significance of Fe contents and temperature, J. Anal. Appl. Pyrolysis. 137 (2019) 259–265. https://doi.org/10.1016/j.jaap.2018.12.003.

[54] W. Huang, F. Gong, M. Fan, Q. Zhai, C. Hong, Q. Li, Production of light olefins by catalytic conversion of lignocellulosic biomass with HZSM-5 zeolite impregnated with 6wt.% lanthanum, Bioresour. Technol. 121 (2012) 248–255. https://doi.org/10.1016/j.biortech.2012.05.141.

[55] W.C. Xu, A. Tomita, Effective Utilization of Coal via Flash Pyrolysis, Isij Int. 30 (1990) 687–698. https://doi.org/10.2355/isijinternational.30.687.

[56] E. Avni, F. Davoudzadeh, R.W. Coughlin, Flash Pyrolysis of Lignin, in: R.P. Overend, T.A. Milne, L.K. Mudge (Eds.), Fundam. Thermochem. Biomass Convers., Springer Netherlands, Dordrecht, 1985: pp. 329–343. https://doi.org/10.1007/978-94-009-4932-4_18.

[57] H. Kawamoto, Lignin pyrolysis reactions, J. Wood Sci. 63 (2017) 117–132. https://doi.org/10.1007/s10086-016-1606-z.

[58] Y. Xue, S. Zhou, X. Bai, Role of Hydrogen Transfer during Catalytic Copyrolysis of Lignin and Tetralin over HZSM-5 and HY Zeolite Catalysts, ACS Sustain. Chem. Eng. 4 (2016) 4237–4250. https://doi.org/10.1021/acssuschemeng.6b00733.

[59] L. Zhang, T.U. Rao, J. Wang, D. Ren, S. Sirisommboonchai, C. Choi, H. Machida, Z. Huo, K. Norinaga, A review of thermal catalytic and electrochemical hydrogenation approaches for converting biomass-derived compounds to high-value chemicals and fuels, Fuel Process. Technol. 226 (2022) 107097. https://doi.org/https://doi.org/10.1016/j.fuproc.2021.107097.

[60] S. Kasakov, H. Shi, D.M. Camaioni, C. Zhao, E. Baráth, A. Jentys, J.A. Lercher, Reductive deconstruction of organosolv lignin catalyzed by zeolite supported nickel nanoparticles, Green Chem. 17 (2015) 5079–5090.

https://doi.org/10.1039/c5gc02160j.

[61] V.M. Roberts, V. Stein, T. Reiner, L. Angeliki, X. Li, J.A. Lercher, Towards Quantitative Catalytic Lignin Depolymerization, Chem. – A Eur. J. 17 (2011) 5939–5948. https://doi.org/10.1002/chem.201002438.

[62] T.D. Matson, K. Barta, A. V. Iretskii, P.C. Ford, One-pot catalytic conversion of cellulose and of woody biomass solids to liquid fuels, J. Am. Chem. Soc. 133 (2011) 14090–14097. https://doi.org/10.1021/ja205436c.

[63] S.C. Qi, L. Zhang, H. Einaga, S. Kudo, K. Norinaga, J. ichiro Hayashi, Nano-sized nickel catalyst for deep hydrogenation of lignin monomers and first-principles insight into the catalyst preparation, J. Mater. Chem. A. 5 (2017) 3948–3965. https://doi.org/10.1039/c6ta08538e.

[64] H. Shafaghat, P.S. Rezaei, W.M.A.W. Daud, Using decalin and tetralin as hydrogen source for transfer hydrogenation of renewable lignin-derived phenolics over activated carbon supported Pd and Pt catalysts, J. Taiwan Inst. Chem. Eng. 65 (2016) 91–100. https://doi.org/10.1016/j.jtice.2016.05.032.

[65] Q. Song, J. Cai, J. Zhang, W. Yu, F. Wang, J. Xu, Hydrogenation and cleavage of the C-O bonds in the lignin model compound phenethyl phenyl ether over a nickel-based catalyst, Cuihua Xuebao/Chinese J. Catal. 34 (2013) 651–658. https://doi.org/10.1016/s1872-2067(12)60535-x.

[66] X. Cui, A.E. Surkus, K. Junge, C. Topf, J. Radnik, C. Kreyenschulte, M. Beller, Highly selective hydrogenation of arenes using nanostructured ruthenium catalysts modified with a carbon-nitrogen matrix, Nat. Commun. 7 (2016). https://doi.org/10.1038/ncomms11326.

[67] P. Zuman, E.B. Rupp, Electrochemical investigations of alkaline cleavage of lignin under mild conditions, Collect. Czechoslov. Chem. Commun. 66 (2001) 1125–1139. https://doi.org/10.1135/cccc20011125.

[68] C. Lan, H. Fan, Y. Shang, D. Shen, G. Li, Electrochemically catalyzed conversion of cornstalk lignin to aromatic compounds: An integrated process of anodic oxidation of a Pb/PbO2 electrode and hydrogenation of a nickel cathode in sodium hydroxide solution, Sustain. Energy Fuels. 4 (2020) 1828–1836. https://doi.org/10.1039/c9se00942f.

[69] J. Zhang, X. Zhang, D. Xie, D. Liu, Z. Li, Effect of technological factors on electrochemical hydrogenation of lignin, Can. J. Chem. Eng. 80 (2002) 1–5. https://doi.org/10.1002/cjce.5450800402.

[70] M. Garedew, C.H. Lam, L. Petitjean, S. Huang, B. Song, F. Lin, J.E. Jackson, C.M. Saffron, P.T. Anastas, Electrochemical upgrading of depolymerized lignin: a review of model compound studies, Green Chem. 23 (2021) 2868–2899. https://doi.org/10.1039/d0gc04127k.

[71] D. Liang, C. Liu, S. Deng, Y. Zhu, C. Lv, Aqueous phase hydrogenolysis of glucose to 1,2-propanediol over copper catalysts supported by sulfated spherical carbon, Catal. Commun. 54 (2014) 108–113. https://doi.org/https://doi.org/10.1016/j.catcom.2014.05.027.

[72] Y. Kwon, M.T.M. Koper, Electrocatalytic hydrogenation and deoxygenation of glucose on solid metal electrodes, ChemSusChem. 6 (2013) 455–462. https://doi.org/10.1002/cssc.201200722.

Chapter 3 Thermal catalytic hydrogenation of alkaline lignin coupled with fast pyrolysis

3.1 Abstract

The current state of lignin has been characterized by these three: (1) as one of the main components in lignocellulosic biomass with an abundant amount; (2) not be taken seriously but treated as a waste product; (3) underutilized due to a complex and stubborn structure. However, lignin can be a rich source for hydrocarbons and aromatic compounds when given appropriate utilization. In this work, the hydrotreatment of alkaline lignin (AL) under relatively mild conditions was addressed as well as further investigated the characterization of hydrogenated alkaline lignin (HAL), particularly the behaviour during fast pyrolysis. The recovery of the HAL decreased with increasing reaction temperature from 60 wt.% to 41 wt.% in the range of 150-250 ℃. The hydrotreated products were analyzed using Elemental Analysis, FTIR (for HAL), and GC-MS (for bio-oil). The HAL samples were found to have a higher hydrogen/carbon atomic effective ratio (H/C_{eff} ratio) than AL. Compared to the internal structure of the lignin before and after hydrotreatment, the side chain groups were removed from AL during the process. After that, from the fast pyrolysis of HAL samples, it was observed that more light hydrocarbons and aromatic compounds were formed than that of AL. Furthermore, fast pyrolysis in the hydrogen atmosphere revealed that more volatile fractions released compared to the helium atmosphere. The total olefins yield for HAL compared to AL increased from 1.02 wt.% to 3.1 wt.% at 250 ℃ for 7 hours. This study of HAL is instructive to some extent for the industrial utilization of lignin.

3.2 Introduction

Lignocellulosic biomass is an abundant renewable resource with a good application prospect, in which lignin typically accounts for 15-30 wt.%[1]. Compared with cellulose and hemicellulose, lignin has often been given insufficient attention, generally been disposed of as a residue in the paper industry. Three monolignols (p-coumaryl alcohol, coniferyl alcohol, and sinapyl alcohol) are cross-linked to form lignin's polymer structure[2]. Alkaline lignin, as a residue, was isolated from cellulose and hemicellulose in an intense alkali process[3]. Generally, the primary utilization of this alkaline lignin is combustion or process heat. However, this is a waste of the abundant aromatic resources in the lignin. The high-value usage of lignin is worth exploring.

Catalytic hydrotreatment includes hydrogenolysis, hydrogenation, and hydrodeoxygenation reaction, which is an effective way to deal with lignin. Most scholars have focused on this technology to liquefy lignin for a high liquefaction rate. Therefore, relatively harsh conditions were used. For instance, the treating temperatures generally ranged between 350 and 450 °C[4]. Moreover, the highest initial hydrogen pressure at room temperature was 100 bar[5][6]. More bio-oil phase, especially monomer compounds, is the main target products of hydrotreatment, while the residue solid was treated as a waste. From the reported principle, the reaction process would impact the solid lignin on chemical structure. This part of residue lignin has a lower molecular weight and a high decomposition rate at a relatively high temperature in thermogravimetric analysis (TGA)[7].

Choosing an appropriate solvent for lignin pretreatment is crucial for effective hydrotreatment of lignin. In this regard, alcohols (i.e., methanol[8] and ethanol) are considered as typical solvents for the hydrotreatment process, as they can enhance the alcoholysis of lignin and incorporate with the samples through alkylation[9]. Moreover, alkali water was used to isolate the lignin from biomass, so-called alkaline lignin, in the

pulping process. Thus, alkali solution was considered a suitable solvent for hydrogenolysis of lignin in other's work[3][10], which can not only dissolve lignin units but suppress the repolymerization during the process[11]. Hydrogen donor solvents like formic acid and tetralin were also used as pretreating solvents of lignin[12][13] and were considered a novel liquid hydrogen source to replace gaseous hydrogen effectively. Therefore, considering the solubility and economy, the alkali water was used as a reaction medium to disperse lignin molecules fully.

As a traditional process, pyrolysis has a wide range of applications in energy utilization and conversion[14][15], which is one of the leading technologies to decompose lignin and produce valuable chemicals, like aromatics and light hydrocarbons[16][17]. The current challenges with lignin pyrolysis are the high yield of carbon-rich char, low conversion rate, and low selectivity of hydrocarbons like aromatics and olefins[18]. Compared with polysaccharides-containing cellulose and hemicellulose, the folded 3D structure and complicated substrates of lignin units limit its further decomposition into light volatiles. The biomass type and isolation methods of lignin are the main factors influencing the pyrolysis behaviour, while alkaline lignin or kraft lignin has been highly modified[19]. The char yield from pyrolysis of alkaline lignin even up to half of the feeding amount, and particularly low olefins can be produced[18].

Catalytic pyrolysis is another strategy for increasing the selectivity of hydrocarbons and aromatic products. Zeolite catalysts loaded on metal particles have been proved that it can in-situ promote more hydrocarbon products and enhance the reformation of aromatics. Yang et al. performed the pyrolysis of alkaline lignin with a 3.0 wt.% of Fe/ZSM-5 catalyst. The maximum carbon yield of light olefins plus aromatic compounds was 12.8 C-mol.%, in which around 3.0 C-mol.% olefins were obtained[20]. Huang et al. have investigated the production of olefins under a La-modified HZSM-5 catalyst. 5.3 wt.% of light olefins can be recovered at 600 ℃, while a trace amount of

olefins can be obtained without catalysts[21]. Nevertheless, providing hydrogen atoms during pyrolysis can promote thermal decomposition better, showing efficiency and performance[22]. Avni et al. studied the effect of different gaseous environments, including 30 vol.% of H_2 in N_2[23]. Kawamoto et al. proposed that hydrogen from cellulose-derived products can stabilize internal mediate radicals and suppress the rearrangement of the methoxyl group[24]. The hydrogen transfer from tetralin to lignin inferred that the hydrocarbons and aromatics increased due to the synergistic function of hydrogen atoms and acidic zeolites[25].

Typical research for hydrotreatment of lignin was put on increasing the liquefaction rate and avoiding coke formation[12][26]. However, the solid residue after hydrotreatment has not been paid much attention. The appropriate pretreatment will be a benefit for the modification of lignin. Hence, in this work, hydrotreatment was considered to hydrogenate the solid lignin, and relatively mild conditions were investigated. Modification of the lignin structure by hydrotreatment under mild conditions was investigated. The pyrolytic properties of lignin before and after hydrotreatment were mainly studied. This paper aims to provide a novel direction for lignin utilization.

3.3 Method and materials

3.3.1 Materials

The alkaline lignin (AL, CAS RN: 8061-51-6), used as the feedstock without pretreatment in this research, was purchased from Tokyo Chemical Industry CO. LTD. Sodium hydroxide (particle, 198-13765), Raney Nickel (181-00025), hydrochloric acid (35-37 wt.%, CAS RN: 7647-01-0), and ethyl acetate (99.5%) were purchased from FUJIFILM Wako Pure Chemical Corporation and were used for the hydrogenation and

sequential separation process. Ruthenium on activated carbon (Ru/C, 5 wt.% Ru loading, 908045-10G) and Rhodium on matrix carbon (Rh/C, 5 wt.% Rh loading, 680710-5G) were purchased from Sigma-Aldrich (Japan), which were pre-dried in the vacuum oven at 60 ℃ for overnight prior to use.

3.3.2 Hydrogenation and separation process

The whole procedure is shown in Fig. 3-1. Lignin sample (200 mg), Raney nickel (200 mg), and sodium hydroxide solution (20 mL, pH=11) were mixed and charged into a 100 mL-scale stainless reactor (Parr 4590 Micro Bench Top Reactor). After being purged with H_2 three times, the reactor was pressurized up to the target pressure at ambient temperature. The mixture was mechanically stirred at 400 rpm for several hours at elevated temperature, and then cooled down to room temperature.

After the reaction, Raney nickel was firstly separated from the mixture by vacuum filtration, and the retained filtrate was acidified to pH=1 with HCl solution for precipitating the solid residue. The solid residue was then dried at 60 ℃ in a vacuum oven overnight, called hydrogenated alkaline lignin (HAL). Liquid-liquid extraction was performed using ethyl acetate to separate the bio-oil phase and water-soluble phase of the filtrate. After that, a rotary evaporator was used to remove ethyl acetate from liquid products. The procedure was performed with care to minimize the error and repeated each experiment at least two times.

The depolymerized lignin was recovered and dried for further characterization. The rest fraction corresponded to the complement of 100 wt.% of the initial lignin was coke, bio-oil phase, and traced gaseous product. The weight of coke was calculated by the difference in the catalyst mixture before and after the reaction. The GC-TCD/FID results showed that the total weight of these gaseous compounds was less than 1 % of the feedstock (AL). Therefore, the gaseous products were ignored here. Then GS-MS

was used to quantify the products in the bio-oil phase. The yield of products was calculated by the following Eq. (3-1)-(3-4).

$$C_A\ (wt.\%) = (W_A\text{-}W_H)/W_A*100\% \quad (3\text{-}1)$$

$$Y_H\ (wt.\%) = W_H/W_A*100\% \quad (3\text{-}2)$$

$$Y_C\ (wt.\%) = W_C/W_A*100\% \quad (3\text{-}3)$$

$$Y_L\ (wt.\%) = (W_A\text{-}W_H\text{-}W_C)/W_A*100\% \quad (3\text{-}4)$$

C_A: the conversion of lignin; Y_H: the yield of HAL; Y_C: the yield of coke; Y_L: the liquefaction rate; W_A: the weight of AL; WH: the weight of HAL; W_C: the weight of coke, calculated by the difference between the catalyst mixture after reaction and catalyst input.

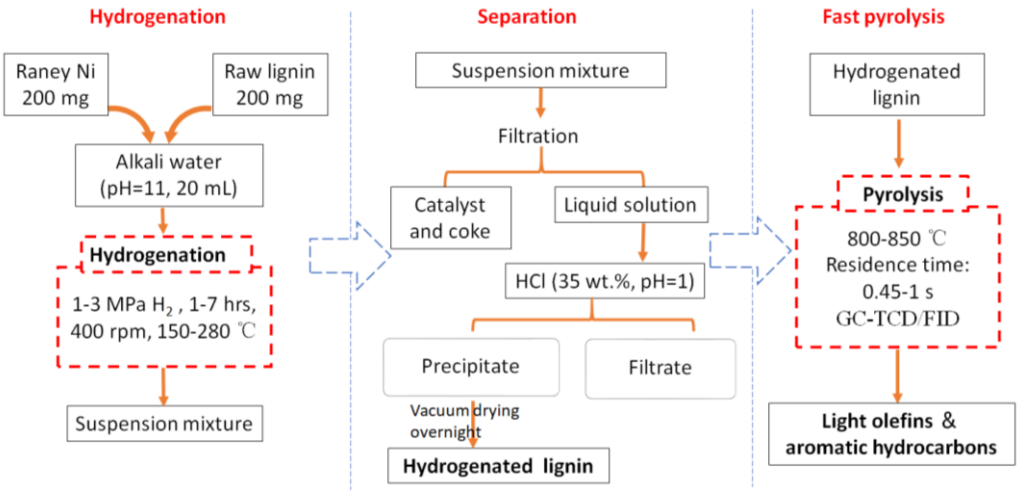

Fig. 3- 1 Two-stage process for lignin conversion to produce olefins and aromatic hydrocarbons.

3.3.3 Characterization

Fourier transform infrared spectrometer (FTIR) was used for investigating the internal functional groups of solid samples, employing the Bruker ALPHA II. A solution

of 1 wt.% lignin in 50 mg of KBr was prepared. The samples were recorded between 400 and 4000 cm^{-1} at a resolution of 4 cm^{-1} in the absorbance mode.

The weight ratio of elements such as carbon, nitrogen, and hydrogen contained in organic compounds was quantified by an elemental analyzer (2400II CHNS/O type manufactured by Perkin Elmer Co., Ltd). The analyzing process was conducted by the column separation method (frontal chromatography) and tested by a TCD. With helium as a carrier gas, around 2 mg of samples were detected each time.

Catalysts' characterization: The crystalline structures of catalysts were detected by X-ray diffraction (XRD) patterns of a Bruker AXS-D8 X-ray diffractometer for the crystalline structures. A target of Cu Kα radiation was equipped in 2θ range of 10-90° with 0.02°/step. The nitrogen adsorption/desorption was carried out on the BELSORP-Minix analyzer to determine the specific surface area of the catalysts. The samples were degassed ahead at 623 K for 3 h in a vacuum to remove surface adsorbed species and moisture on the catalysts. The specific surface area was determined by the adsorption isotherm of nitrogen in the relative pressure range of $0.05 < P/P0 < 0.3$, where p is the partial pressure of nitrogen, and p0 is the saturation pressure at the experimental temperature. The specific surface and pore structure characteristics of the catalyst were calculated by the Brunauer−Emmett−Teller (BET) formula and the Barrett−Joyner−Halenda (BJH) formula, respectively.

3.4 Results and discussion

3.4.1 Hydrogenation condition and products yield

Hydrogenation was performed at different reaction parameters (temperature, reaction time, hydrogen pressure, and metal catalysts), and the results are shown in Fig. 3-2, respectively.

Fig. 3-2(a) shows the influence of hydrogenation temperature on product distribution. When the reaction temperature is below 200 ℃, the yield of products has no apparent change. Around 57 wt.% of hydrogenated lignin can be recovered as solid, and about 11 wt.% of coke formed after the reaction at 150 ℃. With the increase in temperature (over 200 ℃), the conversion rate increased sharply and reached 75 wt.% at 280 ℃. And approximately 24 wt.% of HAL can be precipitated after hydrotreatment at 280 ℃. Moreover, the coke formation has reached 17.9 wt.% at 280 ℃. The severe conditions promoted hydrogenolysis of lignin, and the internal linkages of the lignin structure were cleaved under a high-temperature range. Meanwhile, the repolymerization of lignin units happened competitively at high temperatures on the surface of catalysts to surge in the coke formation. Fig. 3-2(b) shows the product distribution from hydrotreatment at different times. The reaction time did not affect the product yield as much as the reaction temperature did. The conversion rate increased from 41 wt.% to 55 wt.% when reaction time increased from 1 to 7 hours. The longer reaction times are not preferable for hydrogenation, allowing the repolymerization of lignin units on the catalyst surface at the constant reaction temperature. It surmises that a long-time fosters coke formation and slightly encourages the occurrence of hydrogenolysis.

The hydrogenation pressure and catalysts have an impact on the hydrogenated products, as demonstrated in Figures 3-2 (c) and (d). The high hydrogenation pressure ensured sufficient hydrogen transfer to the lignin units, resulting in increased hydrogenated lignin yield from 57.2 wt.% to 68.3 wt.%, and slightly decreased bio-oil yield from 32 wt.% to 26 wt.%. It might be because only some of the branched lignin chains were cleaved at milder temperatures (200 ℃), and the intermediate compounds were reduced under high pressures to form the solid products (HAL). Moreover, the coke formation was decreased in the range of 2-3 MPa. It proves that for the liquefaction of lignin, the temperature has a more significant influence than H_2 pressure.

Furthermore, the temperature is the critical factor for cracking lignin's structure. So, a low-pressure atmosphere (0.9 MPa) would be more suitable for the mild hydrogenation reaction. The three different catalysts (Raney Ni, Ru/C, Rh/C) were checked for the catalytic activity of hydrogenation, shown in Fig. 3-2(d). Noble metal catalysts can further advance the depolymerization of lignin structure, especially Ru/C attributing to the large surface area of Ru/C and Rh/C shown in Table 3-3 (840 m^2/g and 934 m^2/g according to BET results, respectively)[27]. The active sites on the catalyst surface were responsible for the hydrogenation of lignin monomers[28], while high liquefaction results in low HAL yield. Raney Ni has almost no pore structure with 0.67 m^2/g of surface area, and the hydrogenation reaction happened on the surface of the catalysts. More solid hydrogenated lignin has recovered and less coke formed on the Raney Ni surface while liquefaction was progressed on Rh/C and Ru/C surfaces. Considering the HAL yield, the synergistic of Raney Ni and alkali water is appropriate for pretreating lignin's structure, restraining the hydrogenolysis process.

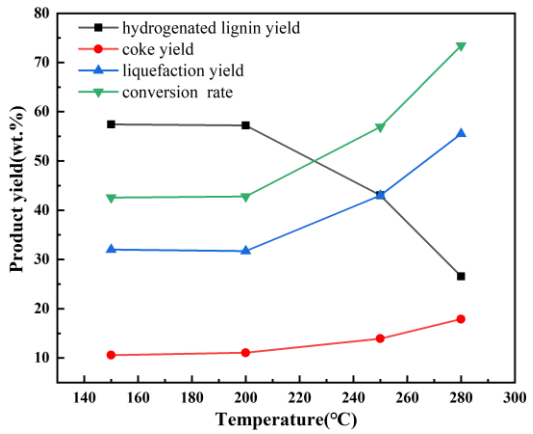

(a)

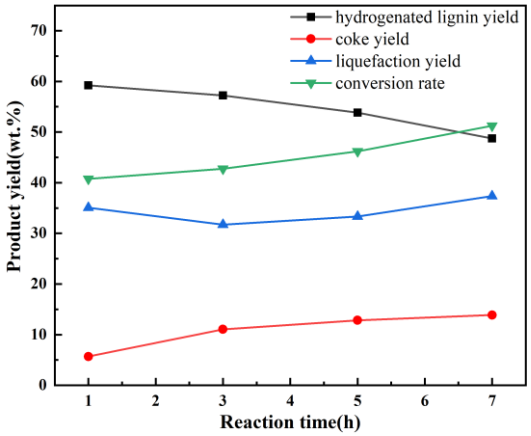

(b)

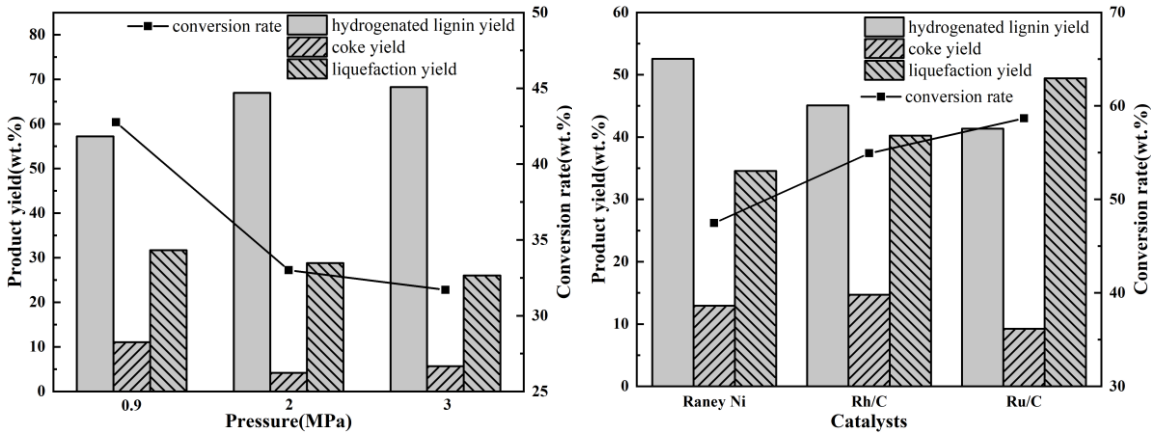

(c) (d)

Fig. 3- 2 The product distribution of hydrotreatment with (a) different temperatures and (b) Reaction time; (c) Pressure; (d) Catalysts. The conditions: (a) Catalyst: Raney Ni; time: 3 hours; pressure: 0.9 MPa H_2. (b) Catalyst: Raney Ni; temperature: 200 ℃; pressure: 0.9 MPa H_2. (c) The product distribution of the hydrotreatment process under different pressure catalyst, the conditions: Raney Ni; reaction time: 3 hours; temperature: 200 ℃. (d) The product distribution of the hydrotreatment process with different metal catalysts. The conditions: temperature: 200 ℃; pressure: 0.9 MPa; reaction time: 7 hours.

3.4.2 Characterization of hydrogenated lignin

The characterisation of HAL samples was done and compared using Elemental analysis and FTIR to determine the structural change of the lignin samples. Table 3-1 shows the elemental composition of AL and HAL samples. Compared with AL, the increase in carbon and hydrogen concentration in HAL is noticeable, especially under high-temperature conditions. The longer time had no significant effect on changing the elemental composition, following the product distribution results. The percentage of oxygen in AL accounts for around 38%, consisting of hydroxyl groups and C-O ether linkages[29]. After hydrotreatment, the oxygen content decreased noticeably due to the

cleavage of the internal bonds and the hydrolysis of hydroxyl groups. Hydrodeoxygenation, one of the main reactions, happened in this process[30]. The nitrogen and sulfur contents are relatively low but still show a clear tendency of reduction.

The Molecular formula of each sample was also calculated, shown in Table 3-1. The H/C_{eff} ratio is an index introduced by Vispute et al.[31], and has been proved to be linearly proportional to the yield of aromatics and olefins due to the intrinsic amount of hydrogen. Here, the H/C_{eff} ratio of AL was 0.003 due to high oxygen yield, while after hydrotreatment, the H/C_{eff} ratio of HAL samples was severely increased to the range of 0.33-0.40. It infers that hydrogenation effectively increases the H/C_{eff} ratio, while the conditions here show a minimal effect. The lowest and highest H/C_{eff} ratio went to HAL-150 and HAL-7, respectively. The degree of unsaturation (Ω) was calculated and listed in Table 2. The unsaturation degree of all HAL samples is higher than that of AL, with a maximum value of 3.89 for HAL-280. The temperature has a significant effect on the degree of unsaturation of the products.

Table 3- 1 The elemental composition of AL and HAL samples.

Samples	**Elemental content (wt.%)[a]**					**Molecular formula**	**H/C_{eff} ratio**	**Ω[d]**
	C	H	N	S	O[b]			
AL	54.67	4.76	0.30	2.43	37.84	$C_6H_{6.26}O_{3.12}N_{0.03}S_{0.1}$	0.003	3.15
HAL-150	63.52	5.33	0.31	2.24	28.60	$C_6H_{6.05}O_{2.03}N_{0.02}S_{0.08}$	0.33	3.60
HAL-200	63.43	5.61	0.26	1.71	28.99	$C_6H_{6.36}O_{2.04}N_{0.02}S_{0.06}$	0.38	3.47
HAL-250	65.81	5.39	0.27	1.24	27.29	$C_6H_{5.9}O_{1.87}N_{0.02}S_{0.04}$	0.36	3.78

HAL-280	66.43	5.29	0.27	0.87	27.14	$C_6H_{5.73}O_{1.84}N_{0.02}S_{0.03}$	0.34	3.89
HAL-1	63.85	5.48	0.26	1.99	28.48	$C_6H_{6.18}O_{2.02}N_{0.02}S_{0.08}$	0.36	3.56
HAL-3	63.43	5.61	0.26	1.71	28.99	$C_6H_{6.36}O_{2.04}N_{0.02}S_{0.06}$	0.38	3.47
HAL-5	63.91	5.49	0.30	1.59	28.71	$C_6H_{6.19}O_{2.02}N_{0.02}S_{0.06}$	0.36	3.57
HAL-7	64.87	5.64	0.28	1.59	27.62	$C_6H_{6.26}O_{1.92}N_{0.02}S_{0.06}$	0.40	3.57

[a] Dry basis

[b] Oxygen was calculated by the difference: $O=100-(C+H+N+S)$

[c] Hydrogen to carbon effective ratio[31]: $H/C_{eff}=(H_{mole}-2*O_{mole})/C_{mole}$

[d] Degree of unsaturation calculated by: $\Omega=1/2*(2C_{mole}+2+N_{mole}-S_{mole}-H_{mole})$

Note: HAL-150: temperature: 150 ℃; HAL-200: temperature: 200 ℃; HAL-250: temperature: 250 ℃; HAL-280: temperature: 280 ℃; other conditions: catalyst: Raney Ni; time: 3 hours; pressure: 0.9 MPa. HAL-1: reaction time: 1 hour; HAL-3: reaction time: 3 hours; HAL-5: reaction time: 5 hours; HAL-7: reaction time: 7 hours; other conditions: temperature: 200 ℃; catalyst: Raney Ni; pressure: 3 MPa.

3.4.3 Characterizations of oil-phase products

The influence of reaction time on the evolution of specific oil products is shown in Table 3-2. The following organic products were detected and quantified in terms of the NIST Standard Reference Database of GC-MS. The chromatograph of bio-oil samples is also shown in Fig. 3-3. In bio-oil 1, guaiacol and vanillin were the main products with the highest concentration, which agrees with the literature[32]. At such a low temperature and short reaction time (200 ℃, 1 hour), the product variety and yield in the oil phase are relatively low. However, increasing the reaction time led to the formation of guaiacol derivatives after 3-hour hydrotreatment. A higher concentration of almost all products can be detected with increasing reaction time until 7 hours. Guaiacol,

catechol, and phenol derivatives are the leading products in the bio-oil 7. In other's work, guaiacol suffered demethoxylation or demethylation to directly form phenol or catechol[32][33]. Dehydration or hydrogenolysis might also be followed, especially under severe conditions. However, the prolonged reaction time slightly increased the yields of almost all the organic compounds in the bio-oil phase, especially guaiacol and its derivatives.

Further increase of bio-oil yield was obtained with a reaction time of more than 5 hours. It infers that the reaction time promotes the sufficient occurrence of depolymerization, and more monomers formation led to higher liquefaction rates. Further monomers reaction, however, requires more severe conditions. At the current condition of 200 ℃, the occurrence of transalkylation or hydrodeoxygenation of formed monomers could not happen to produce light hydrocarbons. Thring et al. also mentioned that guaiacols and alcohols predominated at low severity, while phenol, catechol, and their respective alkyl derivatives were the main products at high severity[34]. The yield of bio-oil products was increased with reaction time. Due to the limitation of GC-MS, dimers, trimers, and oligomers could not be detected. So, in this work, only aromatic monomers were investigated and compared under different hydrogenation times.

Table 3- 2 The main compounds in the bio-oil phase were detected by GC-MS.

Compound	**Structural formula**	**Retention time (min)**	**Bio-oil 1 1 (wt.%)**	**Bio-oil 1 3 (wt.%)**	**Bio-oil 1 5 (wt.%)**	**Bio-oil 1 7 (wt.%)**
2(3H)-Furanone, 5-(acetyloxy)dihydro-5-methyl-	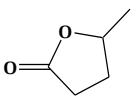	15.925	-	-	-	0.11

Guaiacol	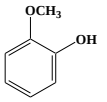	16.287	0.08	0.27	0.50	0.70
Creosol	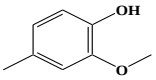	17.225	-	0.07	0.11	0.19
Phenol, 4-ethyl-2-methoxy-	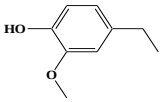	17.948	-	0.14	0.21	0.29
Phenol, 2-methoxy-4-propyl-	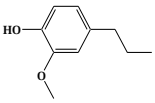	18.631	-	-	0.03	0.03
2,3-Dimethoxyphenol	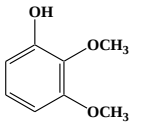	18.76	-	0.02	0.04	0.03
Vanillin	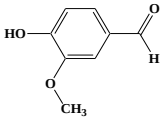	19.63	0.06	0.04	0.10	0.11
Apocynin	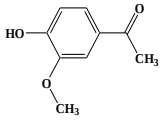	20.196	-	0.03	0.09	0.09
Ethyl homovanillate	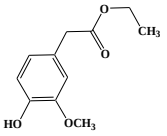	20.892	0.05	0.07	0.15	0.16
3-Allyl-6-methoxyphenol	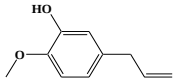	21.838	0.04	0.07	0.14	0.12
Identified oil product			0.24	0.72	1.48	1.87

Note: Bio-oil 1: reaction time: 1 h; Bio-oil 3: reaction time: 3 h; Bio-oil 5: reaction time: 5 h; Bio-oil 7: reaction time: 7 h. Other conditions: temperature: 200 ℃; catalyst: Raney Ni; pressure: 3 MPa.

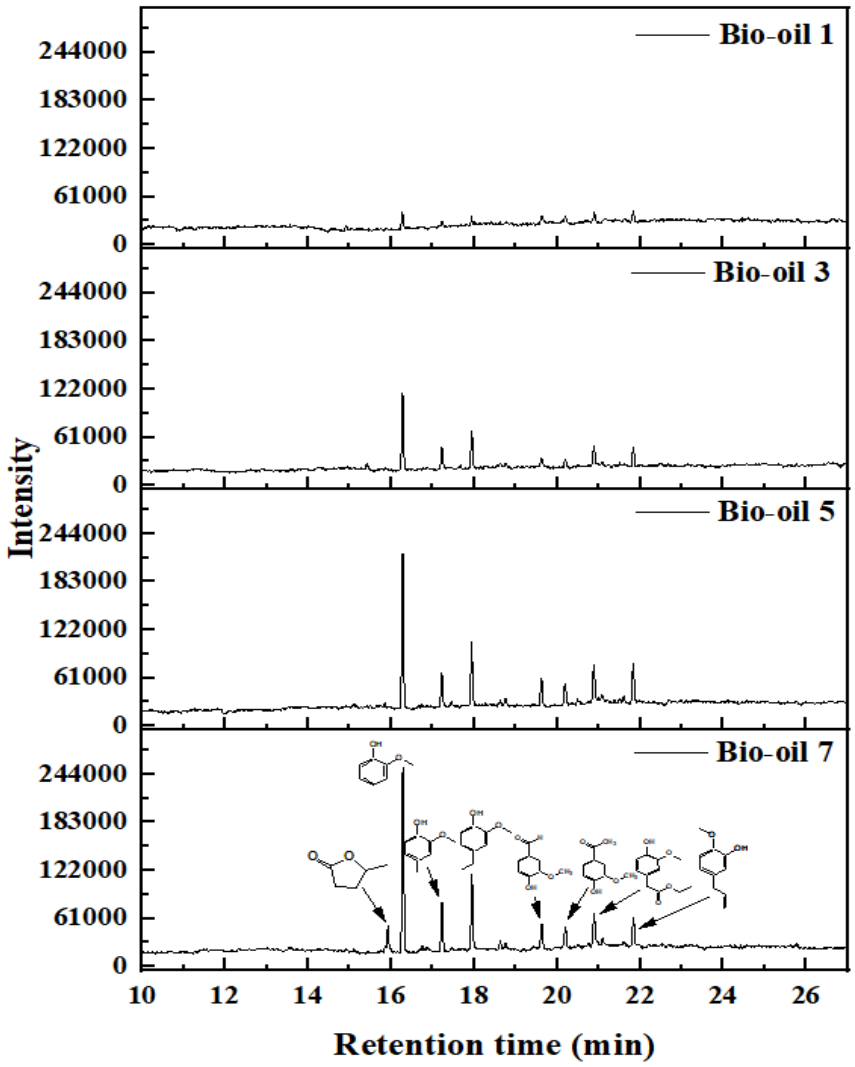

Fig. 3- 3 GC-MS of the bio-oil samples with different reaction times. Bio-oil 1: reaction time: 1 h; Bio-oil 3: reaction time: 3 h; Bio-oil 5: reaction time: 5 h; Bio-oil 7: reaction time: 7 h.

3.4.4 Characterizations of catalysts

Table 3-3 shows the specific surface area and pore structure characteristics of the catalysts from the nitrogen adsorption/desorption. It can be seen that Rh/C and Ru/C have relatively similar pore structures; both contain large specific surface areas and the same pore volume, which may play a positive role in the hydrogenation of monomers. The only difference would be the noble metal type and the synergistic effect with the

solution. Raney nickel is not a porous structure because of the properties of large pore size and low pore volume. Only some large pores formed bumpily on the surface, which supported that the reaction of large lignin compounds happens on the surface of Raney Ni.

Table 3- 3 The specific surface area and pore structure characteristics of the catalysts.

BEL results	Surface area(m^2/g)	Average pore size(nm)	Pore volume(cm^3/g)
Raney Ni	0.668	131.69	0.02
Ru/C	840	4.15	0.87
Rh/C	934	3.73	0.87

Fig. 3-4 shows the XRD profiles of the three catalysts. In Fig. 3-4(a), Raney Ni shows many crystalline peaks which include both Ni_2Al_3 and $NiAl_3$ phases. So, the nickel-aluminium alloy particles are attached to the macroporous surface as crystalline particles. In Fig. 3-4(b), the diffractograms of Ru/C and Rh/C show no obvious crystalline peak, which proves that Ru/C and Rh/C are amorphous. The peaks (2θ is around 43°) correspond to the Ru-containing and Rh-containing phases, respectively. These spectrums of Raney Ni, Ru/C and Rh/C are in agreement with previous findings in the literature[35][36].

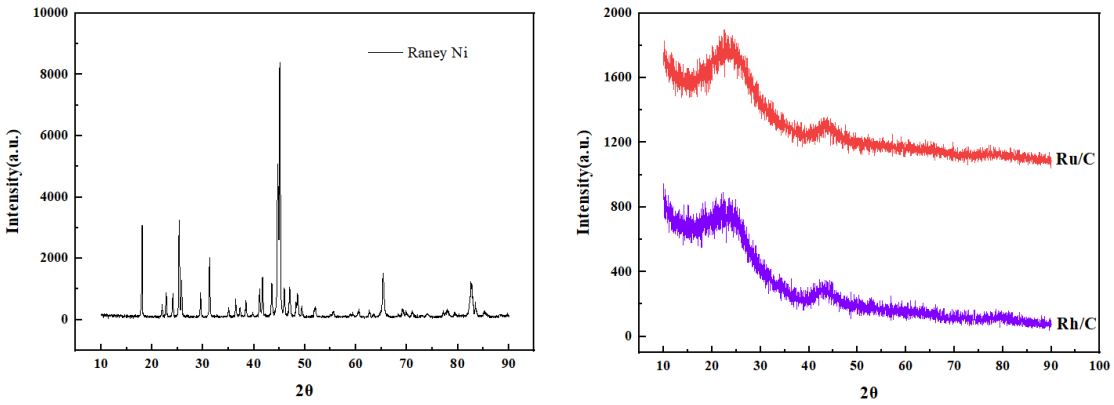

(a) (b)

Fig. 3- 4 XRD profiles of Raney Ni (a), Ru/C and Rh/C (b).

The TG curve of Raney Ni before and after the reaction shows in Fig. 3-5(a). The formation of coke buildup on the catalyst can be seen by comparing the TG curves of Raney Ni before and after the reaction. In Figure 3-5(a), pure Raney Ni does not show any depolymerization within 650 ℃, and the TG curve remains at 100%. After the reaction, the TG curve of the catalyst mixtures is different. The weight loss shown in the TG curve is directly related to the amount of coke produced in the reaction. The more coke form, the higher the mass loss. Here the analysis and comparison of the catalyst mixture after the reaction at different temperatures and pressures were made. The higher the temperature used, the more the coke yield formed. The coke's yield at 2-3 MPa is relatively lower. The weight loss coincides with the pattern of coke yield in Fig. 3-2. However, for Ru/C and Rh/C, the weight loss curves are shown in Fig. 3-5(b). The activated carbon, as a ground substance for metal loading, is also suffered from decomposition in the temperature range of 200-400 ℃. Therefore, the TG curves of Ru/C and Rh/C catalysts before and after the reaction might not be so pronounced, because not only the mass loss of coke formed after the reaction but also the loss of the catalyst itself would occur in the temperature range of 200-400 ℃. So, the TG curves before and after the reaction for Ru/C and Rh/C were not compared here. The yield of coke on the catalysts was only calculated through the weight difference of the catalyst mixture before and after the reaction in this work.

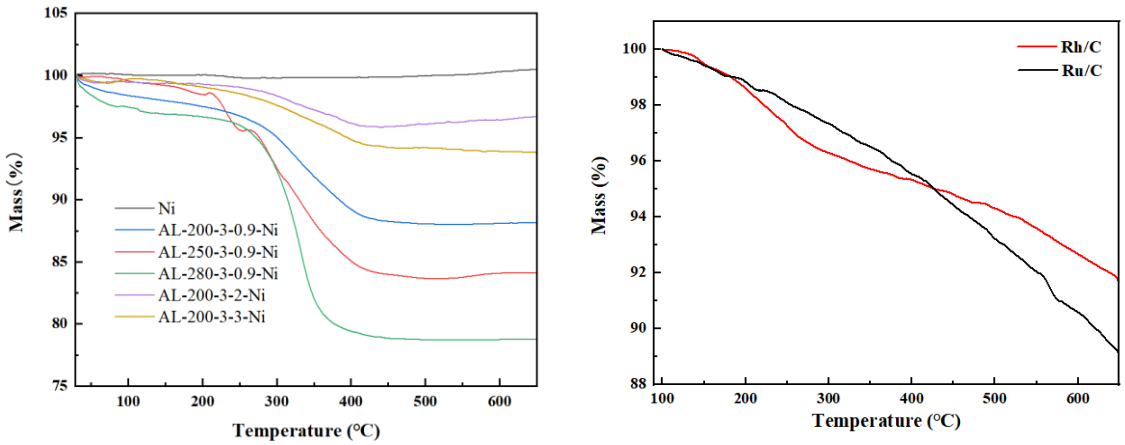

(a) (b)

Fig. 3- 5 Thermogravimetric analysis (TGA) of catalyst mixture, (a) Raney Nickel before and after the hydrogenation reaction; (b) Pure Ru/C and Rh/C before reaction.

3.4.5 Pyrolysis characteristics of lignin for olefins

Changing the pyrolysis condition is aimed at finding out the highest yield of olefins. The temperature and residence time are the main variables that significantly influence on the product distribution in fast pyrolysis. The relationship of olefin yields and selectivity of each compound with temperature and residence time was tested prior to this work.

Many researchers focused on temperature's effect[37][38], while lignin was usually pyrolyzed at 600-650 ℃. From other studies, there is a tendency to increase olefins as the temperature increases[39]. So, the pyrolysis of AL was first compared at a relatively high-temperature range (600-950 ℃). The olefins distribution from fast pyrolysis at 600-950 ℃ is shown in Fig. 3-6(a). The identical residence time was adjusted at various temperatures. The yield of total olefins rose with the temperature increasing, from 0.33 wt.% at 600 ℃ to 0.71 wt.% at 800 ℃. When the temperature is higher than 800 ℃, the total olefins yield starts to decrease significantly. Total olefins yield declined to 0.47 wt.%

when the temperature was increased to 950 ℃. It might be attributed to the intensive decomposition of lignin at high-temperatures. The side-chain groups were immediately cleaved, forming light volatiles such as methane or ethane[40]. The following yield order was observed among the total olefins: ethylene > propylene > butylene. Only a trace amount of butylene (less than 0.02 wt.%) was produced. As for ethylene and propylene's yield, the tendency was first increase and then decrease, the highest value obtained at 850 ℃ (0.63 wt.%) and 750 ℃ (0.22 wt.%), respectively.

The selectivity towards the light olefins upon variation in the residence time is outlined in Fig. 3-6(b). The yield of each olefin has a similar tendency as that of total olefins. When the residence time equaled to 1 second, the olefins yield has reached a peak value, 1.03 wt.%. C2-C4 olefins are the intermediates of fast pyrolysis from the cleavage of side-chain groups, mainly formed at the primary reaction[41]. At the secondary reaction, the heavy oligomer compounds would further decompose to olefins. Simultaneously, the competitive reaction is that olefins would recombine and reform, especially within a long residence time[42][40]. From the above results, the reaction conditions 800 ℃ of temperature and 1 s residence time could be preferred.

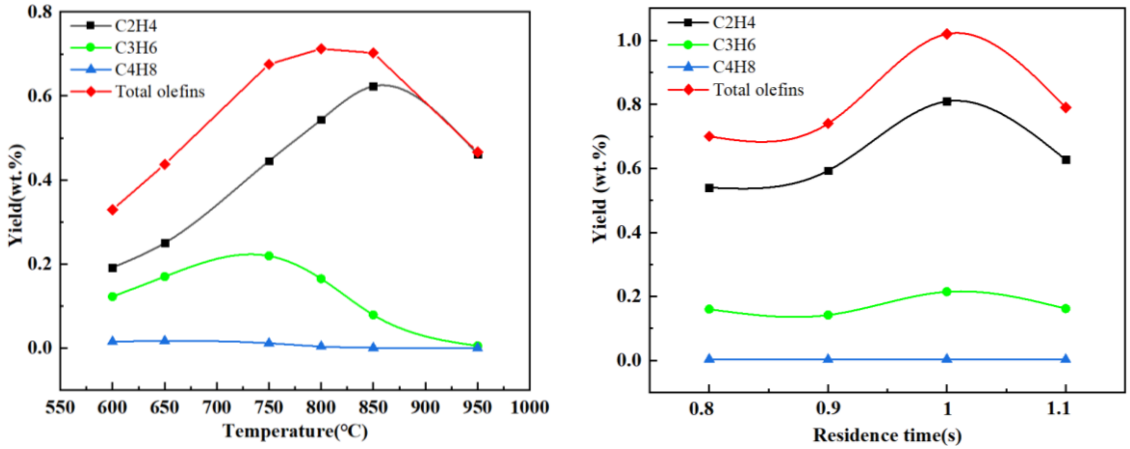

(a) (b)

Fig. 3- 6 The influence of pyrolysis temperature and residence time on the yield of light

olefins at helium atmosphere; (a) residence time: 1 s; (b) temperature: 800 ℃.

3.4.6 Fast pyrolysis of hydrogenated alkaline lignin

Fast pyrolysis of hydrogenated alkaline lignin under helium atmosphere has been shown in Fig. 3-7. The influence of temperature (150-280 ℃) on the distribution of olefins is demonstrated in Fig. 3-7(a). After the hydrogenation process, the HAL samples have higher thermal reactivity, producing more olefins than AL. 250 ℃ is a suitable condition for modifying the lignin structure and improving the yield of olefins (both ethylene and propylene). When the temperature was further increased, the yield of olefins began to drop dramatically. The char yield had a significant increase with increasing temperature. This could be owing to the high temperature exacerbating the process to make the depolymerization more complete, causing the solid product to loses its pyrolytic activity to some extent[43].

The influence of reaction time (1-7 hrs) on the distribution of olefins is shown in Fig. 3-7(b). The reaction time does not significantly impact the propylene and butylene yield, but the extended reaction time has dramatically improved the ethylene yield. The HAL obtained after 7 hours has shown better performance to produce more olefins with less char yield. Thus, the prolonged reaction time could not significantly affect the liquefaction yield but could facilitate the lignin structure change and activate HAL's properties[32].

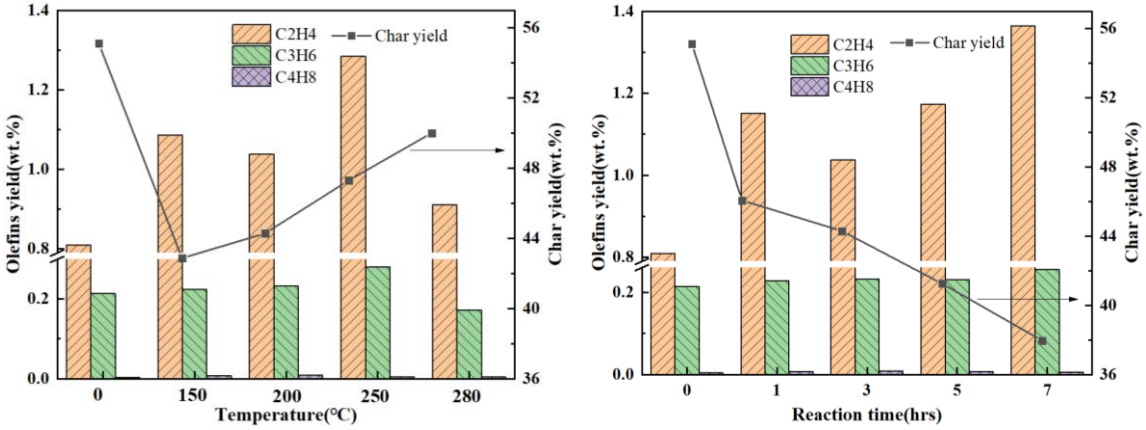

(a) (b)

Fig. 3- 7 The olefins distribution and char yield from the HAL samples with different (a) temperature and (b) reaction time. Pyrolysis condition: 800 ℃; residence time: 1 s; under helium atmosphere.

The other products from fast pyrolysis of lignin before and after hydrogenated samples are listed in Table 3-4. The product distribution is varied before and after hydrogenation. The yield of char and vapour was decreased, and more carbon monoxide was produced from the HAL samples instead of carbon dioxide due to the cleavage of oxygenated functional groups. With the increase of hydrotreatment temperature, char yield continuously raised while carbon monoxide continuously declined. All HAL samples produced more hydrocarbon compounds and aromatics than AL. Methane yield increased from 2.27 wt.% of AL to around 4 wt.% of HAL, but suddenly dropped for HAL-280. The yield of other compounds like ethylene, ethane, propylene, propane, and butane has peaked for HAL-250. The undetected products are the heavy aromatic compounds, which have a significant rising after hydrotreatment. It is worth mentioning that the undetected products have the lowest percentage for HAL-250 and the highest percentage for HAL-280. This surmises that the temperature has a considerable influence on the structure of the solid product. At high hydrogenation temperatures, the functional groups of lignin are severely cleaved, resulting in low yields of light olefins

or low aromatic hydrocarbons during fast pyrolysis. Thus, hydrogenation at higher temperatures leads to form more heavy compounds with more than two rings.

Table 3- 4 The product distribution from fast pyrolysis of AL and HAL samples pretreated at different temperatures. Pyrolysis condition: 800 ℃; residence time: 1 s; atmosphere: helium.

No.	Products	AL	HAL-150	HAL-200	HAL-250	HAL-280
1	Char	55.10	42.86	44.28	47.30	50.00
2	Carbon monoxide	5.08	7.87	7.65	6.70	4.73
3	Carbon dioxide	13.14	7.94	7.31	9.25	4.53
4	Vapor	16.38	16.23	13.15	11.86	13.05
5	Methane	2.27	3.99	3.93	3.97	3.36
6	Ethylene	0.81	1.09	1.04	1.28	0.91
7	Ethane	0.10	0.18	0.21	0.21	0.19
8	Propylene	0.21	0.22	0.23	0.28	0.17
9	Propane	0.002	0.08	0.04	0.08	0.08
10	Butylene	0.004	0.008	0.009	0.005	0.004
11	Butane	0.14	0.22	0.20	0.27	0.16
12	Benzene	0.40	0.97	0.90	0.95	0.72
13	Toluene	0.30	0.49	0.55	0.51	0.46
14	Undetected product*	6.06	17.85	20.5	17.34	21.64

* The undetected product includes the large aromatic compounds that could not be detected by this GC-TCD/FID.

Besides temperature and residence time, the pyrolysis atmosphere is also a critical factor for stimulating the release of volatiles. Xue et al. proposed the extent of coke

reduction and aromatics increase by the co-pyrolysis of lignin with tetralin. This study used tetralin as a hydrogen donor to provoke the lignin's decomposition and suppress the recombination[25]. So, the hydrogen atmosphere was checked in this work. In Fig. 3-8(a), the yield of ethylene and total olefins had an apparent tendency to increase and then decrease with the pyrolysis temperature. The maximum yield of total olefins was obtained at 850 ℃. Furthermore, propylene yield continues to fall from 800 to 1000 ℃. Therefore, further investigation of residence time was performed at 850 ℃. The effect of residence time on olefin products was similar in different atmospheres. Long residence time caused the formed olefins from the primary reaction to recombine and condense in the secondary reaction. Thus, an intermediate residence time of 0.45 s is best suited for producing more light olefins.

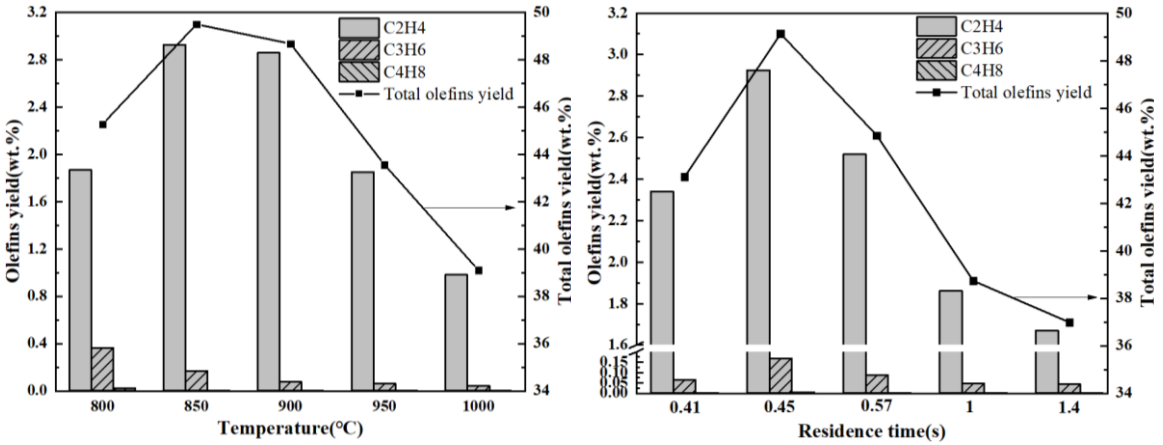

(a) (b)

Fig. 3- 8 The light olefins distribution from fast pyrolysis of HAL (hydrotreatment conditions: 250 ℃, 0.9 MPa for 7 hours with Raney Ni) under hydrogen atmosphere; (a) residence time: 0.45 s; (b) temperature: 850 ℃.

Table 3-5 lists the product distribution of fast pyrolysis of HAL samples. Each HAL sample was performed under the hydrogen and helium atmosphere for comparison. Here,

compared with the inert atmosphere (He), hydrogen gas provoked the release of volatiles. The char yield was reduced for all samples under the hydrogen atmosphere. Moreover, carbon monoxide, vapor, methane, ethylene, ethane, benzene, and toluene have increased to various degrees. The sharp increase of methane under the hydrogen atmosphere accounts for the combination of hydrogen radicals with the methyl radicals generated from the cleavage of C-C or methoxy groups[44]. In addition, gasification of char is inevitably occurred for the first 15 seconds due to the hydrogen atmosphere. The undetected compounds were found to produce more under the inert atmosphere, while hydrogen reacted with large aromatic compounds and simulated volatiles reformation in the hydrogen atmosphere.

Compared with the effects of different catalysts, noble metal-based catalysts have a higher capability for liquefaction, while the yield of HAL is also decreased. In terms of olefin products, after hydrotreatment with Raney Ni, relatively more olefins were produced. Compared with the pyrolyzed products from HAL-Raney Ni-200 and HAL-Raney Ni-250, the yield of char, carbon dioxide, and vapor for HAL-Raney Ni-250 decreased under both helium and hydrogen atmosphere. Instead, the yield of methane, ethylene, ethane, benzene, toluene and undetected products has increased after hydrogenation at 250 ℃. Hydrogenation temperature has little effect on the pyrolysis of HAL for C3-C4 products due to its inherently low yield. HAL samples have better pyrolysis characteristics and generate more light hydrocarbons and aromatic compounds during fast pyrolysis. Catalytic hydrotreatment at 250 ℃ with Raney Ni could be an optimized condition to improve the properties and chemical structure of the hydrogenated products.

Table 3- 5 The comparison for pyrolysis of the HAL samples obtained at 0.9 MPa with 7 hours; HAL-Ru/C: alkaline lignin treated with Ru/C at 200 ℃; HAL-Rh/C: alkaline lignin treated with Rh/C at 200 ℃; HAL-Raney Ni-200: alkaline lignin treated with

Raney Ni at 200 ℃; HAL-Raney Ni-250: alkaline lignin treated with Raney Ni at 250 ℃.

No.	Product compounds	HAL-Ru/C-200		HAL-Rh/C-200		HAL-Raney Ni-200		HAL-Raney Ni-250	
		He	H_2	He	H_2	He	H_2	He	H_2
1	Char	43.62	35.17	47.62	35.34	44.90	39.69	44.57	36.46
2	CO	7.44	7.28	7.22	7.39	7.20	7.62	6.62	8.30
3	CO_2	5.15	5.06	4.83	5.64	4.53	5.21	2.40	2.28
4	Vapor	12.80	20.31	9.97	18.68	13.34	14.32	12.07	13.01
5	Methane	3.54	9.48	3.63	11.28	4.51	10.67	4.56	11.86
6	Ethylene	1.31	2.01	1.08	2.47	1.21	2.49	1.44	2.92
7	Ethane	0.07	0.91	0.11	1.01	0.22	1.33	0.33	1.70
8	Propene	0.11	0.07	0.12	0.08	0.24	0.18	0.30	0.17
9	Propane	0.03	0.04	0.04	0.001	0.06	0.10	0.07	0.05
10	Butylene	0.001	0.001	0.002	0.001	0.008	0.004	0.01	0.004
11	Butane	0.06	0.02	0.11	0.01	0.21	0.03	0.19	0.04
12	Benzene	0.94	2.49	0.98	3.02	1.12	2.37	1.02	2.85
13	Toluene	0.11	0.52	0.39	0.48	0.58	0.79	0.81	0.95
14	Undetected product	24.82	16.64	23.90	14.60	21.87	15.20	25.61	19.41

3.5 Conclusions

Hydrogenation experiments were conducted on AL to observe the effects of hydrotreatment on the solid chemical structure of the lignin. Further, fast pyrolysis was carried out for investigating the pyrolytic properties of HAL samples under different

pyrolysis conditions. The main conclusion that can be drawn is that hydrotreatment is an attractive technology for lignin utilization, not only liquifying lignin to valuable chemicals (guaiacol, creosol, Phenol, 4-ethyl-2-methoxy-, vanillin, etc.) but modifying solid lignin with high quality. A significant decrease of oxygen content and an increase of the H/C_{eff} ratio were found in HAL samples. Notably, HAL has higher pyrolytic activity. 55.1 wt.% of the product of AL is remained as the char in fast pyrolysis, while 44.6 wt.% of char for HAL under same conditions. More valuable light volatiles can be released from lignin samples after hydrotreatment. Furthermore, total olefins yield increased from 1.02 wt.% of AL to 1.75 wt.% of HAL under helium as a carrier gas. Using hydrogen as the pyrolytic atmosphere, the char yield further decreased to 36.5 wt.%, and 3.1 wt.% of total olefins were obtained for HAL (250 ℃, 7 hours, Raney Ni, 0.9 MPa H_2). Thus, our results prove that the HAL samples from the hydrogenation process are worth utilizing as a feedstock for fast pyrolysis, even better than AL. This work provides a good starting point for discussion and further research. Validating the conclusions drawn from this study and optimizing hydrogenation conditions for industrialization are crucial and necessary in the future.

3.6 Reference

[1] Y. Lu, Y.C. Lu, H.Q. Hu, F.J. Xie, X.Y. Wei, X. Fan, Structural characterization of lignin and its degradation products with spectroscopic methods, J. Spectrosc. 2017 (2017). https://doi.org/10.1155/2017/8951658.

[2] I.Z. Awan, N. Tanchoux, F. Quignard, S. Albonetti, F. Cavani, F. Di Renzo, Chapter 13 - Heterogeneous Catalysis as a Tool for Production of Aromatic Compounds From Lignin, in: S. Albonetti, S. Perathoner, E.A.B.T.-S. in S.S. and C. Quadrelli (Eds.), Horizons Sustain. Ind. Chem. Catal., Elsevier, 2019: pp. 257–275. https://doi.org/https://doi.org/10.1016/B978-0-444-64127-4.00013-6.

[3] S.C. Qi, J.I. Hayashi, S. Kudo, L. Zhang, Catalytic hydrogenolysis of kraft lignin to monomers at high yield in alkaline water, Green Chem. 19 (2017) 2636–2645. https://doi.org/10.1039/c7gc01121k.

[4] A. Kloekhorst, H.J. Heeres, Catalytic Hydrotreatment of Alcell Lignin Using Supported Ru, Pd, and Cu Catalysts, ACS Sustain. Chem. Eng. 3 (2015) 1905–1914. https://doi.org/10.1021/acssuschemeng.5b00041.

[5] R.K. Chowdari, S. Agarwal, H.J. Heeres, Hydrotreatment of Kraft Lignin to Alkylphenolics and Aromatics Using Ni, Mo, and W Phosphides Supported on Activated Carbon, ACS Sustain. Chem. Eng. 7 (2019) 2044–2055. https://doi.org/10.1021/acssuschemeng.8b04411.

[6] C.R. Kumar, N. Anand, A. Kloekhorst, C. Cannilla, G. Bonura, F. Frusteri, K. Barta, H.J. Heeres, Solvent free depolymerization of Kraft lignin to alkyl-phenolics using supported NiMo and CoMo catalysts, Green Chem. 17 (2015) 4921–4930. https://doi.org/10.1039/c5gc01641j.

[7] X.-J. Shen, P.-L. Huang, J.-L. Wen, R.-C. Sun, A facile method for char elimination during base-catalyzed depolymerization and hydrogenolysis of lignin, Fuel Process. Technol. 167 (2017) 491–501.

https://doi.org/https://doi.org/10.1016/j.fuproc.2017.08.002.

[8] K. Barta, T.D. Matson, M.L. Fettig, S.L. Scott, A. V. Iretskii, P.C. Ford, Catalytic disassembly of an organosolv lignin via hydrogen transfer from supercritical methanol, Green Chem. 12 (2010) 1640–1647. https://doi.org/10.1039/c0gc00181c.

[9] A. Narani, R.K. Chowdari, C. Cannilla, G. Bonura, F. Frusteri, H.J. Heeres, K. Barta, Efficient catalytic hydrotreatment of Kraft lignin to alkylphenolics using supported NiW and NiMo catalysts in supercritical methanol, Green Chem. 17 (2015) 5046–5057. https://doi.org/10.1039/c5gc01643f.

[10] J. Li, J. Zhang, S. Zhang, Q. Gao, J. Li, W. Zhang, Alkali lignin depolymerization under eco-friendly and cost-effective NaOH/urea aqueous solution for fast curing bio-based phenolic resin, Ind. Crops Prod. 120 (2018) 25–33. https://doi.org/10.1016/j.indcrop.2018.04.027.

[11] J. Long, Y. Xu, T. Wang, Z. Yuan, R. Shu, Q. Zhang, L. Ma, Efficient base-catalyzed decomposition and in situ hydrogenolysis process for lignin depolymerization and char elimination, Appl. Energy. 141 (2015) 70–79. https://doi.org/10.1016/j.apenergy.2014.12.025.

[12] S. Huang, N. Mahmood, M. Tymchyshyn, Z. Yuan, C.C. Xu, Reductive de-polymerization of kraft lignin for chemicals and fuels using formic acid as an in-situ hydrogen source, Bioresour. Technol. 171 (2014) 95–102. https://doi.org/10.1016/j.biortech.2014.08.045.

[13] W.J. Connors, L.N. Johanson, K. V. Sarkanen, P. Winslow, Thermal degradation of kraft lignin in tetralin, Holzforschung. 34 (1980) 29–37. https://doi.org/10.1515/hfsg.1980.34.1.29.

[14] C. Zhang, R. Wu, E. Hu, S. Liu, G. Xu, Coal pyrolysis for high-quality tar and gas in 100 kg fixed bed enhanced with internals, Energy and Fuels. 28 (2014) 7294–7302. https://doi.org/10.1021/ef501923f.

[15] X. Zeng, Y. Wang, J. Yu, S. Wu, J. Han, S. Xu, G. Xu, Gas upgrading in a downdraft fixed-bed reactor downstream of a fluidized-bed coal pyrolyzer, Energy and Fuels. 25 (2011) 5242–5249. https://doi.org/10.1021/ef2012276.

[16] Damayanti, H.S. Wu, Pyrolysis kinetic of alkaline and dealkaline lignin using catalyst, J. Polym. Res. 25 (2018). https://doi.org/10.1007/s10965-017-1401-6.

[17] P.R. Patwardhan, R.C. Brown, B.H. Shanks, Understanding the fast pyrolysis of lignin, ChemSusChem. 4 (2011) 1629–1636. https://doi.org/10.1002/cssc.201100133.

[18] H. Yang, K. Norinaga, J. Li, W. Zhu, H. Wang, Effects of HZSM-5 on volatile products obtained from the fast pyrolysis of lignin and model compounds, Fuel Process. Technol. 181 (2018) 207–214. https://doi.org/10.1016/j.fuproc.2018.09.022.

[19] H. Lange, S. Decina, C. Crestini, Oxidative upgrade of lignin - Recent routes reviewed, Eur. Polym. J. 49 (2013) 1151–1173. https://doi.org/10.1016/j.eurpolymj.2013.03.002.

[20] M. Yang, J. Shao, Z. Yang, H. Yang, X. Wang, Z. Wu, H. Chen, Conversion of lignin into light olefins and aromatics over Fe/ZSM-5 catalytic fast pyrolysis: Significance of Fe contents and temperature, J. Anal. Appl. Pyrolysis. 137 (2019) 259–265. https://doi.org/10.1016/j.jaap.2018.12.003.

[21] W. Huang, F. Gong, M. Fan, Q. Zhai, C. Hong, Q. Li, Production of light olefins by catalytic conversion of lignocellulosic biomass with HZSM-5 zeolite impregnated with 6wt.% lanthanum, Bioresour. Technol. 121 (2012) 248–255. https://doi.org/10.1016/j.biortech.2012.05.141.

[22] W.C. Xu, A. Tomita, Effective Utilization of Coal via Flash Pyrolysis, Isij Int. 30 (1990) 687–698. https://doi.org/10.2355/isijinternational.30.687.

[23] E. Avni, F. Davoudzadeh, R.W. Coughlin, Flash Pyrolysis of Lignin, in: R.P. Overend, T.A. Milne, L.K. Mudge (Eds.), Fundam. Thermochem. Biomass

Convers., Springer Netherlands, Dordrecht, 1985: pp. 329–343. https://doi.org/10.1007/978-94-009-4932-4_18.

[24] H. Kawamoto, Lignin pyrolysis reactions, J. Wood Sci. 63 (2017) 117–132. https://doi.org/10.1007/s10086-016-1606-z.

[25] Y. Xue, S. Zhou, X. Bai, Role of Hydrogen Transfer during Catalytic Copyrolysis of Lignin and Tetralin over HZSM-5 and HY Zeolite Catalysts, ACS Sustain. Chem. Eng. 4 (2016) 4237–4250. https://doi.org/10.1021/acssuschemeng.6b00733.

[26] X.-J. Shen, P.-L. Huang, J.-L. Wen, R.-C. Sun, A facile method for char elimination during base-catalyzed depolymerization and hydrogenolysis of lignin, Fuel Process. Technol. 167 (2017) 491–501. https://doi.org/https://doi.org/10.1016/j.fuproc.2017.08.002.

[27] H. Wu, J. Song, C. Xie, C. Wu, C. Chen, B. Han, Efficient and Mild Transfer Hydrogenolytic Cleavage of Aromatic Ether Bonds in Lignin-Derived Compounds over Ru/C, ACS Sustain. Chem. Eng. 6 (2018) 2872–2877. https://doi.org/10.1021/acssuschemeng.7b02993.

[28] A. Bjelić, M. Grilc, M. Huš, B. Likozar, Hydrogenation and hydrodeoxygenation of aromatic lignin monomers over Cu/C, Ni/C, Pd/C, Pt/C, Rh/C and Ru/C catalysts: Mechanisms, reaction micro-kinetic modelling and quantitative structure-activity relationships, Chem. Eng. J. 359 (2019) 305–320. https://doi.org/10.1016/j.cej.2018.11.107.

[29] J.L. McCarthy, F. Fern, M. Dolk, J.F. Yan, Lignin. 23. Macromolecular Characteristics of Alkali Lignin and Organosolv Lignin from Black Cottonwood, Macromolecules. 19 (1986) 1471–1477. https://doi.org/10.1021/ma00159a032.

[30] A.A. Philippov, A.M. Chibiryaev, O.N. Martyanov, Raney® nickel-catalyzed hydrodeoxygenation and dearomatization under transfer hydrogenation conditions—Reaction pathways of non-phenolic compounds, Catal. Today. 355

(2020) 35–42. https://doi.org/https://doi.org/10.1016/j.cattod.2019.05.033.

[31] T.P. Vispute, H. Zhang, A. Sanna, R. Xiao, G.W. Huber, Renewable chemical commodity feedstocks from integrated catalytic processing of pyrolysis oils, Science (80-.). 330 (2010) 1222–1227. https://doi.org/10.1126/science.1194218.

[32] S. Totong, P. Daorattanachai, A.T. Quitain, T. Kida, N. Laosiripojana, Catalytic Depolymerization of Alkaline Lignin into Phenolic-Based Compounds over Metal-Free Carbon-Based Catalysts, Ind. Eng. Chem. Res. 58 (2019) 13041–13052. https://doi.org/10.1021/acs.iecr.9b01973.

[33] D. Forchheim, U. Hornung, A. Kruse, T. Sutter, Kinetic Modelling of Hydrothermal Lignin Depolymerisation, Waste and Biomass Valorization. 5 (2014) 985–994. https://doi.org/10.1007/s12649-014-9307-6.

[34] R.W. Thring, E. Chornet, R.P. Overend, Thermolysis of glycol lignin in the presence of tetralin, Can. J. Chem. Eng. 71 (1993) 107–115. https://doi.org/10.1002/cjce.5450710115.

[35] Preparation of novel Raney-Ni catalysts and characterization byXRD, SEM and XPS.pdf, (n.d.).

[36] M. Martin-Martinez, J.J. Rodriguez, R.T. Baker, L.M. Gómez-Sainero, Deactivation and regeneration of activated carbon-supported Rh and Ru catalysts in the hydrodechlorination of chloromethanes into light olefins, Chem. Eng. J. 397 (2020) 125479. https://doi.org/https://doi.org/10.1016/j.cej.2020.125479.

[37] D. Ferdous, A.K. Dalai, S.K. Bej, R.W. Thring, N.N. Bakhshi, Production of H2 and medium Btu gas via pyrolysis of lignins in a fixed-bed reactor, Fuel Process. Technol. 70 (2001) 9–26. https://doi.org/10.1016/S0378-3820(00)00147-8.

[38] J.A. Caballero, R. Font, A. Marcilla, Study of the primary pyrolysis of Kraft lignin at high heating rates: Yields and kinetics, J. Anal. Appl. Pyrolysis. 36 (1996) 159–178. https://doi.org/10.1016/0165-2370(96)00929-1.

[39] M. Yang, J. Shao, Z. Yang, H. Yang, X. Wang, Z. Wu, H. Chen, Conversion of

lignin into light olefins and aromatics over Fe/ZSM-5 catalytic fast pyrolysis: Significance of Fe contents and temperature, J. Anal. Appl. Pyrolysis. 137 (2019) 259–265. https://doi.org/10.1016/j.jaap.2018.12.003.

[40] H. YANG, S. APPARI, S. KUDO, J. HAYASHI, S. KUMAGAI, K. NORINAGA, Chemical Structures and Primary Pyrolysis Characteristics of Lignins Obtained from Different Preparation Methods, J. Japan Inst. Energy. 93 (2014) 986–994. https://doi.org/10.3775/jie.93.986.

[41] S. Zhang, M. Yang, J. Shao, H. Yang, K. Zeng, Y. Chen, J. Luo, F.A. Agblevor, H. Chen, The conversion of biomass to light olefins on Fe-modified ZSM-5 catalyst: Effect of pyrolysis parameters, Sci. Total Environ. 628–629 (2018) 350–357. https://doi.org/10.1016/j.scitotenv.2018.01.316.

[42] H.M. Yang, S. Appari, S. Kudo, J.I. Hayashi, K. Norinaga, Detailed Chemical Kinetic Modeling of Vapor-Phase Reactions of Volatiles Derived from Fast Pyrolysis of Lignin, Ind. Eng. Chem. Res. 54 (2015) 6855–6864. https://doi.org/10.1021/acs.iecr.5b01289.

[43] R. Shu, J. Long, Y. Xu, L. Ma, Q. Zhang, T. Wang, C. Wang, Z. Yuan, Q. Wu, Investigation on the structural effect of lignin during the hydrogenolysis process, Bioresour. Technol. 200 (2016) 14–22. https://doi.org/10.1016/j.biortech.2015.09.112.

[44] R. Gautam, S. Shyam, B.R. Reddy, K. Govindaraju, R. Vinu, Microwave-assisted pyrolysis and analytical fast pyrolysis of macroalgae: Product analysis and effect of heating mechanism, Sustain. Energy Fuels. 3 (2019) 3009–3020. https://doi.org/10.1039/c9se00162j.

Chapter 4 Thermal catalytic hydrogenation of organosolv lignin and subsequent fast pyrolysis

4.1 Abstract

Valorization and utilization of lignin have been drawing increasing attention recently. Hydrogenation is one of the main technologies, which can reduce organic compounds and partially depolymerize the macromolecular structure of lignin. The mechanism of lignin hydroprocess has been extensively discussed, focusing on hydrogenolysis. In contrast, the solid residue regarded as unreacted or depolymerized lignin has drawn less attention so far. This study presents an integrated process that consists of catalytic hydrogenation and subsequent fast pyrolysis for valorizing lignin. The results showed that 48-87 wt.% of solid product could be recovered as hydrogenated lignin (H-EOL) after hydrogenation at 200-250 ℃ for 1-7 hours. The chemical structure of H-EOL was comprehensively investigated by the means of Elemental analysis, FTIR, ^{13}C & ^{1}H NMR, and TGA, and the behaviour of fast pyrolysis of H-EOL was detected. H-EOL has higher hydrogen to carbon atomic effective ratio（H/C_{eff} ratio) and achieves the increasing reactivity of thermal decomposition. H-EOL yields light olefins double as much as raw ethanol organosolv lignin (EOL). And the formation of alkanes (C1-C4), benzene, and toluene was promoted to various degrees, while the yield of carbon monoxide, carbon dioxide, and vapour decreased. A novel process and efficient pretreatment method has been provided to verify on organosolv lignin, which is instructive for subsequent research.

4.2 Introduction

Lignin, which serves as a protective cell wall of plants, is the second most abundant biopolymer in lignocellulosic biomass, followed by cellulose, whose content varies from 11 to 40%[1][2]. It is widely accepted that lignin is defined as an amorphous polyphenolic material, which can be formed from an enzyme-mediated dehydrogenative polymerization of three phenylpropanoid monomers (coniferyl, sinapyl and p-coumaryl alcohols)[3]. As a result, lignin could be an attractive starting material to produce hydrocarbon and aromatic chemicals. Simultaneously, the unregular-repeat units and complex three-dimensional structure are still the major challenges for the utilization of lignin. Even though various depolymerization technologies have been of interest in the last a few decades, the major technology is still limited to combustion for providing heat.

Pyrolysis is a relatively mature thermochemical process, and is widely used for the industrial processing of organic materials to obtain oil products or valuable chemicals. However, as for lignin, its cross-linked structure is prone to repolymerization during the thermochemical conversion, resulting in more than half yield of char[4][5]. And the selectivity of pyrolytic products is also relatively low. Currently, catalytic fast pyrolysis (CFP) is one of technologies to improve the selectivity of products, especially olefins and aromatics. Fe-loading zeolite catalysts[6][7], and La-loading HZSM-5[8] have been checked, even increasing the production of light olefins to 8.6 C-mol.%. Indeed, light olefins, regarded as the intermediate products during fast pyrolysis, are hard to be selectively produced[9]. The types of feedstock have a more considerable influence on the yield of olefins compared with temperature, residence time even catalysts, due to their internal structure and chemical properties[8]. Thus, modification of lignin appears to be a viable technique for making better use of lignin and achieving higher olefin and aromatics yields from fast pyrolysis.

Hydrogenation is used to tailor the functional groups, improve lignin’s properties and control the product's distribution. According to the previous reports[10][11][12],

hydroprocess is a common technology for depolymerizing lignin, in which hydrogenolysis is the main reaction on lignin. Meanwhile, lignin also suffers from hydrogenation, and hydrogen atoms transfer into the free radicals of the lignin fraction[13]. Hydrogenation not only saturates lignin molecule but also suppresses the recombination of internal free radicals and the formation of more stubborn char[14][15]. More hydrogenation research was conducted on model compounds of lignin[16][17][18]. Noble metal catalysts (Ru, Rh, Pt and Pd) show a significant catalytic activity for hydrogenolysis of C-O ether bonds and hydrogenation of aromatic rings[19][20]. Although model compounds can illustrate basic units and linkage types in the lignin, it cannot substitute the actual folded structure of lignin in the usual sense.

There are limited research groups focusing on the solid residue from lignin hydrogenation[21][22]. Most of the studies give more attention on liquid products, use high temperatures and severe pressure to improve the liquefaction rate. However, Chio et al. mentioned that the temperature above 240 ℃ could enhance the repolymerization of intermediates of lignin molecule[23]. Shen et al. reported that the partly degraded lignin containing abundant aliphatic C-H bonds, and thermal decomposition started to occur even in the low-temperature range (200-280 ℃)[24]. Long et al. investigated the properties of recovered lignin after catalytic decomposition with the synergic function of NaOH and Ru/C. The recovered lignin possessed a lower molecular weight and lower degree of unsaturation[25].

The lignin's solubility in various solvents is also one of the major factors that profoundly affect the product distribution of the lignin other than temperature. The solubility of lignin depends on the source of the lignocellulose biomass and the isolation methods. Tetrahydrofuran (THF) shows significant solubility for most types of lignin, which has been commonly used as eluent for Gel permeation chromatography)measurement. Long’s group compared the depolymerization behaviour using THF and aqueous alcohol solvents, and obtained a higher conversion rate in the

THF due to its excellent capability of dissolution[26]. So THF was used as a solvent in this work to make sure the totally dispersion of lignin compounds and prevent the alcoholysis effect of alcohols.

It is reasonable speculation that lignin can suffer from hydrogenation at such mild temperatures under suitable catalysts, since a mild condition is proved to result in a significant conversion of lignin and suppressed repolymerization[27]. The pretreated lignin having been reduced is a promising feedstock for producing hydrocarbon chemicals through fast pyrolysis. Therefore, we constructed a novel and integrated process: catalytic hydrogenation of lignin and subsequent fast pyrolysis of hydrogenated lignin at H_2 atmosphere for obtaining more light olefins. This process is dedicated to modifying lignin and improving selectivity of pyrolyzed products.

4.3 Method and materials

4.3.1 Materials

THF (99.5%, with stabilizer), ethanol (99.5%), acetone solvent and DMSO-d_6 (99.9%, 047-29071) were purchased from FUJIFILM Wako Pure Chemical Corporation. Ruthenium on activated carbon (Ru/C, 5 wt.% Ru loading, 908045-10G), Rhodium on matrix carbon (Rh/C, 5 wt.% Rh loading, 680710-5G), and Chromium (III) acetylacetonate (99.99%, 574082-5G) were acquired from Sigma-Aldrich, which were vacuum-dried prior to use. KBr powder was obtained from Pike Technologies. Ethanol organosolv lignin (EOL) was extracted through a methodology followed by Cho et al.[28] with some modifications. Japanese cedar was treated in an ethanol/water mixture (70/30 v/v) with 1.25 wt.% sulfuric acid as a catalyst at 180 °C for 60 min. The ratio of the cedar to the mixture was kept at 1/8 (w/w). The extraction was carried out in a batch reactor. The remained cellulose and hemicellulose were flushed out with 50 mL of

ethanol/water mixture repeatedly three times. Three volumes of ultrapure water were added to the solution to precipitate the lignin in the mixture. Then filtration was performed again to recover the solid phase and dried in a vacuum oven for 24 hours. The solid recovered was called ethanol organosolv lignin (EOL).

4.3.2 Hydrogenation of EOL and separation method

Hydrogenation of EOL was carried out as follows. EOL (100 mg), the catalyst (50 mg), and THF solution (20 mL) were mixed and charged into the batch reactor (Parr 4590 Micro Bench Top Reactor, 100 mL) equipped with a four-blade stirrer, pressure and temperature controllers. The reactor was sealed and purged with H_2 several times to ensure the absence of oxygen, and then pressurized up to 3 MPa at ambient temperature. The mixture was mechanically stirred at 400 rpm at an elevated temperature for a designated time. The temperature and pressure were continuously monitored. After the completion of the hydrogenation, the reactor was quenched with a water bath and rapidly cooled down to room temperature. The procedure was performed with care in order to minimize experimental errors, and reproducibility was confirmed by duplication each run at least two times.

The products after hydrogenation were separated by the following procedures (Fig. 4-1). The gaseous products were collected by the syringe while releasing the pressure in the reactor and analyzed by GC-TCD/FID. The catalyst-coke mixture was separated from the solution by centrifugation with 6000 rpm for 10 min and then washed by THF. The solid mixture was vacuum dried at 60 ℃ for 24 hours. The filtrate was evaporated to remove all reaction medium. The retained product was named hydrogenated lignin (H-EOL), and then dried in the same manner as above. The yield of H-EOL was calculated as a percentage by weight of EOL fed. The weight difference was caused by coke formation. The unrecovered fraction corresponded to the complement of 100 wt.%

of the initial lignin, including oil phase, water, some volatile, and trace gaseous product. Therefore, the yield of products was calculated by the following Eqs. (4-1)-(4-4).

$$C_L\ (wt.\%) = (W_L - W_H)/W_L * 100\% \quad (4\text{-}1)$$

$$Y_H\ (wt.\%) = W_H/W_L * 100\% \quad (4\text{-}2)$$

$$Y_C\ (wt.\%) = W_C/W_L * 100\% \quad (4\text{-}3)$$

$$Y_R\ (wt.\%) = (W_L - W_H - W_C)/W_L * 100\% \quad (4\text{-}4)$$

Where, C, Y, and W are respectively the conversion, yield, and weight, and the subscripts L, H, C, and R denote EOL, H-EOL, coke, and the rest products (liquid and gas), respectively.

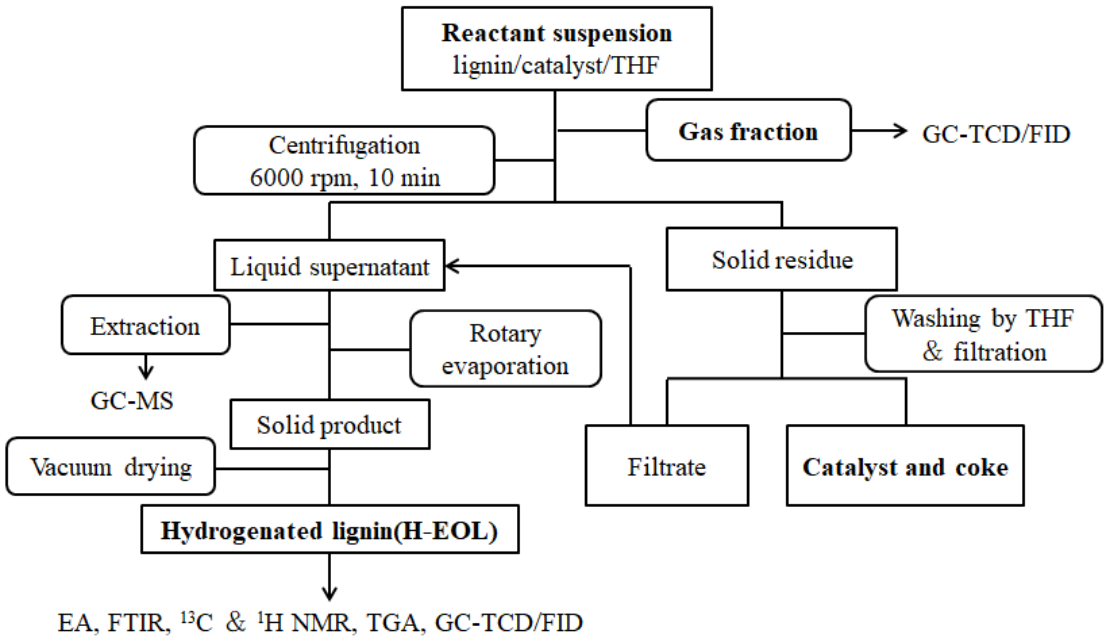

Fig. 4- 1 The flow chart of the products separation process.

4.3.3 Characterization of products

The thermogravimetric analysis (TGA) was used to illustrate the weight loss of lignin by TG curve and revealed the corresponding decomposition rate by DTG

(derivative thermogravimetric) curve, which was carried out in Netzsch STA 2500 Regules. Around 5 mg of the sample was loaded on a crucible. The temperature was first raised from room temperature to 100 ℃ with a rate of 5 °C/min, and maintained at 100 ℃ for 30 min. After that, it was heated to 1000 °C at the same heating rate. The thermal decomposition was performed at a constant N_2 flow rate of 50 ml/min.

Fourier transform infrared spectrometer (FTIR) was used for investigating the internal functional groups of solid samples, employing the Bruker ALPHA II. 1 wt.% of lignin in 50 mg of KBr was prepared. The samples were recorded between 400 and 4000 cm^{-1} at a resolution of 4 cm^{-1} in the absorbance mode.

The weight ratio of elements such as carbon, nitrogen, and hydrogen contained in organic compounds was quantified by elemental analyzer (2400II CHNS/O type manufactured by Perkin Elmer Co., Ltd). The analyzing process was conducted by the column separation method (frontal chromatography) and tested by a TCD. Around 2 mg of samples were detected each time with helium as a carrier gas.

The internal structure of lignin samples was determined by ^{13}C and ^{1}H NMR spectra (Bruker AS300). The details and parameters were following the literature[29]. Sample tubes (OD: 5 mm) was running for concentration of the samples 100 mg dissolved in 0.5 mL of DMSO-d_6. 0.01 M of Chromium (III) acetylacetonate was added to the lignin solution as a relaxation reagent. The quantitative ^{13}C NMR spectra were recorded in the Fourier transformation (FT) mode at 125.7 MHz. The inverse gated decoupling sequence, which allows quantitative analysis and comparison of signal intensities, was used with the following parameters: 30° pulse; 1.4 s acquisition time; 2 s relaxation delay; 64 K data points; and 8000 scans. 1H NMR spectrometer was operated at 500 MHz in FT mode, data acquisition time of about 3.3 s and the number of scans being about 16. Other selection of the operational parameter depends on the nature of ^{1}H NMR spectrometer.

The hydrogenated gaseous product was analyzed by GC 2014 (Shimadzu) equipped

with TCD (Thermal Conductivity Detector) and FID (flame ionization detector) detectors. The gaseous product mainly composed of CH_4 and CO, with minor amounts of CO_2 and C_2 compounds as well. The total weight of these gaseous compounds was however less than 1% of the feedstock. As a result, the yield of gaseous products was overlooked. And the volatiles from fast pyrolysis was also detected by the same GC-TCD/FID equipment with the same program.

4.3.4 Fast pyrolysis

A two-stage tubular reactor (TS-TR), made of quartz with an inner diameter of 4 mm, was used for the fast pyrolysis of lignin. More details about experimental procedure were shown in elsewhere[30][31]. Briefly, about 1 mg of lignin was wrapped every time by a sheet of wire mesh (10×10 mm, SUS316 stainless, 45 μm mesh opening), and the wrapped sample was held by a steel wire hook, so that the sample can be located at the upper part of reactor with the help of a magnet on the outside of reactor in installing the experimental setup. The furnace was insulated before increasing the temperature and verified that the entire system was sealed. After the temperature stabilization, the sample was dropped into the bottom of the reactor, where the preliminary reaction of fast pyrolysis happened. The nascent volatiles were swept into the secondary section by a carrier gas, of which the residence time can be controlled by changing the position of the reactor in the furnace. The actual flow rates of helium and hydrogen were 68.2 and 68.5 mL/min, respectively, so that the corresponding gas residence time of 0.45 s was kept constant.

The TS-TR was connected with the GC-TCD/FID. The volatiles released from the lignin was immediately blown into a packed column (Gaskuropack 54) and then sequentially passed through the TCD and FID sequentially. The quantifications of the products were conducted and calculated based on the external calibration method, the

standard gas consisted in CO (1.0%), CO_2 (0.978%), CH_4 (1.01%), N_2 (balance gas). The conditions for TCD and FID are shown in Table 4-1[32]. The reproducibility was examined, which revealed that the relative errors of the product yield generally within ±5 wt.%.

Table 4- 1 The parameters setup for GC measurement.

Instrument	Analysis conditions	
GC2014-TCD/FID	Separation column	Gaskuropack 54 (packed column, GL Sciences)
	Detector and analytes	TCD: carbon monoxide, carbon dioxide, vapor FID: methane, ethylene, ethane, propylene, propane, methanol, acetaldehyde, butane, butene, isobutylene, ethanol, iso-propanol, cyclopentadiene, acetic acid, benzene, toluene, furfural
	Injector/Detector/Column temperature	200 ℃/220 ℃/40 ℃
	Temperature program	Hold 10 min at 40 ℃, raise temperature to 200 ℃ at a heating rate of 5 ℃/min, then hold 18 min

4.4 Results and discussion

4.4.1 Hydrogenation condition and products yield

The product distribution after catalytic hydrogenation is shown in Fig. 4-2. The influence of catalysts (non, Raney Ni, Ru/C, and Rh/C) on hydrogenation has been observed and shown in Fig. 4-2(a). The products from hydrogenation without catalysts showed almost no liquefaction occurred, around 98.5 wt.% of the product remained as solid product. EOL partially underwent thermal decomposition and hydrogenation under Raney Ni which has been proved to be a suitable catalyst for hydrogenolysis. Low conversion and less coke formation were observed in the results of hydrogenation under Raney Ni, which is caused by the low reactivity of Raney Ni. Hydrogenolysis or hydrogenation can occur only on the macropore surface of Raney Ni, which reduces the catalytic reactivity of hydrogenation and eliminates coke formation. Ru/C and Rh/C both have high capability toward depolymerization of lignin, recovering 74.85 wt.% and 76.21 wt.% of hydrogenated lignin, respectively. The active sites in the large surface area of the catalysts were supplied for hydrogenation[19]. According to the BET results, both Ru/C and Rh/C contain a large surface area (in Chapter 3.3.4), while Ru/C has a relatively larger pore. So that, the conversion rate under Ru/C is slightly high but not obvious.

Fig. 4-2(b) depicts the influence of different solvents (THF, ethanol, acetone) used in the hydrogenation. The solubility is the key factor in this research. Ethanol being widely used for hydrogenolysis of lignin[33][34], from which the H-EOL's yield was lower than that in another two types of solution due to the alcoholysis of ethanol. Since the increasing dispersion is beneficial to prevent the occurrence of repolymerization, EOL completely dissolved in acetone, has less coke formed and more liquid products obtained. It is consistent with the conclusions of Liu's group[35]. As for THF solvent, the excellent dissolution capacity of THF can facilitate the occurrence of hydrogenation. Coke also accounted for a relatively high percentage, because of the recombination of intermediates. Repolymerization of intermediates occurs in parallel with the cleavage of lignin connection bonds.

In Fig. 4-2(c), the H-EOL's yield slightly increased from 74.85 wt.% to 87.11 wt.% with increasing of the reaction time from 1 to 7 hours. That is consistent with the conclusion in the literature that increasing simply the reaction time is insufficient for obtaining high yields of monomers[36]. The coke yield also rose significantly when prolonging the time to 7 hours. Long reaction time causes condensation of lignin-derived molecules, which is also observed in other literature[37]. The plausible reasons for the high yields of coke are the recombination of intermediates or oligomer compounds which are not stable and easy to form the coke products.

As shown in Fig. 4-2(d), less H-EOL was recovered after increasing the temperature. It is widely accepted that the depolymerization of lignin was the first priority to occur, the internal alkyl-aryl ether bonds suffered from the cleavage, especially under high temperatures [14]. The temperature must be the main factor contributed to the depolymerization of lignin. Fig. 4-2(d) shows the depolymerization of EOL is drastically enhanced above 250 °C, and only 47.99 wt.% of the H-EOL can be recovered after the reaction.

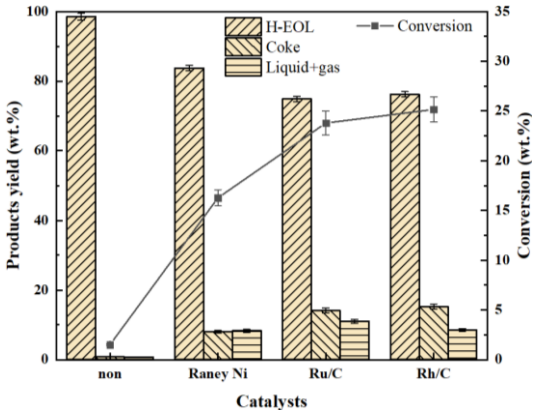

(a)

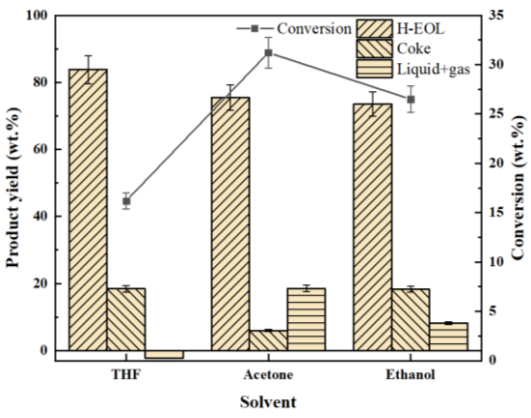

(b)

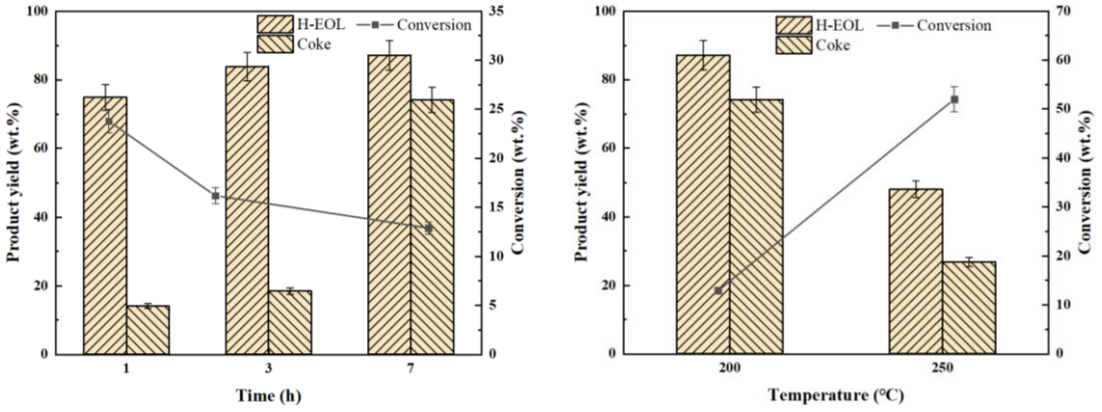

(c) (d)

Fig. 4- 2 The effect of (a) catalysts, (b) solvent, (c) reaction time, (d) temperature on product distribution. Conditions: (a) lignin 100 mg, THF 20 mL, catalyst 50 mg, 200 ℃, 1 hour; (b) lignin 100 mg, solvent 20 mL, Ru/C 50 mg, 200 ℃, 3 hours; (c) lignin 100 mg, THF 20 mL, Ru/C 50 mg, 200 ℃; (d) lignin 100 mg, THF 20 mL, Ru/C 50 mg, 7 hours.

4.4.2 Characterization of hydrogenated organosolv lignin

In the hydrogenation process, EOL underwent the decomposition of macromolecular structure and hydrogen transfer, and then converted into H-EOL samples, liquid products, and coke. In order to reveal the effect of hydrogenation on the chemical structure of lignin, the characterization of EOL and H-EOL samples obtained under different conditions were studied.

Table 4-2 shows the elemental analysis of EOL and H-EOL samples. The percentages of carbon and hydrogen both increased after the hydrogenation with and without the catalysts. At the same time, the yield of oxygen severely reduced, which means the pretreating process is effective for lignin to increase the hydrogen content and reduce the oxygenated compounds. The hydrogen to carbon atomic effective ratio (H/C_{eff} ratio) and degree of unsaturation (Ω) were calculated and shown in Table 4-2.

H/C_{eff} ratio was introduced by Vispute and his groups[38], which is related to the yield of aromatic and olefins. Catalytic hydrogenation can significantly raise H/C_{eff} ratio of lignin to 0.70 and decrease Ω to 3.37 under the function of Ru/C catalyst, even higher under Rh/C. Pan and co-workers also found that in a course of preheating Hami sub-bituminous coal, the addition of hydrogen sources achieved to raise the hydrogen-to-carbon ratios and the thermal reactivity of solid residue[39]. Ru/C and Rh/C both exhibited excellent performance for hydrogenation with high activity.

Table 4- 2 The elemental composition of EOL and H-EOL samples pretreated with the presence of different catalysts.

Sample		**Elemental composition[a]**					**H/C_{eff}**	**Ω[d]**
	Catalysts	C	H	O	S	N	**ratio[c]**	
EOL	-	68.42	5.94	25.34	0.12	0.18	0.49	3.73
	non	69.85	6.27	23.73	0.02	0.13	0.57	3.69
H-EOL[b]	Ru/C	70.00	6.92	22.89	0.07	0.12	0.70	3.37
	Rh/C	70.38	7.13	22.29	0.08	0.12	0.74	3.30

[a]: On a dry basis

[b]: The H-EOL samples were both prepared at 200 ℃ for 1 hour with 3 MPa H_2, THF as solvent.

[c]: $H/C_{eff}=(H-2O)/C$[38]

[d]: Degree of unsaturation $\Omega=(2C+2-H)/2$

FTIR spectroscopy of EOL and H-EOL samples are shown in Fig. 4-3. According to the FTIR spectra assignment (Table 4-3)[40], the peak in the range of 3000-3600 cm^{-1} is assigned to the O-H stretching in phenolic and aliphatic groups. The decreasing of O-H group proved that the hydrodeoxygenation reaction took place. The ether linkages

(β-O-4, α-O-4 and 4-O-5) are weaker and easier to be cleaved than C-C bonds (β-1, α-1 and 5'-5) considering the bond dissociation enthalpies[41]. Thus, the peaks of C-O ether (1212-1224 cm^{-1}), hydroxyl group, and carbonyl group (1674-1709 cm^{-1}) obviously decreased after hydrogenation. And aliphatic ($-CH_3$, $-CH_2$, C=C) group was the only functional group increased after hydrogenation, which is in agreement with the conclusion of Iretskii' s group[13]. They suggested that the elevated number of aliphatic groups means ring alkylation may occur concurrently with the reduction. It reveals the occurrence dominate of alkylation, which was proved to be produced even in the oil phase[42]. Elemental results in this work are consistent with the above descriptions. As observed in Fig. 4-3(a), the synergetic effects of Ru/C catalyst and THF might suppress the depolymerization of lignin and improve the stretching vibration of aliphatic groups, which proved well the occurrence of alkylation[43]. Reaction time shows less effect on the functional groups than catalysts (in Fig. 4-3(b)). Slightly reduction of oxygenated groups has been observed on H-EOL when increasing the reaction time. The reaction time over 3 hours could result in the slightly grown-up of aromatic groups and aliphatic groups' vibration.

Table 4- 3 The assignment and functional groups for FTIR.

Functional group	**Assignment**	**Absorption (cm^{-1})**
O-H stretching in aliphatic and phenolic groups	phenol, alcohols	3600-3000
C=C stretching	Alkene group	2956
$-CH_3$ stretching	Alkane group	2928
$-CH_2$ stretching	Aliphatic methylene	2865
Non-conjugated C=O stretching	carbonyl/carboxyl	1709

Conjugated C=O stretching		1674
Aromatic skeleton vibration Conjugated C=C stretching	Aromatic rings	1600, 1513, 1462
Aliphatic C−H in methyl groups and phenolic	Phenolic group	1310-1390
O-H stretching, O-H deformation		
C-O stretching	Aromatic ether	1270
C−O stretching	Aryl-alkyl ether linkage	1224-1212
C-O stretching	Alcohols	1153, 1091, 1031
C-O stretching	Alkyl ether	1124
Benzene derivatives	-	858, 810,768

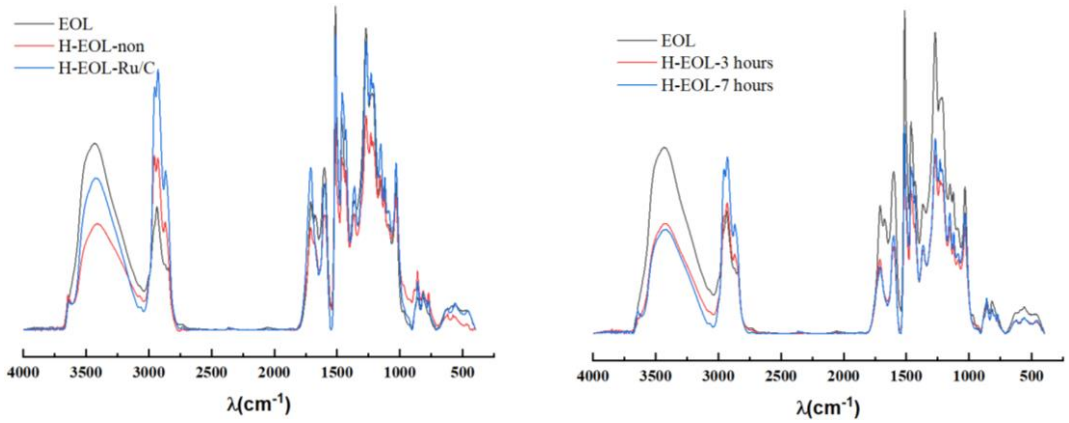

(a) (b)

Fig. 4- 3 The FTIR spectroscopy of EOL and H-EOL samples. (a) H-EOL samples with and without catalyst (other conditions: 200 ℃, 1 hour, 3 MPa H_2); (b) H-EOL samples pretreated for 3 hours and 7 hours (other conditions: 200 ℃, Ru/C, 3 MPa H_2).

Chemical assignments for major peaks in ^{1}H NMR and ^{13}C NMR spectra are according to the literature[29], showing in Table 4-4 and 4-5. Fig. 4-4 and Fig. 4-5 are showing ^{1}H NMR patterns of EOL and H-EOL, respectively.

Table 4- 4 Chemical shift assignments for major peaks in ^{1}H NMR spectrum

δ/ppm	**Assignment**
0.7-1.4	Non-oxygenated aliphatic region
1.6-2.2	Aliphatic acetate
2.2-2.5	Aromatic acetate
2.5-3.0	Hydrogens on C-β in acetylated β and β-β substructures. Also, hydrogens on $-CH_2COOH$ moieties of fatty acids
3.0-3.5	Hydrogen in methoxyl groups
3.5-4.0	Methoxyl hydrogens in aromatic moieties of acetylated substructures, hydrogens on C-β of β-5 and axial bydrogens on C-γ of β-β substructures
4.5-5.2	Hydrogens on C-β of acetylated β-O-4 substructures, on C-γ of cinnamyl alcohol acetate moieties in acetylated substructures, and on C-α of acetylated β-β substructures.
6.1-8.0	Aromatic region
9.0-10.0	Hydrogens of aldehyde groups in acetylated substructures of cinnamaldehyde moieties

Table 4- 5 Chemical shift assignments for major peaks in ^{13}C NMR spectrum

δ/ppm	**Assignment**
193.4	C=O in φ–CH=CH–CHO, C=O in φ–C(=O)CH(–O φ)–C–
191.6	C=O in φ–CHO
169.4	Ester C=O in $R–C(=O)OCH_3$
166.2	C=O in φ–COOH, ester C=O in φ–C(=O)OR
156.4	C–4 in H-units
152.9	C–3/C–3’ in etherified 5–5 units, C–α in φ–CH=CH–CHO units

152.1	C–3/C–5 in etherified S units and B ring of 4–O–5 units
151.3	C–4 in etherified G units with α–C=O
149.4	C–3 in etherified G units
149.1	C–3 in etherified G type β–O–4 units
146.8	C–4 in etherified G units
146.6	C–3 in non-etherified G units (β–O–4 type)
145.8	C–4 in non-etherified G units
145.0	C–4/C–4’ of etherified 5–5 units
143.3	C–4 in ring B of β–5 units, C–4/C–4’ of non–etherified 5–5 units
134.6	C–1 in etherified G units
132.4	C–5/C–5’ in etherified 5–5 units
131.1	C–1 in non–etherified 5–5 units
129.3	C–β in φ–CH=CH–CHO
128.0	C–α and C–β in φ–CH=CH–CH2OH
125.9	C–5/C–5’ in non–etherified 5–5 units
122.6	C–1 and C–6 in φ–C(=O)C–C units
119.9	C–6 in G units
118.4	C–6 in G units
115.1	C–5 in G units
114.7	C–5 in G units
111.1	C–2 in G units
110.4	C–2 in G units
71.8	C–α in G type β–O–4 units (*erythro*)
71.2	C–α in G type β–O–4 units (*threo*), C–γ in G type β–β
63.2	C–γ in G type β–O–4 units with α–C=O
62.8	C–γ in G type β–5, β–1 units

60.2	C–γ in G type β–O–4 units
55.6	C in φ–OCH3
53.9	C–β in β–β units
53.4	C–β in β–5 units
29.1	Aliphatic
15.2	Aliphatic

* G = guaiacyl, S = syringyl.

The ^{1}H Nuclei in lignin present in similar but not identical, and chemical environments give rise to intensive overlap of signals in a spectra, so that the presence of carbohydrates would make the spectra even more complex[44]. According to Table 4-4, the signals in the range of 2.2-2.5 ppm, 3.5-4 ppm, and 6.1-8.0 ppm are assigned to aromatic acetate, hydrogen in the methoxyl groups of aromatic acetylated substructures and connection bonds (β-O-4, β-β, β-1and C-α), as well as aromatic region, respectively. It is apparent that the intensity of the above signals has a sharp decrease after hydrogenation, especially the intensity of the peak for hydrogen in methoxyl groups and connection bonds. The reason might be related to the cleavage of ether bonds and demethoxylation reaction of syringyl (S) type units and guaiacyl (G) units during this process. Combined with above characterization, the content of aliphatic -OH diminished, while -COOH group (2.5-3 ppm) increased during the depolymerization. The drop in the aromatic region and no change of the aliphatic region (0.7-2.2 ppm) may be attributable to the following reasons: (1) hydrogenation of raw lignin also formed cyclohexanes, which also decreases the aromatic region and generates signal of aliphatic; (2) side chains in lignin cleaved and/or rearranged under the hydrogenation process.

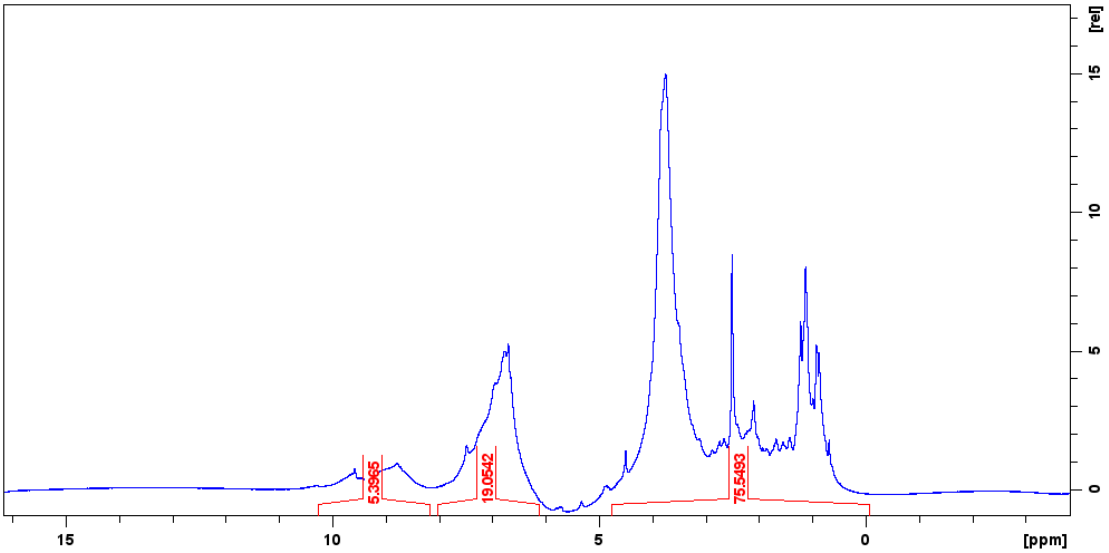

Fig. 4- 4 The ^{1}H NMR spectra of EOL.

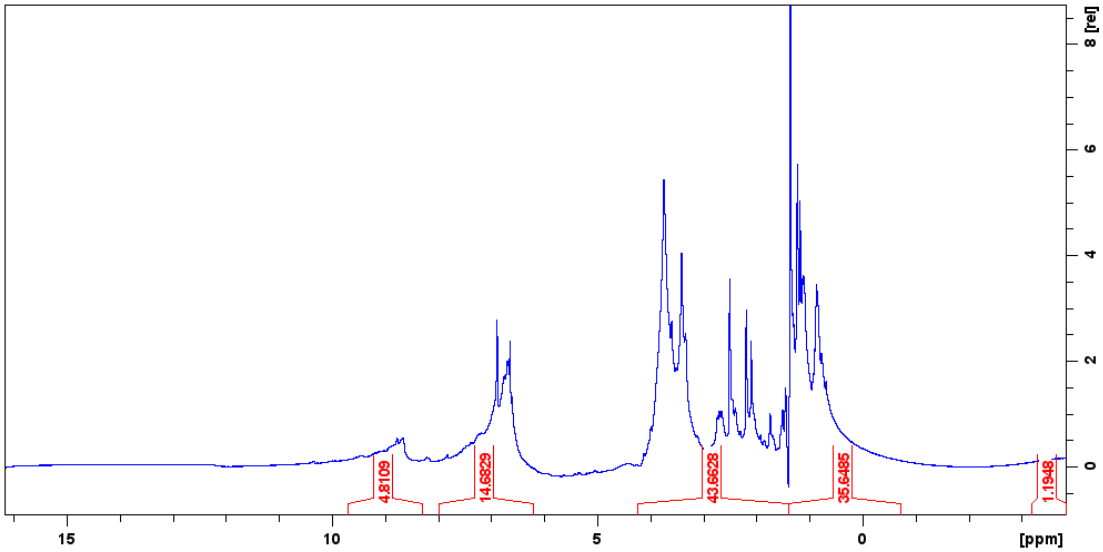

Fig. 4- 5 The ^{1}H NMR spectra of H-EOL (hydrogenation conditions: 250 ℃, 3 MPa, Ru/C, 3 hours).

The ^{13}C NMR spectra of EOL and H-EOL are demonstrated in Fig. 4-6 and Fig. 4-7, respectively. Generally, DMSO-d6 is acquired at around 40 ppm of ^{13}C NMR spectra. As shown in Fig. 4-6 and Fig. 4-7, the ^{13}C NMR intensity of H-EOL is stronger than that of EOL, which might be attributed to the sensitivity of ^{13}C NMR is too low for macromolecular cross-linked compounds. So that, the peaks of spectroscopy (Fig. 4-6)

are limited, even preparing high concentration of lignin solution for detection. However, it can be seen that the spectrum of H-EOL shows many peaks, which should be due to partial depolymerization of lignin through pretreatment, and the structure of H-EOL becomes more evident and detectable. The signals in the range of 60-72 ppm, 110-120 ppm, and 145-152 ppm appear to be apparent spectral peaks, which all represent carbon in G-type units. It is probably attributable to the fact that S-type units were more susceptible to performing demethoxylation reaction than G-type units[24]. Furthermore, the aliphatic region (15-29.1 ppm) also shows significantly in H-EOL's spectra, in agreement with the corresponding FTIR spectroscopy.

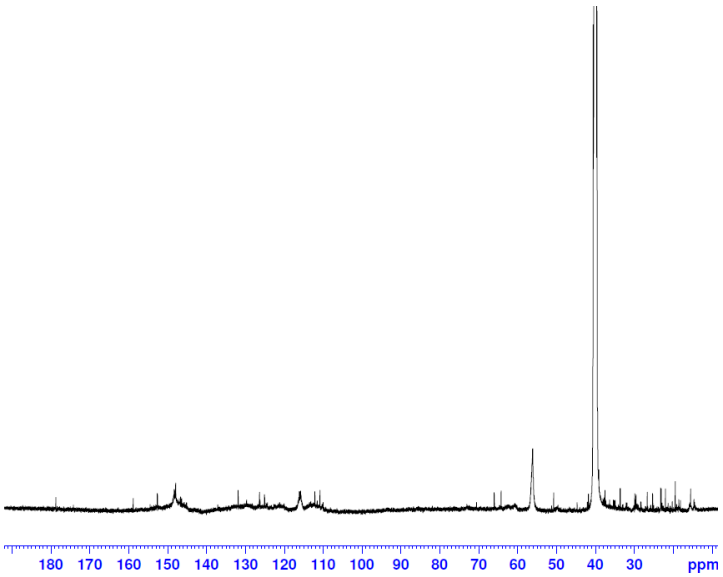

Fig. 4- 6 The ^{13}C NMR spectra of EOL.

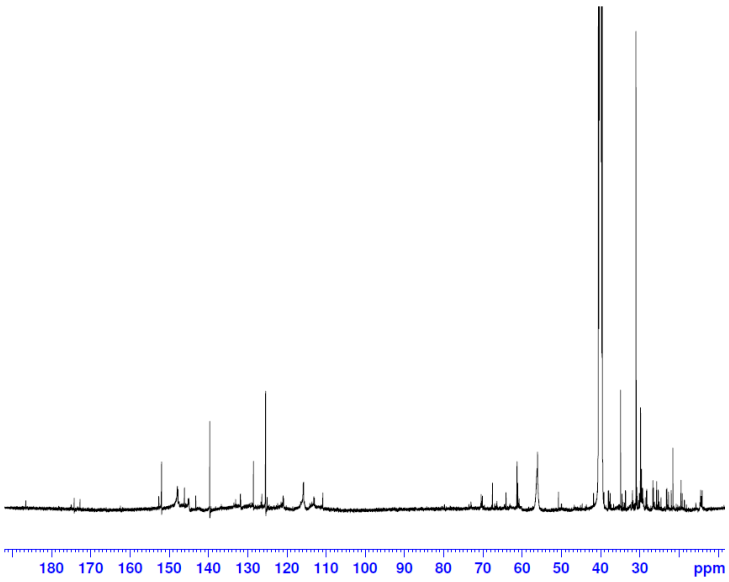

Fig. 4- 7 The ^{13}C NMR spectra of H-EOL (hydrogenation conditions: 250 ℃, 3 MPa, Ru/C, 3 hours).

Thermal degradation of lignin is mainly related to its inherent structure and internal functional groups. Further characterization of lignin samples after hydrogenation is presented by TG and DTG curves.

As shown in Fig. 4-8, the TG and DTG curves of H-EOL samples were totally different from those of EOL. For the DTG curve of EOL, the main degradation process can be clearly seen occurring in the wide range of 200-600 ℃. But for H-EOL, the DTG curve was separated into three stages. The first stage was 100-150 ℃, which was attributed to the dehydration of inherent moisture or the cleavage of hydroxyl groups[45]. When the temperature increases to 150-300 ℃, there is another small peak shown, which is different from the EOL. This is attributed to the occurrence of catalytic depolymerization and the presence of lignin fragments during hydrogenation. According to the modification scheme proposed by Hrutfiord[46], hydrolysis and thermolysis reactions are the initial step that partially break down the lignin into fragments. The third is the major decomposition stage in the range of 300-600 ℃, which is severe than

that of EOL.

In Fig. 4-8(a), the DTG curves of H-EOL samples with and without Ru/C have similar decomposition periods. However, the peaks' intensity of the H-EOL obtained with catalyst was higher than that without catalyst. From the TG curve, the yield of char residue decreased from 50 wt.% of EOL to 32 wt.% of H-EOL after hydrogenation with Ru/C. After pretreating the lignin samples with the hydrogenation process, fewer residues remained in the thermal depolymerization process. Lignin oligomers were formed owing to the catalyst, which can be easily suffered from thermal degradation at lower temperatures.

The influence of reaction time on thermal degradation of lignin samples is shown in Fig. 4-8(b). Further increasing reaction time to 7 hours has a limited effect on the TG and DTG curves of H-EOL. The reaction time does not dramatically change the decomposition properties of H-EOL samples, which is in accord with the above characterization of H-EOL samples.

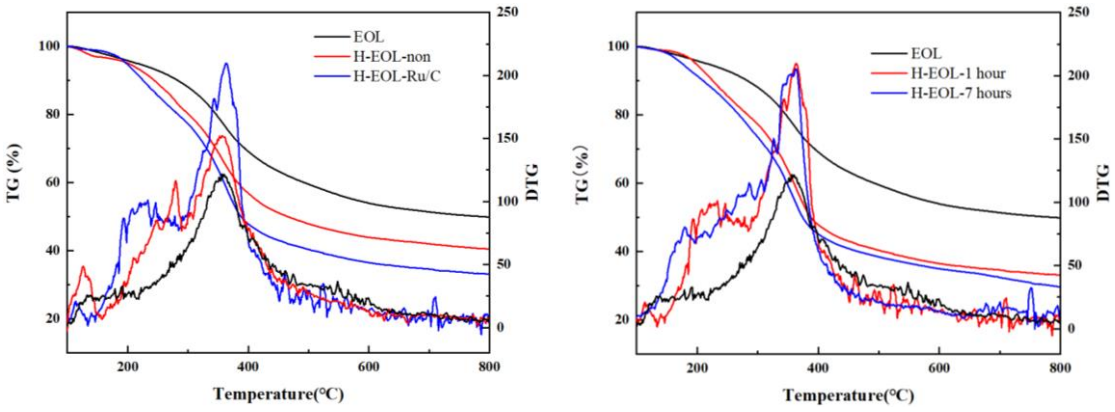

(a) (b)

Fig. 4- 8 The TG/DTG curves of the EOL and H-EOL samples. (a) effects of catalyst (with and without catalyst); (b) effects of reaction time (reaction time: 1 and 7 hours). Other conditions: EOL: 100 mg; solvent: THF 20 mL; H_2: 3 MPa; temperature: 200 °C.

4.4.3 Fast pyrolysis of hydrogenated organosolv lignin

Under different hydrogenation conditions, the chemical properties and molecular structure of solid products are various. The pyrolyzed products from EOL and H-EOL were detected by GC-TCD/FID, shown in Table 4-6. Fast pyrolysis of EOL and H-EOL samples were all performed at 850 ℃ under a hydrogen atmosphere. H-EOL1 recovered from the hydrogenation in the absence of catalyst mainly suffered from depolymerization of side chains. Therefore, less yield of CO, CO_2, H_2O and CH_4 than that of EOL and obviously yielding the char to 25.24 wt.% have been observed here. Compared with H-EOL1, the other H-EOL samples had higher thermal activity after hydrogenation, the char yield of both H-EOL2 and H-EOL3 even decreased to around 10 wt.%. The inorganic oxygenated products (CO_2 and H_2O) from H-EOL2 and H-EOL3 decreased lower than that from H-EOL1. The C1-C3 hydrocarbons, benzene, and toluene from H-EOL2 and H-EOL3 have further increased to a similar percentage. Ru/C and Rh/C have similar catalytic functions on hydrogenation, which is in accordance with the elemental analysis and FTIR spectra of H-EOL.

When further increasing the hydrogenation temperature to 250 ℃ (H-EOL4 and H-EOL5), the char yield increased to 14.29 wt.% and 15.38 wt.%, respectively. It proves that the H-EOL samples have been pretreated under higher temperatures suffered from more cleavage of functional groups and became more stable. The yield of hydrocarbon compounds from H-EOL4 has increased after pretreating at 250 ℃ for 3 hours, and has slight further increased with increasing the reaction time to 7 hours (see the results of H-EOL5). Jongerius et al. also got the conclusion that higher amounts of deoxygenated products could be obtained with the increase of hydrogenation time and temperature[37]. The total olefins' yield went up to the maximum value (9.94 wt.%) from H-EOL5, mostly composed of ethylene whose selectivity went to 97.08%. It is thus suggested that hydrogenation can increase the thermal reactivity and selectivity of

hydrocarbon products. It is possibly attributed to the increase of H/C_{eff} ratio in the lignin molecules, proposed by Vispute's research group[38]. However, the further severe condition will enhance the liquefaction of lignin and the formation of coke. Therefore, appropriate hydrogenation conditions should be designed to pretreat raw lignin well.

Table 4- 6 The pyrolyzed products from EOL and H-EOL samples were derived from the different hydrogenation conditions. H-EOL1: non-catalyst, 1 h, 200 ℃; H-EOL2: Ru/C, 1 h, 200 ℃; H-EOL3: Rh/C, 1 h, 200 ℃; H-EOL4: Ru/C, 3 hrs, 250 ℃; H-EOL5: Ru/C, 7 hrs, 250 ℃.

No.	**Pyrolyzed products (wt.%)**	**Retention time (min)**	**Feedstock**					
			EOL	**H-EOL1**	**H-EOL2**	**H-EOL3**	**H-EOL4**	**H-EOL5**
1	CO	0.82	14.63	13.06	15.07	13.34	12.75	11.36
2	CO_2	1.89	4.09	3.32	3.08	2.76	3.13	2.46
3	H_2O	9.45	15.52	11.91	10.48	10.43	9.02	8.2
4	CH_4	1.08	21.16	17.04	22.96	23.69	23.77	23.95
5	C_2H_4	3.43	4.98	5.99	8.31	8.30	9.33	9.65
6	C_2H_6	4.85	1.65	2.04	3.24	3.36	3.23	3.9
7	C_3H_6	17.15	0.09	0.09	0.12	0.13	0.16	0.21
8	C_3H_8	18.27	0.002	0.005	0.007	0.007	0.007	0.01
9	CH_3OH	21.75	0.05	0.09	0.12	0.14	0.08	0.09
10	C_4H_8	26.83	0.03	0.04	0.06	0.06	0.07	0.08
11	C_4H_{10}	27.51	0.33	0.004	0.006	0.006	0.008	0.008
12	C_2H_5OH	27.89	0.004	0.006	0.008	0.009	0.01	0.01
13	Iso-PrOH	30.40	0.005	0.001	0.001	-	0.001	0.01
14	Acetic acid	33.92	0.85	0.93	1.13	1.2	1.04	1.44
15	Benzene	40.65	5.09	4.57	6.38	6.61	6.42	6.62
16	Toluene	47.36	0.77	0.98	1.31	1.65	1.39	1.77
Char			17.24	25.34	10.83	10.0	14.29	15.38
Undetected product (diff.)			13.51	14.58	16.89	18.31	15.294	14.85
Total			100	100	100	100	100	100

A more intuitive comparison is shown in Fig. 4-9. Considering about solid yield from hydrogenation and olefins yield from fast pyrolysis, H-EOL4 recovered from the

hydrogenation condition (250 °C, 3 hours, THF, Ru/C, 3 MPa H_2) was chosen to compare with EOL here. The yield of alkanes and olefins has been found to increase simultaneously and obviously, methane and ethylene are the main compounds in these two groups, respectively. Caballero et al. also claimed that the formation of ethylene is linearly correlated with that of methane, and methane formation is favoured at low yields of CO and CO_2[47]. Besides that, the aromatics (benzene and toluene) yield also increased from 5.85 wt.% of EOL to 7.81 wt.% of H-EOL4. The inorganic compounds, including CO, CO_2 and H_2O, had a sharp reduction after hydrogenation due to the cleavage of side-chain groups. The formation of the oxygenated compounds (CH_3OH, C_2H_5OH, iso-propanol, acetic acid) is mainly attributed to the increased carbonyl groups, and reacted with hydrogen atoms in the subsequent fast pyrolysis process.

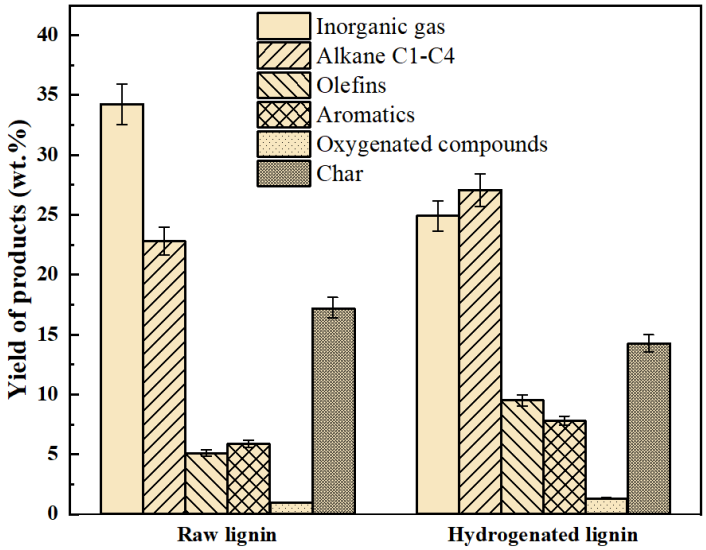

Fig. 4- 9 The comparison of derived volatile products from raw organosolv lignin (EOL) and hydrogenated lignin (H-EOL4).

There listed some recent literature about using catalytic fast pyrolysis to improve the selectivity of products, where zeolite-type catalysts proving to be the most selective for olefins and aromatic hydrocarbon products (Table 4-7). We can see, without catalyst

(Entry 1), only a trace number of olefins can be obtained and 56.4 wt.% of kraft lignin was transferred into useless char. With the HZSM-5 catalyst (Entry 7), the olefins and aromatics yield slightly increased to 1.3 wt.% and 0.78 wt.%, while char yield also increased. In these literature, the highest olefins' yield is 5.3 wt.% and yield of benzene and toluene is 2.23 wt.%, which is catalyzed by 6 wt.% La/HZSM-5 (Entry 2). In this work, the lignin pretreated under hydrogenation can produce 9.94 wt.% of light olefins and 8.39 wt.% of benzene and toluene. The hydrogenation process as a pretreatment, changes the structure of the lignin, and partial depolymerization as well as reduction makes the H-EOL more suitable as a pyrolysis feedstock. Low polymerization and high H/C_{eff} ratio allow producing more olefins and aromatic hydrocarbons. This method seems to be more efficient than catalytic fast pyrolysis to obtain olefins and aromatic hydrocarbons.

Table 4- 7 The comparison of olefins and aromatics yield with other literature.

Entry	Feedstock	Catalyst	Temperature	Olefins and aromatics yield	Char yield	Ref.
1	Kraft lignin	-	650 ℃	Olefins: 0.2 wt.% Aromatics: 0.1 wt.%	56.4 wt.%	[48]
2	Lignin	6 wt.% La/HZSM-5	600 ℃	Olefins: 5.3 wt.% Benzene and toluene: 2.23 wt.%	53.7 C-mol.%	[49]
3	Alkali lignin	3 wt.% Fe-ZSM-5	600 ℃	Olefins: 3.8 C-mol.% Benzene and toluene: 2.9 C-mol.%	-	[6]
4	Lignin	3 wt.% Fe-ZSM-5	600 ℃	Olefins: 1.26 wt.% Oil: 31.69 wt.%	59.77 wt.%	[7]
5	Milled wood lignin	HZSM-5	500 ℃	Olefins: 4.0 C-mol.% Benzene and toluene: 1.7 C-mol.%	41.2 C-mol.%	[50]
6	Klason lignin	HZSM-5	650 ℃	Olefins: 3.64 wt.% Benzene and toluene: 5.7 wt.%	-	[9]
7	Kraft	HZSM-5-25	650 ℃	Olefins: 1.3 wt.%	65.5	[48]

	lignin			Benzene and toluene: 0.78 wt.%	wt.%	
This work	Hydrogenated lignin	-	850 ℃	Olefins: 9.94 wt.% Benzene and toluene: 8.39 wt.%	14.29 wt.%	-

4.4.4 The proposed reaction pathways

Combination of the above findings, the proposed reaction scheme of lignin hydrogenation is illustrated in Figure 4-10. There are three kinds of parallel process for catalytic hydrogenation of raw lignin. Hydrogenolysis predominately happened on the ether bonds (β-O-4, α-O-4 and 4-O-5), the hydrogen atoms were then added into free radicals[51]. In this process, phenolic intermediates were formed, which subsequently followed hydrogenation and hydrodeoxygenation. Hydrogenation might happen on aromatic rings or C=O groups through catalysis of Ru/C, the extent of which is dictated by the free energy barrier for this pathway and the availability of the catalyst's active sites on the surface. It should be noted that the occurrence of hydrolysis or hydrodeoxygenation is the main reason for decreasing of oxygen, like, -OH group and $-OCH_3$ group, especially in S-type units. Nevertheless, higher bond dissociation energies of Caryl-methoxyl bonds than those of C-O bonds in aryl ethers makes the rate of demethoxylation slower than the decomposition of connection bonds[14].

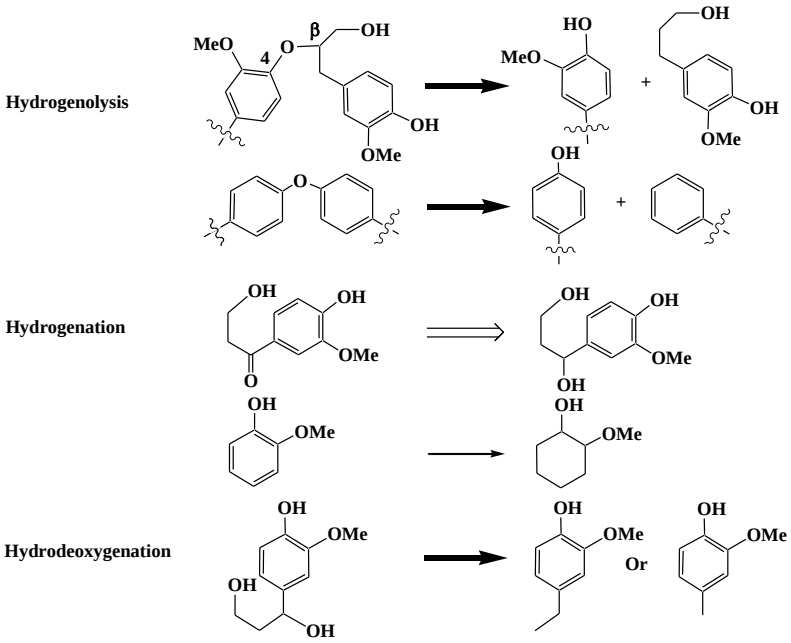

Fig. 4- 10 The proposed schematic of reaction pathways for lignin hydrogenation.

4.5 Conclusions

Hydrogenation is a promising technology to change the structure and modify the chemical properties of lignin. The present study checked the characterization of the H-EOL under different hydrogenation conditions, and investigated the thermal decomposition properties of H-EOL. The following conclusions were drawn.

(1) The yield of H-EOL showed a direct correlation with catalysts, solvent, time, and temperature. Among them, the temperature was a crucial parameter for yielding the solid product. The H-EOL yield sharply decreased from 87.11 to 47.99 wt.% when the hydrogenation temperature increased from 200 to 250 ℃, which signifies higher temperature encourages more cleavage of internal linkages and functional groups.

(2) Compared with EOL, the H/C_{eff} ratio of H-EOL samples has increased. The content of oxygen and sulfur significantly decreased after pretreatment due to the thermal decomposition of ether bonds and side-chain groups. The vibrational stretching of O-H groups C-O, and C=O of H-EOL becomes weaker, while the aliphatic group is

the only functional groups increased after hydrogenation. This phenomenon can be more pronounced in response to a higher temperature and longer reaction time. Hydrogenolysis of ether bonds, hydrodeoxygenation of hydroxyl group, demethoxylation and alkylation happened in the hydrogenation process successively

(3) EOL can produce more light hydrocarbons through the fast pyrolysis at the hydrogen atmosphere. An activated atmosphere can promote thermochemical decomposition. Almost all compounds except CO_2 detected by GC-TCD/FID were intensively yielded. Less char was remained after pyrolysis under hydrogen atmosphere, since the hydrogen can react with the intermediates and suppress the repolymerization.

(4) The TGA results signify that H-EOL samples have higher reactivity which can be easily decomposed at relatively low temperatures. At the same time, fast pyrolysis of H-EOL samples has been checked, in which the maximum yield of light olefins is 9.94 wt.% from H-EOL5. Moreover, the yield of methane, alkane, benzene, and toluene also has a marked increase after hydrogenation pretreatment. The effective hydrogenation pretreatment can valorize the lignin sample. More than 85 wt.% of H-EOL can be converted into volatile.

(5) Considering the H-EOL yield of hydrogenation and the product distribution of fast pyrolysis, the hydrogenation condition for H-EOL4 is considered as a picked condition. When the time was further prolonged (H-EOL5), only around half of feedstock can be recovered as the solid product from hydrogenation. Thus, more effective pretreatment conditions are required. Suppressing liquefaction of lignin and modification of lignin structure would be further looked forward. That should be the outlook of future work for this integrated process.

4.6 Reference

[1] E. Novaes, M. Kirst, V. Chiang, H. Winter-Sederoff, R. Sederoff, Lignin and biomass: A negative correlation for wood formation and lignin content in trees, Plant Physiol. 154 (2010) 555–561. https://doi.org/10.1104/pp.110.161281.

[2] J. Zakzeski, A.L. Jongerius, P.C.A. Bruijnincx, B.M. Weckhuysen, Catalytic lignin valorization process for the production of aromatic chemicals and hydrogen, ChemSusChem. 5 (2012) 1602–1609. https://doi.org/10.1002/cssc.201100699.

[3] S.A.-Q. Quideau S. A4 - Ralph, J., Facile large-scale synthesis of coniferyl, sinapyl, and p-coumaryl alcohol, J. Agric. Food Chem. v. 40 (1992) 1108-1110–1992 v.40 no.7. https://doi.org/10.1021/jf00019a003.

[4] G. Jiang, D.J. Nowakowski, A. V. Bridgwater, Effect of the temperature on the composition of lignin pyrolysis products, Energy and Fuels. 24 (2010) 4470–4475. https://doi.org/10.1021/ef100363c.

[5] K. Wang, K.H. Kim, R.C. Brown, Catalytic pyrolysis of individual components of lignocellulosic biomass, Green Chem. 16 (2014) 727–735. https://doi.org/10.1039/c3gc41288a.

[6] M. Yang, J. Shao, Z. Yang, H. Yang, X. Wang, Z. Wu, H. Chen, Conversion of lignin into light olefins and aromatics over Fe/ZSM-5 catalytic fast pyrolysis: Significance of Fe contents and temperature, J. Anal. Appl. Pyrolysis. 137 (2019) 259–265. https://doi.org/10.1016/j.jaap.2018.12.003.

[7] S. Zhang, M. Yang, J. Shao, H. Yang, K. Zeng, Y. Chen, J. Luo, F.A. Agblevor, H. Chen, The conversion of biomass to light olefins on Fe-modified ZSM-5 catalyst: Effect of pyrolysis parameters, Sci. Total Environ. 628–629 (2018) 350–357. https://doi.org/10.1016/j.scitotenv.2018.01.316.

[8] W. Huang, F. Gong, M. Fan, Q. Zhai, C. Hong, Q. Li, Production of light olefins

by catalytic conversion of lignocellulosic biomass with HZSM-5 zeolite impregnated with 6wt.% lanthanum, Bioresour. Technol. 121 (2012) 248–255. https://doi.org/https://doi.org/10.1016/j.biortech.2012.05.141.

[9] H. Yang, K. Norinaga, J. Li, W. Zhu, H. Wang, Effects of HZSM-5 on volatile products obtained from the fast pyrolysis of lignin and model compounds, Fuel Process. Technol. 181 (2018) 207–214. https://doi.org/10.1016/j.fuproc.2018.09.022.

[10] K.M. Torr, D.J. van de Pas, E. Cazeils, I.D. Suckling, Mild hydrogenolysis of in-situ and isolated Pinus radiata lignins, Bioresour. Technol. 102 (2011) 7608–7611. https://doi.org/https://doi.org/10.1016/j.biortech.2011.05.040.

[11] W. Xu, S.J. Miller, P.K. Agrawal, C.W. Jones, Depolymerization and hydrodeoxygenation of switchgrass lignin with formic acid, ChemSusChem. 5 (2012) 667–675. https://doi.org/10.1002/cssc.201100695.

[12] K. Barta, G.R. Warner, E.S. Beach, P.T. Anastas, Depolymerization of organosolv lignin to aromatic compounds over Cu-doped porous metal oxides, Green Chem. 16 (2014) 191–196. https://doi.org/10.1039/c3gc41184b.

[13] K. Barta, T.D. Matson, M.L. Fettig, S.L. Scott, A. V. Iretskii, P.C. Ford, Catalytic disassembly of an organosolv lignin via hydrogen transfer from supercritical methanol, Green Chem. 12 (2010) 1640–1647. https://doi.org/10.1039/c0gc00181c.

[14] S. Kasakov, H. Shi, D.M. Camaioni, C. Zhao, E. Baráth, A. Jentys, J.A. Lercher, Reductive deconstruction of organosolv lignin catalyzed by zeolite supported nickel nanoparticles, Green Chem. 17 (2015) 5079–5090. https://doi.org/10.1039/c5gc02160j.

[15] R. Shu, Y. Xu, P. Chen, L. Ma, Q. Zhang, L. Zhou, C. Wang, Mild Hydrogenation of Lignin Depolymerization Products over Ni/SiO2 Catalyst, Energy and Fuels. 31 (2017) 7208–7213.

https://doi.org/10.1021/acs.energyfuels.7b00934.

[16] S.C. Qi, L. Zhang, H. Einaga, S. Kudo, K. Norinaga, J. ichiro Hayashi, Nano-sized nickel catalyst for deep hydrogenation of lignin monomers and first-principles insight into the catalyst preparation, J. Mater. Chem. A. 5 (2017) 3948–3965. https://doi.org/10.1039/c6ta08538e.

[17] Q. Song, J. Cai, J. Zhang, W. Yu, F. Wang, J. Xu, Hydrogenation and cleavage of the C-O bonds in the lignin model compound phenethyl phenyl ether over a nickel-based catalyst, Cuihua Xuebao/Chinese J. Catal. 34 (2013) 651–658. https://doi.org/10.1016/s1872-2067(12)60535-x.

[18] X. Cui, A.E. Surkus, K. Junge, C. Topf, J. Radnik, C. Kreyenschulte, M. Beller, Highly selective hydrogenation of arenes using nanostructured ruthenium catalysts modified with a carbon-nitrogen matrix, Nat. Commun. 7 (2016). https://doi.org/10.1038/ncomms11326.

[19] A. Bjelić, M. Grilc, M. Huš, B. Likozar, Hydrogenation and hydrodeoxygenation of aromatic lignin monomers over Cu/C, Ni/C, Pd/C, Pt/C, Rh/C and Ru/C catalysts: Mechanisms, reaction micro-kinetic modelling and quantitative structure-activity relationships, Chem. Eng. J. 359 (2019) 305–320. https://doi.org/10.1016/j.cej.2018.11.107.

[20] I. Hita, P.J. Deuss, G. Bonura, F. Frusteri, H.J. Heeres, Biobased chemicals from the catalytic depolymerization of Kraft lignin using supported noble metal-based catalysts, Fuel Process. Technol. 179 (2018) 143–153. https://doi.org/10.1016/j.fuproc.2018.06.018.

[21] V.M. Roberts, V. Stein, T. Reiner, L. Angeliki, X. Li, J.A. Lercher, Towards Quantitative Catalytic Lignin Depolymerization, Chem. – A Eur. J. 17 (2011) 5939–5948. https://doi.org/10.1002/chem.201002438.

[22] T.D. Matson, K. Barta, A. V. Iretskii, P.C. Ford, One-pot catalytic conversion of cellulose and of woody biomass solids to liquid fuels, J. Am. Chem. Soc. 133

(2011) 14090–14097. https://doi.org/10.1021/ja205436c.

[23] C. Chio, M. Sain, W. Qin, Lignin utilization: A review of lignin depolymerization from various aspects, Renew. Sustain. Energy Rev. 107 (2019) 232–249. https://doi.org/10.1016/j.rser.2019.03.008.

[24] X.-J. Shen, P.-L. Huang, J.-L. Wen, R.-C. Sun, A facile method for char elimination during base-catalyzed depolymerization and hydrogenolysis of lignin, Fuel Process. Technol. 167 (2017) 491–501. https://doi.org/https://doi.org/10.1016/j.fuproc.2017.08.002.

[25] J. Long, Y. Xu, T. Wang, Z. Yuan, R. Shu, Q. Zhang, L. Ma, Efficient base-catalyzed decomposition and in situ hydrogenolysis process for lignin depolymerization and char elimination, Appl. Energy. 141 (2015) 70–79. https://doi.org/10.1016/j.apenergy.2014.12.025.

[26] J. Long, Q. Zhang, T. Wang, X. Zhang, Y. Xu, L. Ma, An efficient and economical process for lignin depolymerization in biomass-derived solvent tetrahydrofuran, Bioresour. Technol. 154 (2014) 10–17. https://doi.org/https://doi.org/10.1016/j.biortech.2013.12.020.

[27] X.-J. Shen, P.-L. Huang, J.-L. Wen, R.-C. Sun, A facile method for char elimination during base-catalyzed depolymerization and hydrogenolysis of lignin, Fuel Process. Technol. 167 (2017) 491–501. https://doi.org/https://doi.org/10.1016/j.fuproc.2017.08.002.

[28] J.M. Cho, S. Chu, P.J. Dauenhauer, G.W. Huber, Kinetics and reaction chemistry for slow pyrolysis of enzymatic hydrolysis lignin and organosolv extracted lignin derived from maplewood, Green Chem. 14 (2012) 428.

[29] T.-Q. Yuan, S.-N. Sun, F. Xu, R.-C. Sun, Characterization of Lignin Structures and Lignin–Carbohydrate Complex (LCC) Linkages by Quantitative 13C and 2D HSQC NMR Spectroscopy, J. Agric. Food Chem. 59 (2011) 10604–10614. https://doi.org/10.1021/jf2031549.

[30] H.-M. Yang, S. Appari, S. Kudo, J. Hayashi, K. Norinaga, Detailed Chemical Kinetic Modeling of Vapor-Phase Reactions of Volatiles Derived from Fast Pyrolysis of Lignin, Ind. Eng. Chem. Res. 54 (2015) 6855–6864. https://doi.org/10.1021/acs.iecr.5b01289.

[31] K. Norinaga, O. Deutschmann, Detailed kinetic modeling of gas-phase reactions in the chemical vapor deposition of carbon from light hydrocarbons, Ind. Eng. Chem. Res. 46 (2007) 3547–3557. https://doi.org/10.1021/ie061207p.

[32] H.-M. Yang, S. Appari, S. Kudo, J. Hayashi, K. Norinaga, Detailed Chemical Kinetic Modeling of Vapor-Phase Reactions of Volatiles Derived from Fast Pyrolysis of Lignin, Ind. Eng. Chem. Res. 54 (2015) 6855–6864. https://doi.org/10.1021/acs.iecr.5b01289.

[33] I. Kristianto, S.O. Limarta, H. Lee, J.M. Ha, D.J. Suh, J. Jae, Effective depolymerization of concentrated acid hydrolysis lignin using a carbon-supported ruthenium catalyst in ethanol/formic acid media, Bioresour. Technol. 234 (2017) 424–431. https://doi.org/10.1016/j.biortech.2017.03.070.

[34] K. Wu, C. Yang, Y. Zhu, J. Wang, X. Wang, C. Liu, Y. Liu, H. Lu, B. Liang, Y. Li, Synthesis-Controlled α- And β-Molybdenum Carbide for Base-Promoted Transfer Hydrogenation of Lignin to Aromatic Monomers in Ethanol, Ind. Eng. Chem. Res. 58 (2019) 20270–20281. https://doi.org/10.1021/acs.iecr.9b04910.

[35] Z. Liu, F.S. Zhang, Effects of various solvents on the liquefaction of biomass to produce fuels and chemical feedstocks, Energy Convers. Manag. 49 (2008) 3498–3504. https://doi.org/10.1016/j.enconman.2008.08.009.

[36] A.L. Jongerius, P.C.A. Bruijnincx, B.M. Weckhuysen, Liquid-phase reforming and hydrodeoxygenation as a two-step route to aromatics from lignin, Green Chem. 15 (2013) 3049–3056. https://doi.org/10.1039/c3gc41150h.

[37] A.L. Jongerius, R.W. Gosselink, J. Dijkstra, J.H. Bitter, P.C.A. Bruijnincx, B.M. Weckhuysen, Carbon nanofiber supported transition-metal carbide catalysts for

the hydrodeoxygenation of guaiacol, ChemCatChem. 5 (2013) 2964–2972. https://doi.org/10.1002/cctc.201300280.

[38] T.P. Vispute, H. Zhang, A. Sanna, R. Xiao, G.W. Huber, Renewable chemical commodity feedstocks from integrated catalytic processing of pyrolysis oils, Science (80-.). 330 (2010) 1222–1227. https://doi.org/10.1126/science.1194218.

[39] P. Hao, Z. Bai, R. Hou, J. Xu, J. Bai, Z. Guo, L. Kong, W. Li, Effect of solvent and atmosphere on product distribution, hydrogen consumption and coal structural change during preheating stage in direct coal liquefaction, Fuel. 211 (2018) 783–788. https://doi.org/10.1016/j.fuel.2017.09.122.

[40] C.G. Boeriu, D. Bravo, R.J.A. Gosselink, J.E.G. Van Dam, Characterisation of structure-dependent functional properties of lignin with infrared spectroscopy, Ind. Crops Prod. 20 (2004) 205–218. https://doi.org/10.1016/j.indcrop.2004.04.022.

[41] R. Parthasarathi, R.A. Romero, A. Redondo, S. Gnanakaran, Theoretical study of the remarkably diverse linkages in lignin, J. Phys. Chem. Lett. 2 (2011) 2660–2666. https://doi.org/10.1021/jz201201q.

[42] M. Kleinert, T. Barth, Towards a lignincellulosic biorefinery: Direct one-step conversion of lignin to hydrogen-enriched biofuel, Energy and Fuels. 22 (2008) 1371–1379. https://doi.org/10.1021/ef700631w.

[43] R. Shu, J. Long, Y. Xu, L. Ma, Q. Zhang, T. Wang, C. Wang, Z. Yuan, Q. Wu, Investigation on the structural effect of lignin during the hydrogenolysis process, Bioresour. Technol. 200 (2016) 14–22. https://doi.org/10.1016/j.biortech.2015.09.112.

[44] C.-L. Chen, D.B.T.-M. in E. Robert, Characterization of lignin by 1H and 13C NMR spectroscopy, in: Biomass Part B Lignin, Pectin, Chitin, Academic Press, 1988: pp. 137–174. https://doi.org/https://doi.org/10.1016/0076-6879(88)61017-2.

[45] Z. Luo, S. Wang, X. Guo, Selective pyrolysis of Organosolv lignin over zeolites with product analysis by TG-FTIR, J. Anal. Appl. Pyrolysis. 95 (2012) 112–117. https://doi.org/10.1016/j.jaap.2012.01.014.

[46] C.W. Dence, The Determination of Lignin, in: S.Y. Lin, C.W. Dence (Eds.), Methods Lignin Chem., Springer Berlin Heidelberg, Berlin, Heidelberg, 1992: pp. 33–61. https://doi.org/10.1007/978-3-642-74065-7_3.

[47] J.A. Caballero, R. Font, A. Marcilla, Pyrolysis of Kraft lignin: Yields and correlations, J. Anal. Appl. Pyrolysis. 39 (1997) 161–183. https://doi.org/10.1016/S0165-2370(96)00965-5.

[48] X. Li, L. Su, Y. Wang, Y. Yu, C. Wang, X. Li, Z. Wang, Catalytic fast pyrolysis of Kraft lignin with HZSM-5 zeolite for producing aromatic hydrocarbons, Front. Environ. Sci. Eng. China. 6 (2012) 295–303. https://doi.org/10.1007/s11783-012-0410-2.

[49] W. Huang, F. Gong, M. Fan, Q. Zhai, C. Hong, Q. Li, Production of light olefins by catalytic conversion of lignocellulosic biomass with HZSM-5 zeolite impregnated with 6wt.% lanthanum, Bioresour. Technol. 121 (2012) 248–255. https://doi.org/10.1016/j.biortech.2012.05.141.

[50] K. Wang, P.A. Johnston, R.C. Brown, Comparison of in-situ and ex-situ catalytic pyrolysis in a micro-reactor system, Bioresour. Technol. 173 (2014) 124–131. https://doi.org/https://doi.org/10.1016/j.biortech.2014.09.097.

[51] Y. Wang, D. Wang, X. Li, G. Li, Z. Wang, M. Li, X. Li, Investigation on the Catalytic Hydrogenolysis of Lignin over NbOx-Ni/ZnO-Al2O3, Ind. Eng. Chem. Res. 58 (2019) 7866–7875. https://doi.org/10.1021/acs.iecr.9b00376.

Chapter 5 Lignin modification and hydrogenation though electrochemical hydrogenation process

5.1 Abstract

Lignin is one of the most promising biopolymers for producing hydrocarbons and aromatic compounds in nature. Electrochemical conversion of lignin is regarded as an attractive technology for producing various aromatic chemicals which are generally derived from fossil fuels. The author reports an electrochemical approach for hydrogenating alkaline lignin (AL), which uses relatively low-cost Ni foam as a working electrode under alkali electrolyte. The primary factors (such as power input, reactor type, temperature, reaction time, catalysts, and electrode substrates) of electrochemical hydrogenation were used to control the products' yield and features. The redox characteristics of the reaction system were directly compared with the cyclic voltammetry measurement under different parameters. After electrochemical hydrogenation (ECH), fast pyrolysis was conducted on HAL samples to investigate the influence of electrochemical reactions on lignin. The maximum olefins and aromatics yield from HAL was increased to more than three times AL, accounting for 2.22 wt.% and 4.07 wt.%, respectively. Then, thermogravimetric analysis (TGA), elemental analysis (EA), Fourier-transform infrared spectroscopy (FTIR), and heteronuclear single quantum coherence (HSQC) NMR were employed to characterize hydrogenated lignin samples (HAL), as well as gas chromatography–mass spectrometry (GC-MS) was conducted to investigate the oil-phase products. This work focused on this electrochemical hydrogenation coupled with fast pyrolysis process to give a possibility that converting lignin into not only liquid oil products, but solid hydrogenated lignin can be used to produce more olefins and aromatics in fast pyrolysis.

5.2 Introduction

For lignin, olefins and aromatic compounds are the major research topic[1], which can be used as raw materials for derivatives of aromatic hydrocarbon compounds or as fuel sources. Some chemical conversion technologies have been investigated, like pyrolysis[2], gasification[3], hydroprocess[4], liquefaction[5], and oxidation[6]. Generally, due to lignin's cross-linking structure, most of the conversion processes for lignin require severe conditions, like pyrolysis with high temperature (600-1000 ℃)[7,8], or hydrogenation with high temperature and pressure (200-450 ℃, 1-10 MPa)[9], even some processes under specific catalysts[10,11]. Yang et al. conducted pyrolysis of alkaline lignin under a 3.0 wt.% Fe/ZSM-5 catalyst. A maximum 3.0 C-mol.% of light olefins and 9.8 C-mol.% of aromatic compounds was obtained[12]. Long et al. performed depolymerization on lignin through hydrogenolysis, the recovered lignin after the reaction possessed lower molecular weight and higher H/C ratio[13]. Zhang and her groups have investigated the effect of hydrogenation on the pyrolytic properties of organosolv lignin[14] and alkaline lignin[15]. They also discovered that after hydrogenation, hydrogenated lignin samples both have a higher H/C_{eff} ratio, and twice olefins yield can be achieved for organosolv lignin and triple olefins yield for alkaline lignin compared with raw lignin. Hydrogenation proved to be a more effective pretreatment to modify lignin and obtain more olefins.

Electrochemical conversion of waste lignin from the pulp and paper industry is an alternative process for renewably utilizing lignin to generate chemicals[16]. Electrochemical conversion may afford better control over the conversion and require mild reaction conditions than traditional thermochemical conversion. Lan et al. have studied electrochemically catalytic conversion on cornstalk lignin, including anodic oxidation to form lignin fragments and cathodic hydrogenation on lignin fragments[17].

Fang et al. have performed electrocatalytic reduction on both lignin β-O-4 models and lignin, while the product distribution from lignin was shown in the literature[18]. Meanwhile, Zhang et al. have investigated the effect of technological factors on the electrochemical hydrogenation of lignin[19]. They found that obtained hydrogenated lignin showed hydrogen content and H/C ratio increased by 1.7% and 0.04, respectively. These suggest that electrochemical hydrogenation is a potential technology for treating lignin in the current context of low carbon and emission reduction. Since the lignin after electrochemical hydrogenation has higher H/C ratio and lower molecular weight, it may have a higher potential to obtain more olefins and aromatic hydrocarbon compounds from hydrogenated lignin. This paper would like to provide a new prospect for the electrochemical hydrotreating of lignin as a pretreatment technology, which not only to convert lignin into liquid products by the electrochemical reaction, but also to obtain solid hydrogenated lignin with higher pyrolytic properties. The exploration of electrochemical hydrogenation on lignin is still at an early stage and its implementation in the large-scale industry requires further investigation [20].

In this research, the hydrogenated lignin conducted via the electrochemical process went through fast pyrolysis to transfer lignin to valuable chemicals. Various factors of the electrochemical hydrogenation process presented in this work verified the influence on the yield of ECH products and the yield of light olefin and aromatics in fast pyrolysis. Furthermore, the oil-phase products after electrochemical hydrogenation were also qualified by GC-MS. On the one hand, the comprehensive characterization of the products allows a better understanding of the reaction mechanism. And on the other hand, it could be found that not only the hydrogenated lignin but also the oil-phase products could be obtained after electrochemical hydrogenation reaction. It becomes possible to propose this two-stage process technology for the converting of lignin to obtain more fine chemical derivatives and renewable energy. Thus, this study aims to contribute to this growing area of research by exploring pretreatment technology for

lignin to modify the structure and improve the selectivity of pyrolyzed products and validate its feasibility.

5.3 Experimental method and materials

5.3.1 Chemicals and material

Alkaline lignin (CAS RN: 8061-51-6) was used as the feedstock without any pretreatment in this research, purchased from Tokyo Chemical Industry CO. LTD. Sodium hydroxide (particle, 198-13765), Raney Nickel (181-00025), hydrochloric acid (35-37 wt.%, CAS RN: 7647-01-0), and ethyl acetate (99.5%) were provided from FUJIFILM Wako Pure Chemical Corporation. The commercial 5 wt.% Ru/C and 5 wt.% Rh/C catalyst, Nafion perfluorinated resin solution (5 wt.%) were purchased from Sigma-Aldrich, Japan. All chemicals were used for the electrochemical reaction and sequential separation process without any pretreatment. Carbon paper (CP, thickness 0.3 ±0.01 mm, electric resistivity: 3 mΩ/cm^2) was ordered from XIAMEN TOB NEW ENERGY TECHNOLOGY Co., LTD., China. Ni foam (NF), purity > 99.99%, was purchased from MTI Japan. Nafion membrane N117 was purchased from Furukawa agency, Japan. Pt mesh (35*25 mm with 80 mesh) was purchased from EC FRONTIER CO. Ltd. The ultrapure water was 18.2 MΩ·cm for all the experiments, which was prepared with a water purification system (YAMATO Scientific CO. Ltd).

5.3.2 Experiment and separation procedure

The typical reaction systems and characterization analysis used in this work are shown in Fig. 5-1. Potentiostat ECstat 301 (EC-frontier, Japan) was used to provide constant current (Chronoamperometry) or potential (Chronopotentiometry). 1cell (undivided cell) and H-cell (divided cell) reactors were used to conduct electrochemical

hydrogenation (ECH). And, 1 M NaOH was used as an electrolyte to dissolve alkaline lignin (AL). A three-electrode system was used, in which Pt wire and Hg/HgO were fixed as the counter electrode (CE) and reference electrode (RE), respectively. The working electrode (WE) as one of the main parameters was studied in this work. After a certain time, the hydrogenated products were separated by the following procedures. First, the catalyst-coke mixture was separated from the electrolyte by filtrating. Next, the filtrate solution was acidified to around pH=1 with HCl (35%) solution for precipitating the solid residue. Then the solid residue was filtrated and dried in a vacuum oven at 60 ℃ overnight, called hydrogenated lignin (HAL). Liquid-liquid extraction was performed using ethyl acetate to separate the bio-oil phase and water-soluble phase of the filtrate. After that, a rotary evaporator was used to remove ethyl acetate from the oil product. The HAL and oil phase yields were calculated as a weight percentage by the mass of AL fed. The unrecovered fraction in water corresponded to the complement of 100 wt.% of the initial lignin, including water-soluble products (lignin oligomers and light compounds). Therefore, the yield of products was calculated by the following Eqs. (5-1) - (5-4).

$$C_L\ (wt.\%) = (W_L - W_H)/W_L * 100\% \quad (5\text{-}1)$$

$$Y_H\ (wt.\%) = W_H/W_L * 100\% \quad (5\text{-}2)$$

$$Y_O\ (wt.\%) = W_O/W_L * 100\% \quad (5\text{-}3)$$

$$Y_W\ (wt.\%) = W_L - W_H - W_O\ /W_L * 100\% \quad (5\text{-}4)$$

Where, C, Y, and W are respectively the conversion, yield, and weight, and the subscripts L, H, O, and W denote AL, HAL, oil-phase products, and water-soluble products, respectively.

In the subsequent experiment, a two-stage tubular reactor (TS-TR) coupled with gas chromatography (GC2014 and GC2010) was used to check the pyrolysis characteristic of HAL samples. More details about the experimental procedure are shown in Table

5-1[21]. Briefly, about 1 mg of lignin sample was tested each time and wrapped with a sheet of wire mesh (SUS316 stainless mesh with 10×10 mm, 45 μm mesh opening), and held by a steel wire hook. Then the prepared sample was placed on the upper part of the U-type reactor with the help of a magnet on the reactor outside before the experiment setup. After the temperature stabilization and GC setup, the sample was dropped into the bottom of the reactor, where the preliminary reaction of fast pyrolysis occurred. The volatiles was swept into GC by H_2 carrier gas. The actual flow rate of hydrogen gas was 68.5 mL/min, so the corresponding gas residence time of 0.45 s was kept constant.

The volatiles released from the lignin blown into GC2014 with a packed column (Gaskuropack 54), were tested through the thermal conductivity detector (TCD) and flame ionization detector (FID) sequentially. Another identical fast pyrolysis experiment was used to analyze larger aromatic compounds through another GC2010 equipped with a capillary column (TC-1701). The quantifications of the products were conducted and calculated based on the external calibration method, and the standard gas consisted of CO (1.0%), CO_2 (0.978%), CH_4 (1.01%), and N_2 (balance gas). And the undetected products can be assumed as heavy oil which was calculated by the difference method. The conditions for the two GC apparatuses are shown in the previous work[22]. In addition, the reproducibility was examined, which revealed that the relative errors of the product yield were generally within ±5 wt.%.

Table 5- 1 The parameters setup for GC measurement.

Instrument	**Analysis conditions**	
GC2014-TCD/FID	Separation column	Gaskuropack 54 (packed column, GL Sciences)
	Detector and analytes	TCD: carbon monoxide, carbon dioxide, vapor FID: methane, ethylene, ethane, propylene,

		propane, methanol, acetaldehyde, butane, butene, isobutylene, ethanol, iso-propanol, cyclopentadiene, acetic acid, benzene, toluene, furfural
	Injector/Detector/Column temperature	200 ℃/220 ℃/40 ℃
	Temperature program	Hold 10 min at 40 ℃, raise temperature to 200 ℃ at a heating rate of 5 ℃/min, then hold 18 min
GC2010-FID	Separation column	TC-1701 (capillary column)
	Detector and analytes	FID: benzene, toluene, styrene, indene, phenol, naphthalene, 2-methyl-naphthalene, acenaphthylene, fluorene, phenanthrene, anthracene, fluoranthene, pyrene, chrysene
	Injector/Detector/Column temperature	300 ℃/320 ℃/40 ℃
	Temperature program	Hold 10 min at 40 ℃, raise temperature to 250 ℃ at a heating rate of 4 ℃/min, then hold 20 min

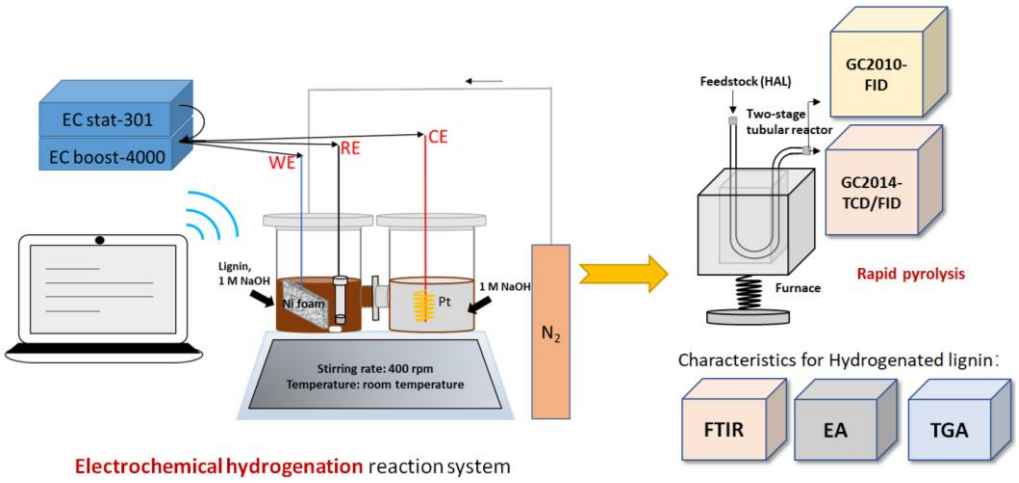

Fig. 5- 1 Electrochemical hydrogenation coupled with pyrolysis system.

Typical catalytic electrodes were prepared by following Fig. 5-2. Carbon paper (CP, size 2 cm × 2 cm) was used as the electrode substrate, which was immersed in 1 M sulfuric acid for 3 hours ultrasonic at first and then in ethanol for another 3 hours ultrasonic to improve hydrophilicity properties. After overnight drying in a vacuum oven, it was reserved for use. Raney Ni coated carbon paper: 20 mg of commercial 5 wt.% Rh/C powder was dispersed in the 87 μL of 5 wt.% Nafion, 261 μL of ethanol, and 652 μL of deionized water, followed by ultrasonic treatment for 60 min until achieving a uniform dispersion. Then, the dispersion was loaded onto the pretreated CP in batches, and dried in the air overnight at room temperature. The loading amount of Raney Ni on CP was ~ 2.5 mg·cm^{-2}. Moreover, other catalysts were loaded on CP in the same method as above. In addition, Ni foam (NF) was pretreated in a similar process as above, except replaced sulfuric acid with nitric acid. Then, the pretreated NF was loaded with different catalysts by the same method, while the loading amount of 5 wt.% Rh/C catalyst on NF was ~ 2.5 mg·cm^{-2}.

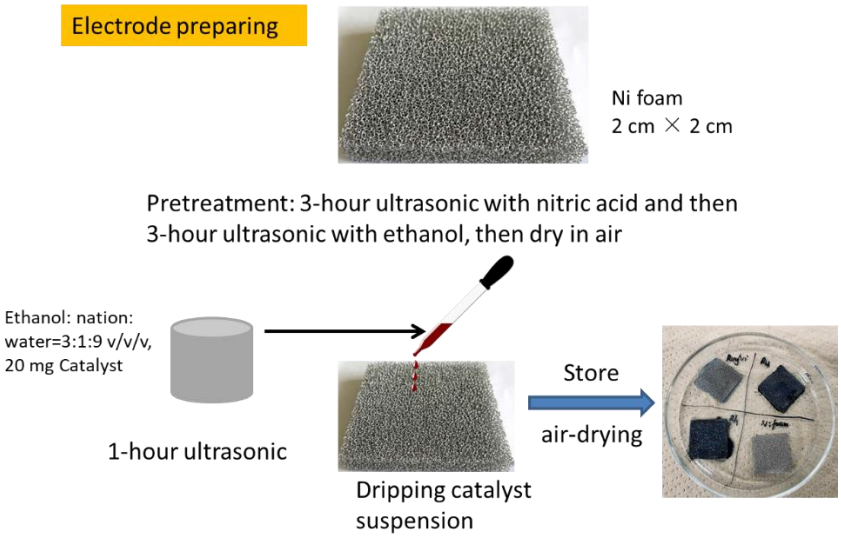

Fig. 5- 2 Diagram of preparing process for catalytic electrodes.

5.3.2 Characterization method

The diverse characterizations of HAL samples were also needed to check the influence of ECH on lignin.

Thermogravimetric analysis (TGA) was performed in Netzsch STA 2500 Regules. TG curve was used to illustrate the weight loss of lignin, and the corresponding decomposition rate was revealed by the derivative thermogravimetric (DTG) curve. Around 5 mg of the sample was loaded on a Pt crucible each time. The temperature was raised from room temperature to 1000 ℃ with a rate of 5 °C/min, and held for 10 min at 1000 ℃ for stabilization. The thermal decomposition was conducted at a constant N_2 flow rate of 50 mL/min.

Fourier transform infrared spectrometer (FTIR) was used to examine the internal functional groups of the samples. Bruker ALPHA II was employed for the prepared sample, 1 wt.% of lignin in 50 mg of KBr for each test. The samples were recorded between 400 and 4000 cm^{-1} at a resolution of 4 cm^{-1} in the absorbance mode.

The weight ratio of elements such as carbon, hydrogen, nitrogen, and sulfur contained in organic compounds was quantified by elemental analysis (2400II CHNS/O

type manufactured by Perkin Elmer Co., Ltd). The analysis process was conducted by the column separation method (frontal chromatography) and tested by a TCD. Around 2 mg of the sample was detected each time with helium as the carrier gas.

GC-MS (Gas Chromatography-Mass Spectrometry) was used to analyze the compounds in oil-phase after ECH. A capillary column (TC-5, inner diameter: 0.25 mm) was employed in the SHIMADZU GC2030, and the samples were identified using a mass spectrometer detector with a flame ionization detector. The oven temperature was kept at 40 ℃ for 4 min and raised to 300 ℃ with 10 ℃/min of heating rate and keep at 300 ℃ for 10 min. The injector temperature is 220 ℃. And injection volume is 2 μL with a 19:1 split ratio. The compounds were determined by comparison with the National Institute of Standards and Technology Chemistry WebBook (NIST 2017).

More information on side-chain linkages and the C9 units of lignin samples was determined by 2D NMR HSQC (heteronuclear single quantum coherence) spectroscopy (JNM-ECZ400 (JEOL)). The methodology was followed by the literature[23]. Sample tubes (OD: 5 mm) were running for the sample (90 mg of lignin samples dissolved in 0.5 mL of DMSO-d6 solvent). 0.01 M of Chromium (III) acetylacetonate was added as a relaxation reagent to the sample solution. For the ^{1}H dimension, the number of collected complex points was 1024, and the recycle delay was 1.5 s. For the ^{13}C dimension, the number of transients was 64, and 256-time increments were recorded. The number of the scan was 8. The DMSO-d6 solvent was used as an internal chemical shift reference point (δC/δH 39.5/2.49). The assignments of 2D HSQC spectra were referred literature [23,24], shown in Table 5-2.

Table 5- 2 Assignment of main signals in HSQC spectra of the lignin samples.

Label	**δ_C/δ_H**	**Assignment**
-OCH_3	55.9/3.73	C−H in methoxyls

A_γ	59.6−59.8/3.41−3.65	C_γ−H_γ in β-O-4′ substructures (A)
C_γ	62.7/3.69	C_γ−H_γ in phenylcoumaran substructures (C)
B_γ	71.4/3.81, 4.18	C_γ−H_γ in resinol substructures (B)
G_2	111.1/6.97	C_2−H_2 in guaiacyl units (G)
G_2'	111.4/7.51	C_2−H_2 in oxidized (C_α=O) guaiacyl units(G′)
G_5	114.9/6.77	C_2−H_2 in guaiacyl units (G)
G_6	119.3/6.79	C_6−H_6 in guaiacyl units (G)
G_6'	123.2/7.61	C_6−H_6 in oxidized (C_α=O) guaiacyl units (G′)
$H_{3,5}$	113.2/6.69	$C_{3,5}$−$H_{3,5}$ in p-hydroxyphenyl units (H)
$H_{2,6}$	128.4/7.19	$C_{2,6}$−$H_{2,6}$ in p-hydroxyphenyl units (H)
J_β	126.1/6.76	C_β−H_β in cinnamaldehyde end groups (J)
$PCA_{3,5}$	115.5/6.77	C_3−H_3 and C_5−H_5 in p-coumarate (PCA)

5.4 Results and discussion

5.4.1 Optimized conditions investigation

Electrochemical hydrogenation (ECH) in this work was conducted with a three-electrode configuration in 1.0 M NaOH electrolyte. Alkaline water can dissolve lignin to form a homogeneous solution and provide a good conductivity for the electrochemical reaction. Before that, cyclic voltammetry (CV) was used to study the redox property of the reaction processes. CV curves investigated different scan rates (20-60 mV/s) in Fig. 5-3(a). The oxidation and reduction peaks show in the range of 0.25 to 0.55 V and -0.25 to -0.4 V, respectively. From the results, we can see that the reduction peaks intensity increased proportionally with the increase of the scan rate, that related to the process is irreversible. Thus, 50 mV/s of scan rate generally chosen in the literature was selected to perform further experiments.

The effect of lignin concentration on the redox property of the reaction system is reported in Fig. 5-3(b). Comparing the reaction system without AL, the lignin loading shows a more intensive redox reaction. The lignin concentration affected the oxidation process, while the lignin concentration did not change the reduction peaks. Accordingly, the higher lignin concentration leads to more lignin molecules absorbed on the surface of Pt mesh. The excessive concentration of lignin would harm the electrochemical reaction[25].

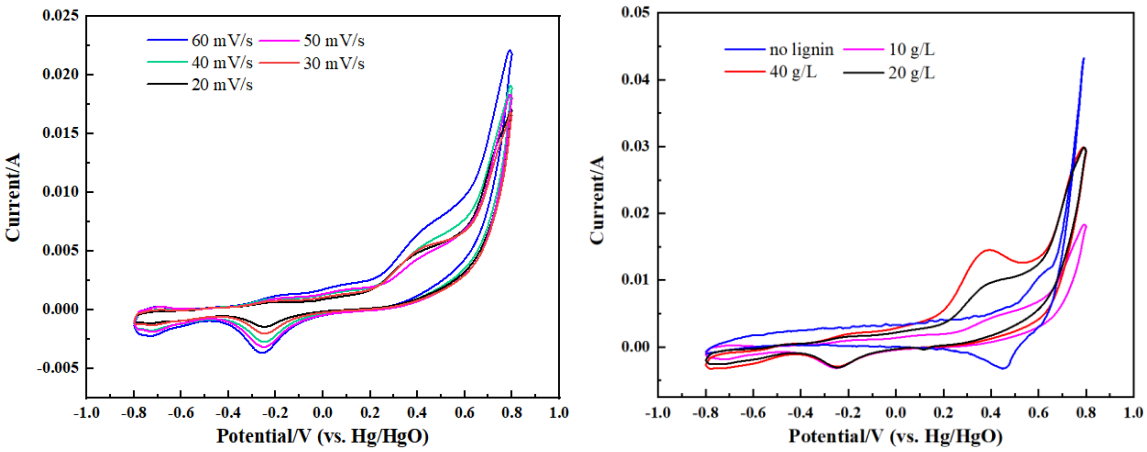

(a) (b)

Fig. 5- 3 The CV curve of the reaction system. (a) The CV curve of the reaction system (WE: Pt mesh; CE: Pt wire; RE: Hg/HgO) with different scan rates (20-60 mV/s); (b) The CV curve with different lignin proportion, testing conditions: 1cell, Pt mesh as WE, electrolyte: 1 M NaOH, room temperature.

The undivided cell (1cell) and the divided cell (H-cell) were studied as Fig. 5-4(a). In CV curves, oxidation peaks show outstanding signals under H-cell that separate anode and cathode reactions by proton exchange membrane. H-cell avoids co-existing and interacting with each other in the undivided cell. The reaction temperature was investigated in the range from 25 ℃ to 60 ℃ (Fig. 5-4(b)). The temperature shows a

relatively noticeable effect on the oxidation reaction, while no significant changes show for the hydrogenation reaction. This is consistent with the literature, where high temperatures promote oxidation reactions and thus increase the depolymerization rate of lignin generally[26,27]. However, in this work, only the electrochemical hydrogenation reaction of lignin was considered. It seems that temperature has less influence on the reduction reaction, so there were no significant changes in the yield of the products under the same electrochemical reaction conditions.

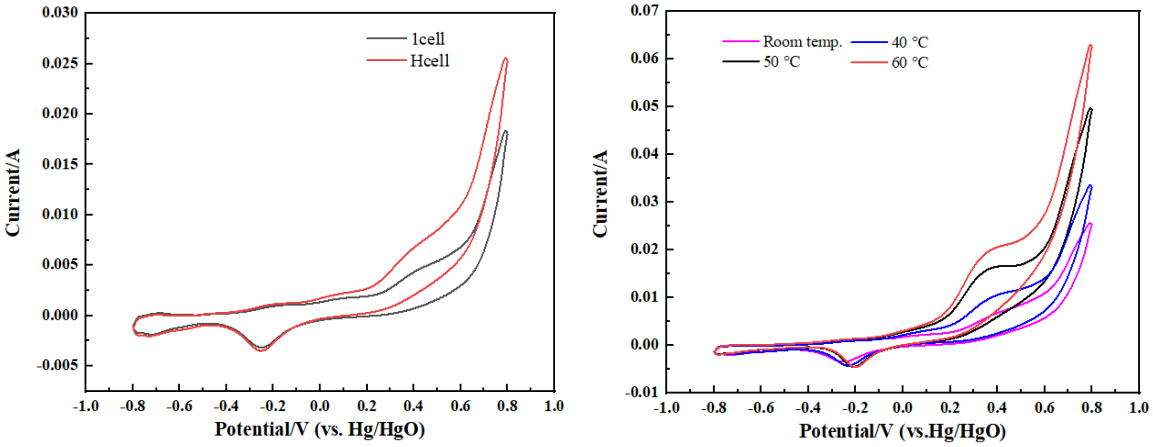

(a) (b)

Fig. 5- 4 The CV curves of the electrochemical reaction system in 1cell and H-cell (a) and under different temperatures (b). (a) Conditions: 10 g/L lignin conc., Pt mesh as WE, electrolyte: 1 M NaOH, 50 mV/s, room temperature. (b) The CV curve of the electrochemical reaction system under different temperatures. Conditions: 10 g/L lignin conc., Pt mesh as WE, electrolyte: 1 M NaOH, 50 mV/s, H-cell.

One factor that affects the large improvement of hydrogenation efficiency is electrode materials. In general, commercially available carbon paper (CP) and nickel foam (NF) are widely used in electrochemical application. which were directly utilized as a substrate to support catalysts loading. Rh/C, Ru/C, and Raney Ni as common

hydrogenation catalysts were loaded on CP and NF here. The CV curve of various electrode substrates is slightly different. Commercial Pt mesh compared with carbon paper loaded with the catalysts are displayed in Fig. 5-5(a) and (b). The Pt mesh electrode showed a reduction peak at -0.25 V, while carbon paper was not found redox peaks during the CV test. According to the Pt electrode is one of the most active materials for the reduction reaction. However, the advantage of Pt is the cost effect issue. Thus, NF substrate was used to support different catalysts as shown in Fig. 5-5(c). By comparison, the loaded catalysts (Raney Ni, Ru/C, and Rh/C) had more effect on both reduction and oxidation than bare nickel foam. Especially, Raney Ni-NF outstands superior activity on reduction due to the unique properties of Ni foam, such as large surface area, mass transport, and high resistance under strong alkaline solutions[28]. Furthermore, Raney nickel as an electrode has also shown good performance on electrocatalytic hydrogenation on lignin phenolic models[29]. Fig. 5-5(d) also compared the systems with and without lignin by using the Ru/C-NF electrode. The presence of lignin can promote the redox reaction, and the higher the lignin concentration, the more intense the reaction is, as seen in the CV plots.

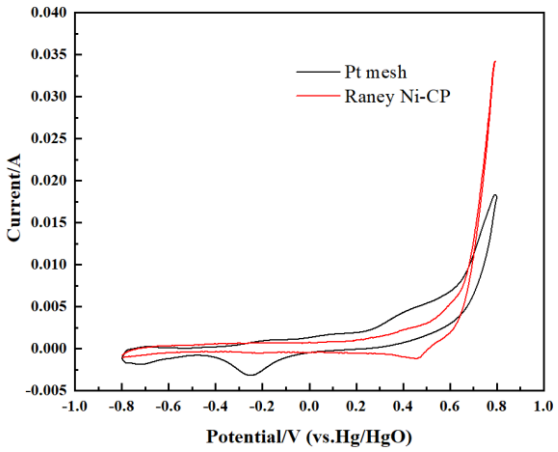

(a)

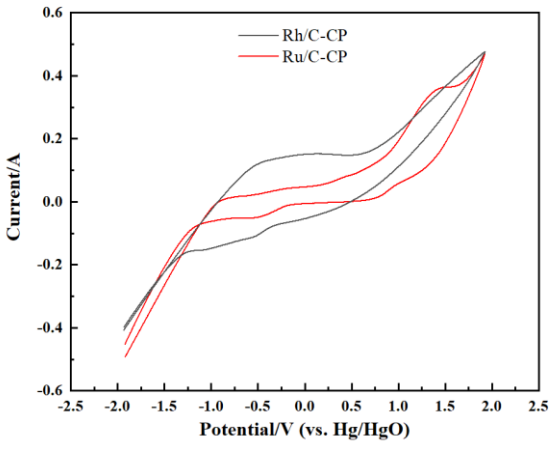

(b)

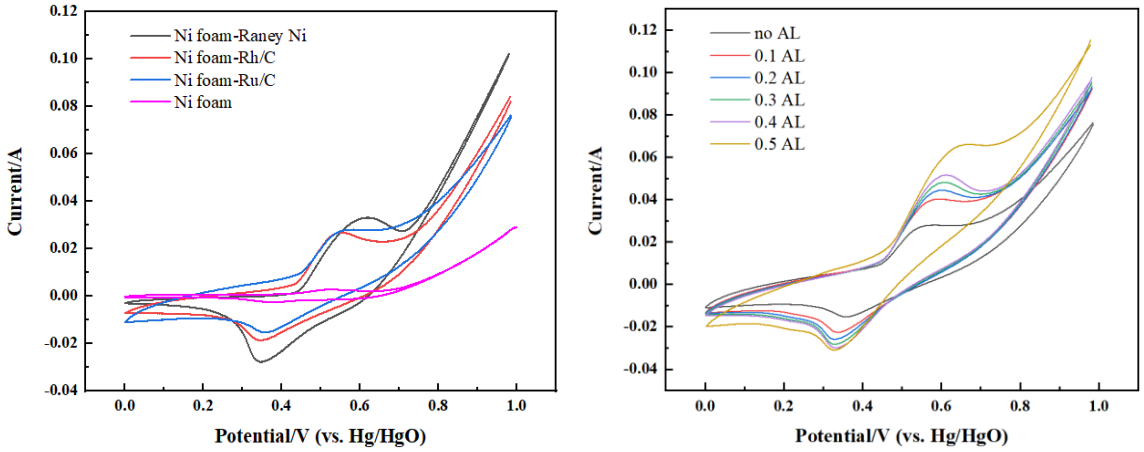

(c) (d)

Fig. 5- 5 Checking the performance of the reaction systems with various WE through the CV curve. Conditions: 10 g/L lignin conc., 50 mV/s, room temperature, RE: Hg/HgO, CE: Pt wire. (a) WE: Pt mesh, and Raney Ni-CP; (b) WE: Rh/C and Ru/C on CP. (c) WE: Raney Ni, Ru/C, and Rh/C on NF; (d) WE: Ru/C-NF.

Table 5-3 shows the details of reaction conditions and the product distribution of ECH. The effect of input current or potential on the yield of HAL has been described below. It can be seen that the yield of HAL increased with the current to 87.01 wt.% at 220 mA, while the oil-phase product has the opposite trend. When the experiments were performed using a constant voltage (Entry 6), the lignin conversion was significantly increased. Thus, the constant potential was used to demonstrate in this research. And the specific input voltage was determined by the potential corresponding to the reduction peak in the relative CV curve. However, the limitations of the undivided cell led to the fact that the electrochemical reaction does not occur exclusively as a reduction reaction on the lignin. Thus, the cell type is one of the crucial points to avoiding this problem. H-cell (Entry 7) separated the oxidation and reduction reactions by proton exchange membrane to avoid the effect of oxidative depolymerization on lignin, so that more HAL was recovered after ECH. Furthermore, the HAL samples were recovered after a

long-duration reaction via an H-cell reactor. In terms of product distribution of ECH, a longer reaction time resulted in a higher lignin conversion rate and more oil phase. While increasing the reaction temperature to 60 °C slightly increased the oil-phase products. Actually, the temperature has been wildly investigated in other electrochemical research, which both showed the temperature has a positive effect on the oxidation reaction and conversion rate[29,30].

Table 5- 3 The details of electrochemical hydrogenation conditions and product yield.

Entry	**Lignin /Conc.**	**Electrolyte**	**WE/CE/RE**	**Constant current (mA)/ potential (V)**	**Reactor types**	**Temperature**	**Time (h)**	**Conv. rate**	**Product yield (wt.%)**	
									HAL	**Oil**
1	AL/ 10 g/L	1 M NaOH	Pt / Pt/ Hg|HgO	44	1cell	RT	2	25.71	74.29	28.93
2	AL/ 10 g/L	1 M NaOH	Pt / Pt/ Hg|HgO	88	1cell	RT	2	21.55	78.45	22.12
3	AL/ 10 g/L	1 M NaOH	Pt / Pt/ Hg|HgO	132	1cell	RT	2	15.48	84.52	22.05
4	AL/ 10 g/L	1 M NaOH	Pt / Pt/ Hg|Hg	176	1cell	RT	2	13.16	86.84	23.16

			O							
5	AL/ 10 g/L	1 M NaOH	Pt / Pt/ Hg|HgO	220	1cell	RT	2	12.99	87.01	8.57
6	AL/ 10 g/L	1 M NaOH	Pt / Pt/ Hg|HgO	-0.25	1cell	RT	2	33.31	66.69	12.35
7	AL/ 10 g/L	1 M NaOH	Pt / Pt/ Hg|HgO	-0.25	H-cell	RT	2	18.05	81.95	5.69
8	AL/ 10 g/L	1 M NaOH	Pt / Pt/ Hg|HgO	-0.25	H-cell	RT	16	28.85	71.15	12.17
9	AL/ 10 g/L	1 M NaOH	Pt / Pt/ Hg|HgO	-0.3	H-cell	60 ℃	2	17.80	82.20	7.75

Note: 1cell: undivided cell; H-cell: divided cell; RT: room temperature.

5.4.2 The products distribution of Electrochemical hydrogenation and fast pyrolysis

Electrochemical hydrogenation (ECH) in this work was conducted with a three-electrode configuration in 1.0 M NaOH electrolyte. Alkaline water can dissolve lignin to form a homogeneous solution and provide a good conductivity for the electrochemical reaction. Product distribution from ECH with different lignin concentrations is shown in Fig. 5-6(a). Less HAL can be recovered as the solid product when increasing AL loaded. It confirms the previous phenomenon that the higher lignin concentration promotes the adsorption of lignin on the electrode for a specific time,

fostering conversion rate (especially oxidation). Thus, it can be explained that a higher lignin concentration allows partial depolymerization accompanied by the hydrogenation reaction to occur on the lignin macromolecules. Less HAL can be obtained, and higher oligomers (water phase) and low oil phase yield were found in the 1cell. However, the lignin oligomers in the water phase after ECH were not detected in this work, which is a challenge in future research. From Fig. 5-6(b), the light olefins yield (such as ethylene, propylene, and butylene) from HAL samples both have various degrees of increase with the increase of lignin concentration. As for aromatic products, benzene and xylene yield had decreased first and then increased when increased lignin concentrations, reaching a maximum at a lignin concentration of 10 g/L. Toluene maintained an upward trend during the rise in lignin concentration. The reason is that the production of benzene depends mainly on the thermal decomposition and recombination of HAL samples, which depend not only on the effect of ECH but also on the fast pyrolysis process. Toluene yield is mainly due to the degree of hydrogenolysis of HAL.

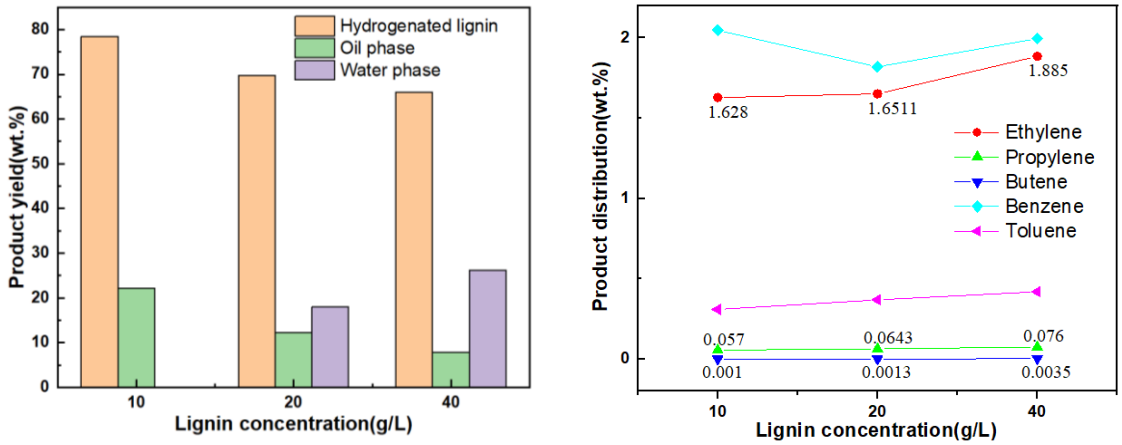

(a) (b)

Fig. 5- 6 The product distribution from ECH (a) with different lignin concentrations and the products of fast pyrolysis (b). (a) The product yield of ECH results with different lignin concentrations. Conditions: 20 mA/cm^2, 2 hours, and room temperature. (b) Fast

pyrolysis of HAL samples treated with various lignin concentrations. Pyrolysis conditions: 850 ℃, residence time: 0.45 s, atmosphere: H_2.

The effect of input power was verified by introducing various currents and potentials to the reaction system in Fig. 5-10. Since the contact area of WE is uniformly 4.4 cm^2, 44-220 mA current represents 10-50 mA/cm^2 current density, respectively. From Fig. 5-7(a), it can be seen that the higher the current input is, the higher the yield of HAL is obtained after electrochemical hydrogenation. On the one hand, it may be attributed to the high current promoting the intense reaction in water, which might replace the hydrogenation of AL as the main reaction in the reaction system. On the other hand, the excessive current might be over the range of the redox reaction that happened, which caused more unreacted lignin to remain. So, the experiments also were carried out with a constant potential by applying the voltage corresponding to the reduction peak characteristic in the CV curves (Fig. 5-5(a)), which followed the methodology of Yan, et al.[31]. It can be seen that less than 70 wt.% (64.08 wt.%) of the solid was recovered as HAL after 2 hours of reaction under a constant potential of 0.25 V. It implies more reactions happened on the lignin.

The main pyrolysis products of HAL samples are shown and compared in Figure 5-7(b). It can be seen that when the current input was higher during ECH, the lower the pyrolysis capacity of HAL was, and fewer olefins and aromatics could be produced. This also confirms that the electrochemical reaction of water was promoted more at the high current range. Here, the highest yields of ethylene, benzene, and toluene were obtained, accounting for 1.93 wt.%, 2.14 wt.%, and 0.4 wt.%, respectively, when a constant potential of 0.25 V was input. Thus, applying the suitable potential for the system is more selective and efficient for the hydrogenation of lignin.

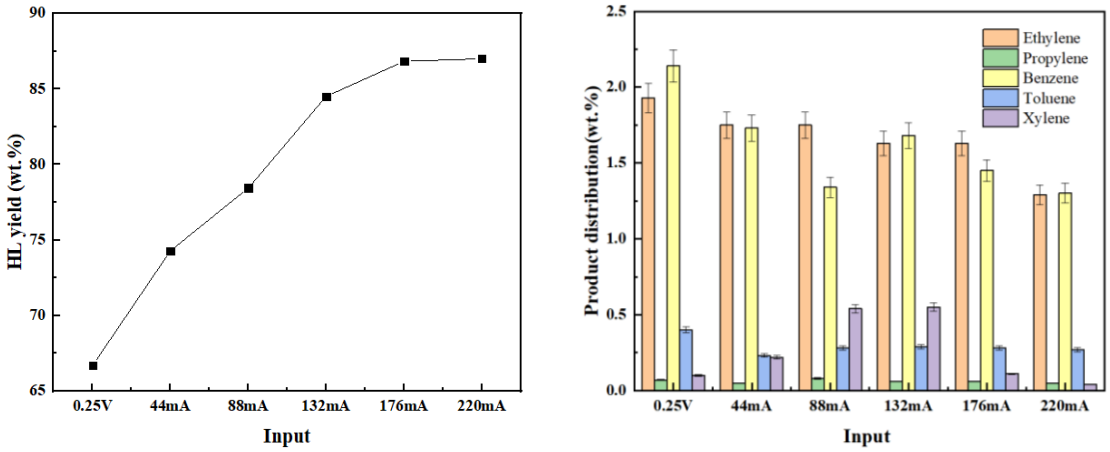

(a) (b)

Fig. 5- 7 The products yield from ECH (a) with different input power and the products of fast pyrolysis (b). (a) The yield of HAL samples after pretreating with ECH under different input current/potential. Conditions: 1cell, room temperature, WE: Pt mesh, 2 hours. (b) Pyrolyzed products from HAL samples treated with different input current/potential.

The undivided cell (1cell) and the divided cell (H-cell) were studied as Fig. 5-8. In CV curves (Fig. 5-4 (a)), oxidation peaks show outstanding signals under H-cell that separate anode and cathode reactions by proton exchange membrane. H-cell avoids co-existing and interacting with each other in the undivided cell. As a result, the ECH under H-cell provided high HAL at 81.95 wt.%. The main products from fast pyrolysis of lignin samples are shown in Fig. 5-8. Concerning the product yield of HAL samples, more pyrolyzed products can be produced after ECH. The reaction conducted in H-cell slightly promoted olefins yield (2.05 wt.%) and xylenes from HAL samples while benzene and toluene yield became slightly lower. Lower char yield (41.55 wt.%) can be obtained after pretreating with H-cell simultaneously. It might be attributed to the H-cell reactor can increase the reaction efficiency with no interfering reactions[32]. Furthermore, separating the oxidation reaction from lignin molecules caused the

hydrogenated lignin could be recovered more in H-cell. In brief, HAL from treating in H-cell had better pyrolytic activity and more volatile fraction released than HAL in 1cell. Hence, the subsequent reactions were carried out using H-cell.

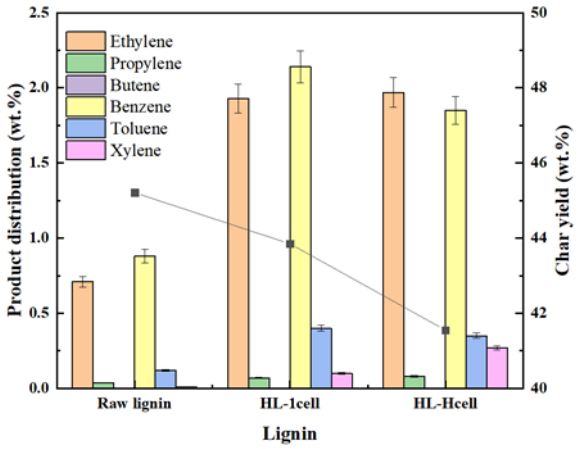

Fig. 5- 8 The pyrolysis distribution of raw lignin (AL) and hydrogenated lignin samples from the undivided cell (HAL-1cell) and divided cell (HAL-Hcell). Conditions: 10 g/L of lignin conc., 2 hours, Pt mesh as WE, electrolyte: 1 M NaOH, room temperature, input: -0.25 V. Pyrolysis conditions: 850 ℃, residence time: 0.45 s, atmosphere: H_2.

Table 5-4 lists the distribution of the products for fast pyrolysis of lignin samples. Fast pyrolysis experiments were conducted under the same conditions. The effects of reactor type, reaction time, and temperature on the pyrolysis products were compared here. Electrochemical hydrogenation produces more organic volatile fractions and less char yield than AL. Compared to the two different reactor types, the yield of olefins from HAL-1cell was lower than that of HAL-Hcell, which was probably due to the oxidation reaction. HAL-1cell has a lower molecular weight and can produce more methane as well as aromatics through thermal cracking.

According to the product from fast pyrolysis, HAL pretreated with a long-time reaction produced fewer olefins but more aromatic products (especially benzene,

styrene, indene, phenol, and naphthalene). Jia et al. reported the effect of reaction time on cumulative yield[33]. They found the cumulative yield of hydrogenation products was proportional to the increase of time. However, the ratio became gradually small and then stable after 4-5 hours. Thus, this study found that extending the electrochemical hydrogenation time allows the hydrogenated lignin to produce more aromatic compounds. For the effect of temperature, comparing HAL-Hcell (RT) and HAL-60 (60 ℃), it can be found that increasing the reaction temperature leads to a decrease in olefin yield without much change in total aromatic hydrocarbon yield, and an increase in char yield. Some statements show that although increasing the temperature accelerates the lignin molecular movement, it also has a negative impact on the electrochemical hydrogenation reaction[19]. One reason is that the temperature is not high enough to be able to influence the hydrogenation reaction, and another reason is that the temperature also promotes the intermolecular repolymerization along with the depolymerization reaction.

Table 5- 4 The products yield from fast pyrolysis of AL and HAL samples.

No.	**Pyrolyzed products (wt.%)**	**Retention time (min)**	**Lignin samples**				
			AL	**HAL-1cell**	**HAL-Hcell**	**HAL-16**	**HAL-60**
GC2014-TCD (Gaskuropack 54 column)							
1	CO	0.84	4.50	5.69	4.90	5.22	4.83
2	CO_2	1.88	11.00	6.90	6.40	7.55	6.62
3	H_2O	9.42	26.10	17.19	16.08	20.49	17.42
GC2014-FID (Gaskuropack 54 column)							
4	CH_4	1.11	5.18	8.42	7.60	7.75	6.92
5	C_2H_4 (C_2H_2)	3.48	0.71	1.93	1.97	1.65	1.43
6	C_2H_6	4.87	0.50	0.77	0.85	0.75	0.71
7	C_3H_6	17.06	0.04	0.07	0.08	0.05	0.05

8	C_3H_8	18.24	0.002	0.02	0.02	0.002	0.006
9	CH_3OH	21.24	0.29	0.18	0.16	-	0.08
10	CH_3CHO	26.81	0.02	0.05	0.05	0.027	0.031
11	C_4H_{10}	27.5	0.001	0.002	0.002	0.002	0.001
12	C_4H_8	27.86	0.001	0.001	0.001	0.003	0.001
13	Iso-C_4H_{10}	29.25	0.003	0.003	0.005	0.001	0.002
14	C_2H_5OH	29.96	0.001	0.003	0.005	-	0.002
15	Iso-C_3H_7OH	32.23	0.02	0.006	0.008	0.006	0.004
16	Cyclopentadiene	33.72	0.08	0.16	0.12	0.089	0.12
17	CH_3COOH	34.44	0.11	0.06	0.04	0.06	0.07
18	C_6H_6	40.65	0.88	2.14	1.85	2.17	1.73
19	C_7H_8	47.36	0.12	0.40	0.35	0.27	0.30
20	Furfural	51.45	0.071	0.072	0.05	0.077	-
21	m-, o-, p-Xylene	57-62	0.01	0.10	0.27	0.35	0.65
GC2010-FID (TC-1701 capillary column)							
22	Styrene	17.18	0.005	0.034	0.034	0.076	0.022
23	Indene	25.61	0.058	0.249	0.234	0.307	0.182
24	Phenol	29.49	0.059	0.249	0.077	0.388	0.132
25	Naphthalene	32.36	0.092	0.506	0.278	0.518	0.281
26	2-methyl naphthalene	36.459	0.002	0.039	0.007	0.041	0.010
27	Acenaphthylene	42.82	0.004	0.007	0.001	0.008	0.002
28	Fluorene	46.78	0.001	-	0.001	0.002	-
29	Phenanthrene	53.317	0.001	-	0.001	0.001	0.001

30	Anthracene	53.611	0.003	-	0.001	-	-
31	Floranthene	61.237	0.002	0.001	0.001	0.002	0.001
32	Pyrene	62.563	0.002	0.001	-	0.001	0.001
33	Total olefins yield		0.751	2.001	2.051	1.703	1.481
34	Total aromatics yield		1.229	3.626	2.835	3.784	2.899
35	Char		45.21	43.85	41.55	40.17	44.53
Undetected product (diff.)			6.04	12.53	18.75	13.55	15.37

Note: HAL-1cell: hydrogenated lignin treated in the undivided cell, HAL-Hcell: hydrogenated lignin treated in the divided cell, HAL-16: hydrogenated lignin treated with 16 hours (H-cell, RT), HAL-60: hydrogenated lignin treated under 60 ℃ (H-cell, 2 hours). Pyrolysis conditions: 850 ℃, residence time: 0.45 s, atmosphere: H_2.

Figures 5-9(a) and (b) below show the comparison of the results obtained from the experiments (ECH and fast pyrolysis) conducted under the conditions of using Pt and CP as the electrode substrate. And (c) and (d) are the results of the experiments (ECH and fast pyrolysis) conducted with NF as the electrode substrate. After ECH, the HAL samples' yield was between 64-80 wt.%, and the oil yield was 13-38 wt.%. The lowest hydrogenated lignin (64.08 wt.%) yield was obtained when Raney Ni-NF was used as WE, and the highest hydrogenated lignin yield (80.10 wt.%) was obtained when Ru/C-CP was used as WE. The yield of HAL after ECH has a similar value when used Ru/C-CP, Ru/C-NF, NF, and Pt as the electrode. The main pyrolyzed products from HAL samples were tested and listed in (b) and (d). In terms of olefin yields, Pt, Ru/C-CP, Rh/C-NF, and NF used as electrodes have similar ethylene yields (1.6-1.7 wt.%), while propylene and butene yields were quite low. However, the propylene production from HAL samples under NF as electrode substrate generated a higher yield than that of CP

as the electrode substrate. The hydrogenated lignin treated with Raney Ni-NF can obtain the highest olefins yield 2.22 wt.%. And benzene, toluene, and xylenes yield from HAL treated with Raney Ni-NF were also higher than other catalysts. The reason might be that Ni foam has a higher conductivity than carbon paper, and a more pronounced reduction peak was found in the CV curves (Fig. 5-5(b) and (c)).

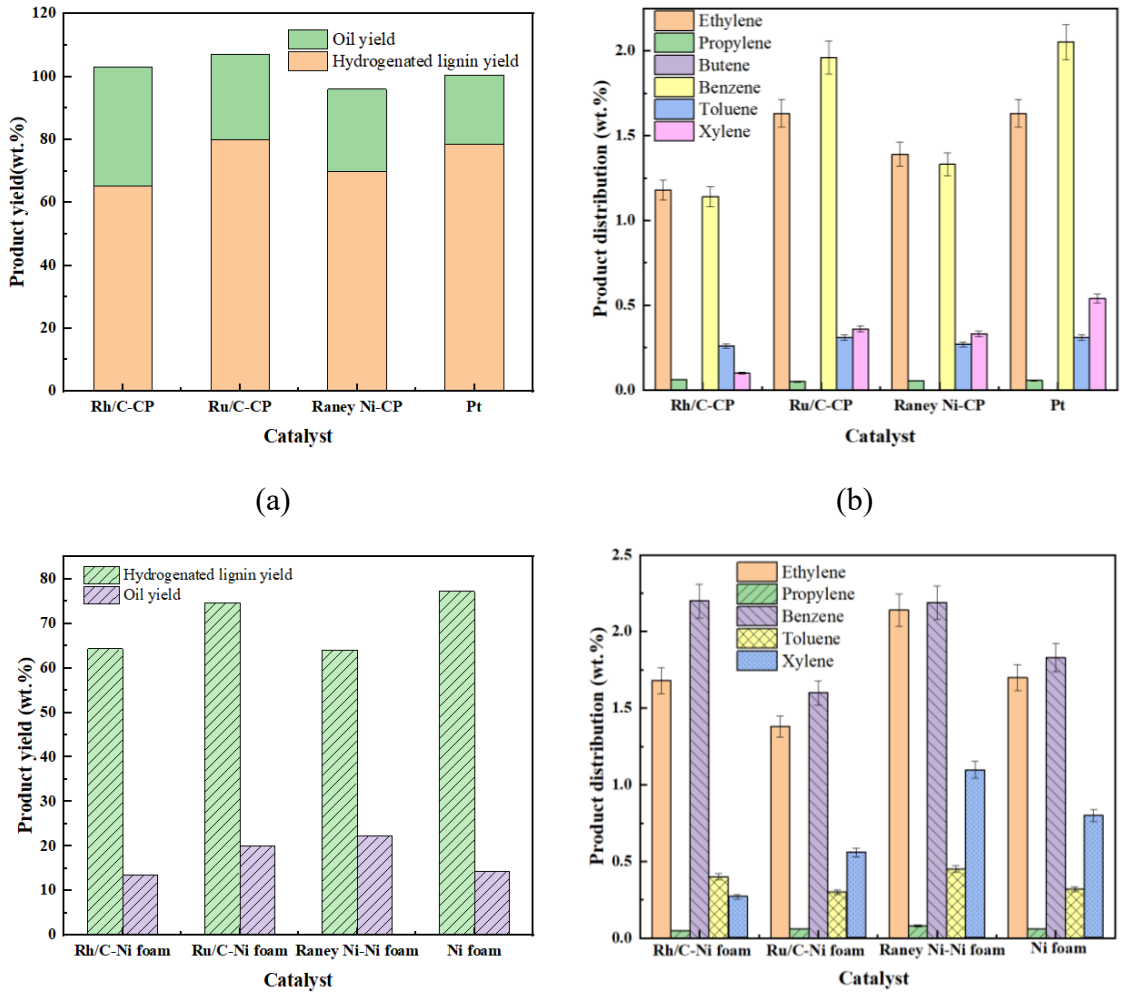

Fig. 5- 9 The product distribution after ECH and fast pyrolysis reactions. (a) The product yield after the electrochemical hydrogenation process, conditions: 10 g/L lignin conc., 2 hours, constant current: 88 mA, 1 M NaOH. (c) The product yield after ECH, conditions: 10 g/L lignin conc., 2 hours, constant potential: 0.3 V, 1 M NaOH. (b) & (d)

The products from fast pyrolysis, conditions: 850 ℃, residence time: 0.45 s, H_2.

All the volatile compounds from fast pyrolysis were tested and quantified. The gas chromatography is shown with the same scale in Fig. 5-10. Twice pyrolysis experiments were performed with the same conditions but conducted on two GC apparatus with different columns. Raw lignin (AL) and hydrogenated lignin (HAL) were used to compare. HAL here was selected after being treated with the best conditions found (Cell type: H-cell; Working electrode: Raney Ni-NF; Input: constant voltage, 0.3 V; Reaction time: 2 hours; Temperature: room temperature). It is clear from the graph below that carbon dioxide and vapour have slightly decreased, while other hydrocarbons and aromatic compounds have significantly increased after the electrochemical hydrogenation reaction. However, in the GC2010-FID of HAL, the product peaks after a retention time greater than 40 min were barely detectable, which proves that no 3-ring and 4-ring aromatic clusters appeared in the pyrolysis after the electrochemical hydrogenation reaction.

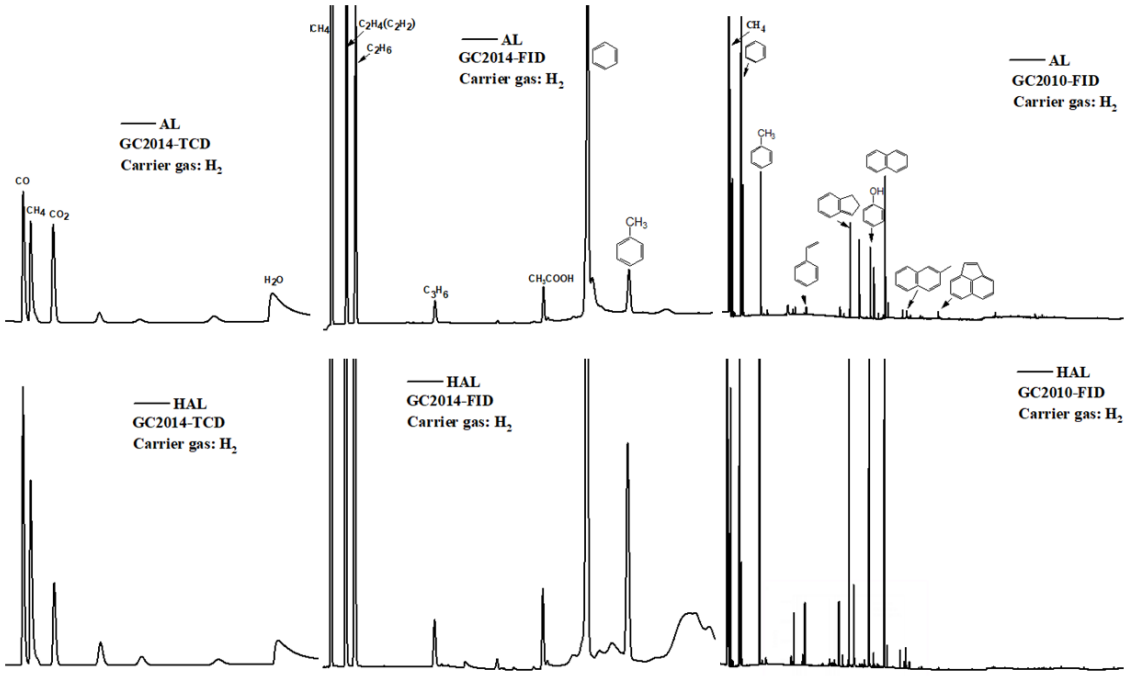

Fig. 5- 10 Comparison of the GC diagrams of the pyrolysis products from AL and HAL (Conditions: Raney Ni-NF, 0.3 V, 2 hours, H-cell).

Simultaneously, the pyrolyzed products were classified and compared in Fig. 5-11. It can be seen that after ECH, HAL produces less char, inorganic gas (CO, CO_2, H_2O), and light oxygenates carbon (including methanol, acetaldehyde, ethanol, and so on) in fast pyrolysis. In contrast, the yields of major hydrocarbons (alkanes and alkenes), as well as aromatic compounds, increased significantly. The yield of olefins (including ethylene, propylene, and butylene) and aromatics (including benzene, toluene, xylenes, and other aromatics listed in Table 1) from HAL is more than three times that of AL. For AL, only 0.75 wt.% of olefins and 1.23 wt.% of aromatics were produced, while for HAL, 2.22 wt.% (olefins) and 4.07 wt.% (aromatics) were obtained from HAL. This implies that lignin treated with electrochemical hydrogenation has a more significant potential to become an alternative to fossil energy and to achieve efficient use of renewable energy.

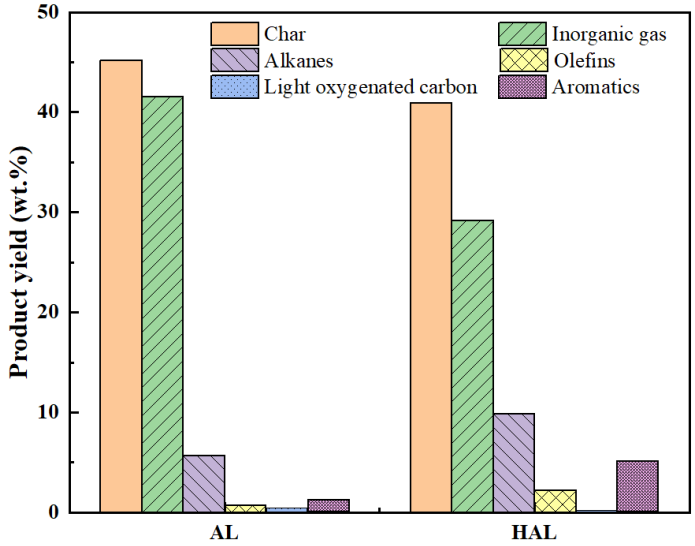

Fig. 5- 11 Comparison of product distribution for fast pyrolysis of AL and HAL (ECH conditions: Raney Ni-NF, 0.3 V, 2 hours, H-cell).

5.4.3 Characterization of hydrogenated products

Elemental analysis is used to probe the internal elemental structure of the lignin macromolecules. Compared to AL in Table 5-5, the HAL samples showed varying decreasing trends in the content of both sulfur and nitrogen compounds. This is due to the chain breakage of some branched functional groups of lignin during the electrochemical reaction. As for the carbon and hydrogen contents, HAL samples treated with Ni foam and Raney Ni-NF electrode showed an increasing trend, while the hydrogen content of HAL samples treated with Pt and Raney Ni-CP electrode had an opposite trend. The carbon content of HAL treated with Raney Ni-CP even decreased, which means the electrochemical reaction with the Raney Ni-CP electrode is not proper for the occurrence of hydrogenation. Because the conductivity of CP substrate is lower than that of Ni foam. Consequently, the Raney Ni-CP electrode does not show an obvious redox peak for the reaction (Figure 5-5(a)). Another one is that constant current seems to promote only the redox reaction of water, so the elemental analysis results obtained are opposite to the others.

Compared to bare Ni foam, the loading of Raney Ni on NF substrate resulted in a higher H/C_{eff} ratio and higher unsaturation. This is due to the excellent catalytic capability of Raney Ni, which promotes the depolymerization reaction of lignin, especially the cleavage of internal ether bonds. So, the oxygen, sulfur, and nitrogen content decreased, and the carbon and hydrogen content increased to 62.40 and 4.94 maximum. And the H/C_{eff} ratio increased from 0.006 (AL) to 0.23 (HAL under Raney Ni-NF), which was mainly due to the increase in hydrogen content and the decrease in oxygen content after ECH. The increased H/C_{eff} ratio demonstrates the increased ability of the feedstock to produce olefins and aromatics[34]. On the other hand, the breakage

of lignin functional groups in ECH makes the unsaturation of HAL decrease, which tends to be similar to that of benzene (Ω=4). This indicates that the aromatic ring hydrogenation did not occur, but some of the oxygen-containing functional groups were broken by electrochemical reduction.

Table 5- 5 The elemental composition of AL and HAL samples was pretreated with the presence of different electrodes.

Sample		**Elemental composition**[a]					**H/C$_{eff}$ ratio**[c]	**Ω**[d]
	Electrode	**C**	**H**	**O**	**S**	**N**		
AL	-	54.67	4.76	37.86	2.43	0.30	0.006	3.19
HAL[b]	Pt	57.64	4.69	34.99	2.42	0.26	0.066	3.59
	Raney Ni-CP	50.39	4.01	43.47	1.88	0.24	-0.34	3.31
	Ni foam	58.38	4.89	34.08	2.40	0.25	0.13	3.55
	Raney Ni-NF	62.40	4.94	30.01	2.38	0.27	0.23	3.87

[a]: On a dry basis

[b]: The HAL samples were prepared at room temperature for 2 hours, with 1 M NaOH as electrolyte.

[c]: Hydrogen to carbon atomic effective ratio, H/C$_{eff}$ ratio=(H-2O)/C, where C = number of carbons, H = number of hydrogens, O = number of oxygens.

[d]: Degree of unsaturation Ω=(C+1) + N/2-H/2, where C = number of carbons, H = number of hydrogens, N = number of nitrogens.

The HAL samples treated with different electrodes with and without catalysts were tested by FTIR (Fig. 5-12). The recorded spectra of lignin samples were analyzed based on assignments in the literature[35]. After the electrochemical reaction, C=O groups showed in hydrogenated lignin samples, which were attributed to the cleavage of internal ether bonds. On the other hand, after the treatment with Raney Ni-NF and Pt, the intensity of carbonyl/carboxyl groups became lower due to hydrogenation further occurring. So that, C-O deformation in secondary alcohols, C-O in aryl-alkyl and O-H groups stretching both increased after the ECH pretreatment. Moreover, -CH_3 alkane and –CH_2 methylene groups of HAL samples treated with Raney Ni-NF and Pt also

slightly increased. And the peaks of aromatic groups that became more intensive might attribute to the partial decomposition of side groups during the electrochemical reaction. And in all the HAL samples, HAL treated with Raney Ni-NF has a higher intensity of functional groups mentioned above, next is Pt. However, due to complex bonds and various vibration modes, the spectral below 1400 cm^{-1} was hard to analyze exactly.

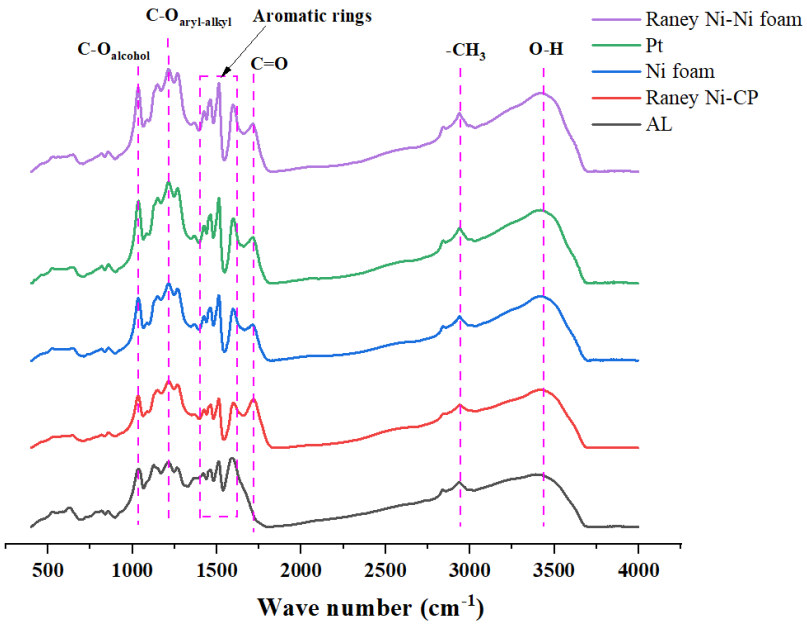

Fig. 5- 12 FT-IR spectroscopy of AL and HAL samples with various electrodes.

HSQC NMR was used to provide more detailed information about lignin structure before and after ECH, which has allowed for the resolution of overlapping resonances observed in either the ^{1}H or ^{13}C NMR spectra[36]. The side-chain and aromatics regions in HSQC spectra can be identified in the range of δC/δH 50-90/2.5-6.0 and δC/δH 100-135/5.5-8.5, respectively[23]. The HSQC spectra of AL and HAL are shown in Fig. 5-13, and the assignments of the main cross signals detected are listed in Table 5-2.

As shown in Fig. 5-13, the C-H in methoxyl has a major signal in the side-chain regions. The C_{γ}-H_{γ} correlations in β-O-4′ substructures (A), resinol substructures (B),

and phenylcoumaran substructures (C) were shown at δC/δH 59.5-59.7/3.4-3.63, 71.0/3.82, 4.18, and 62.5/3.73, respectively. These signals proved that the alkaline lignin was partially acylated at γ-position carbon in β-O-4′ linkages[37]. However, the signals for C_α-H_α, and C_β-H_β were not found in the side-chain regions. G-type lignin units (guaiacyl units) showed a prominent signal in the alkaline lignin, and the correlations for C_2-H_2, C_5-H_5, and C_6-H_6 at δC/δH 110.9/6.98, 114.9/6.77, and 119.0/6.8 were found in the aromatic regions. Moreover, C_2-H_2 and C_6-H_6 in oxidized G′ units were observed at δC/δH 111.4/7.51 and 118.9/6.07, respectively. C_3–H_3 and C_5–H_5 in p-coumarate (PCA) were also clearly detected. And minor correlations from $C_{3,5}$-$H_{3,5}$ and $C_{2,6}$-$H_{2,6}$ in p-hydroxyphenyl units (H) were observed in the spectra. After pretreating with the electrochemical hydrogenation process, the spectra of HAL have no obvious differences from that of AL. Only C_6-H_6 in oxidized G′ units were observed to disappear after ECH due to the occurrence of the reduction reaction. And the signals of G2′ also show weak after ECH. No apparent changes were found in the side-chain regions of the HSQC spectra. Because the electrochemical hydrogenation reaction occurs under very mild conditions, even the methoxyl groups, which are prone to bond breakage, are well preserved. In fact, due to the properties of alkaline lignin, it does not dissolve well in the DMSO-d6 solution, so the 2D NMR spectra obtained do not show all the lignin structures. Therefore, the quantification of the lignin structure is quite difficult.

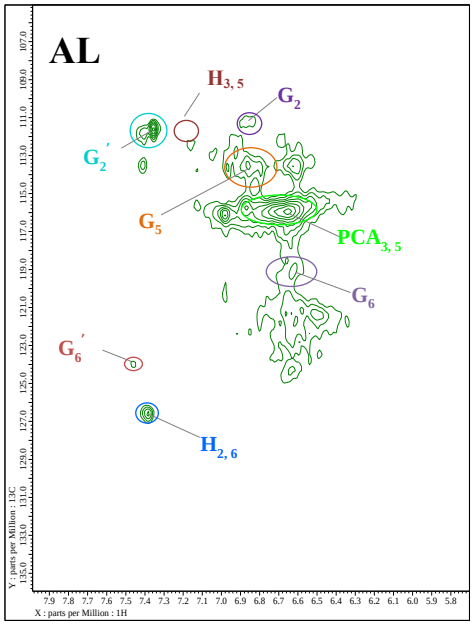
AL
H3, 5
G2
G2′
G5
PCA3, 5
G6
G6′
H2, 6
Y : parts per Million : 13C
X : parts per Million : 1H

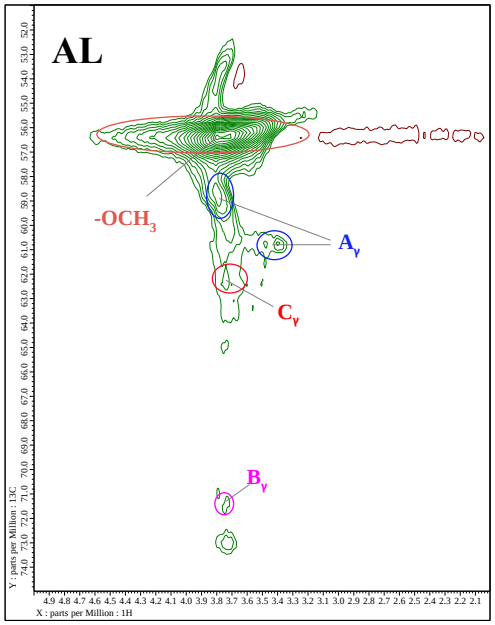
AL
-OCH3
Aγ
Cγ
Bγ
Y : parts per Million : 13C
X : parts per Million : 1H

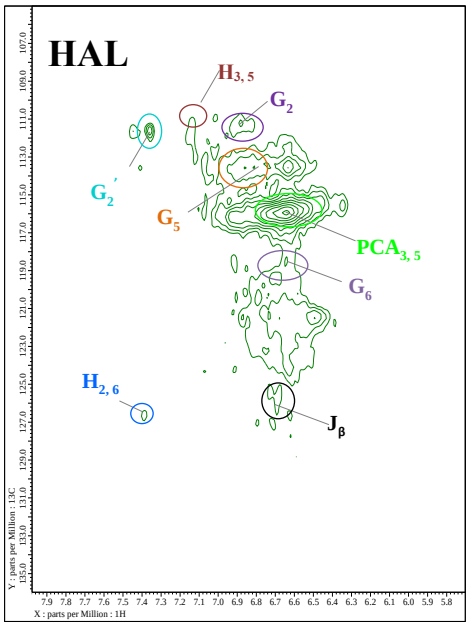
HAL
H3, 5
G2
G2′
G5
PCA3, 5
G6
H2, 6
Jβ
Y : parts per Million : 13C
X : parts per Million : 1H

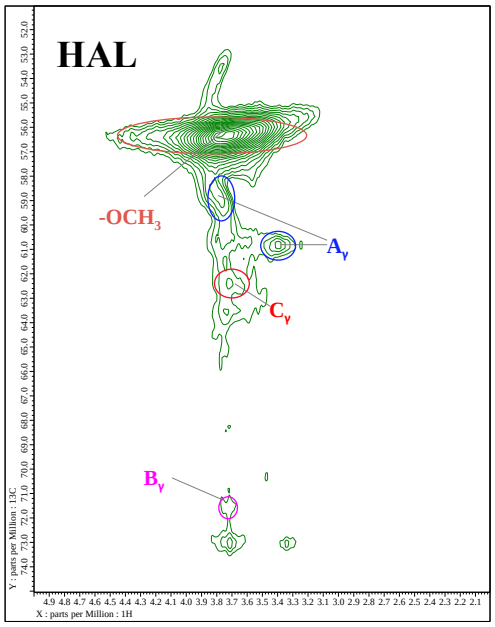
HAL
-OCH3
Aγ
Cγ
Bγ
Y : parts per Million : 13C
X : parts per Million : 1H

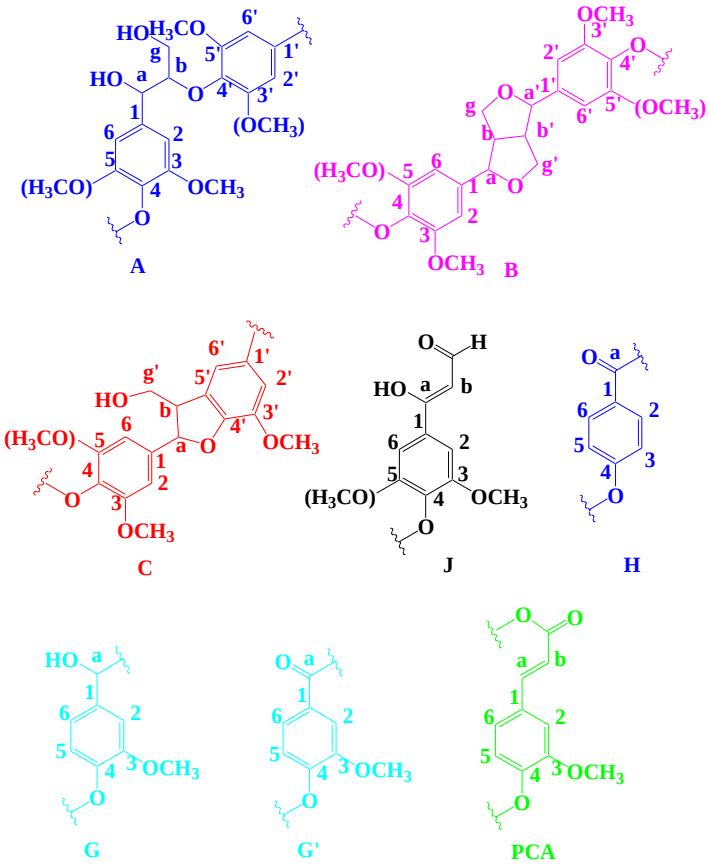

Fig. 5- 13 The ^{1}H-^{13}C HSQC NMR spectra (δC/δH 105-136/5.7-8.0 ppm, 51-75/2.0-5.0 ppm, 31-55/2.0-3.2 ppm) for alkaline lignin and hydrogenated lignin. HAL was pretreated with Raney Ni-NF in H-cell for 2 hours. The primary substructures (involving different side-chain linkages and aromatic units) identified are listed in the right column.

TG analysis was used to test the thermal decomposition regularity of lignin samples within 1000 ℃. From the TG diagram (Fig. 5-14(a)), it can be seen that the lignin samples have a maximum weight loss slope between 200-500 °C, which is the main temperature range for releasing volatile fractions. The DTG curve can clearly show the reaction rate at each temperature point. Compared with AL (red line in Fig. 5-14(b)), the DTG peaks of HAL samples all shifted to a higher temperature, around 350 ℃. Furthermore, HAL samples treated with NF and Raney Ni-NF have a more intensive

mass reduction rate at a higher temperature range. This suggests that the electrochemical hydrogenation reaction results in a better thermal reactivity of hydrogenated lignin. In the temperature range from 800 ℃ to 1000 ℃, there are some fluctuations in HAL samples that might be due to the instability of instrument measurements at high temperatures.

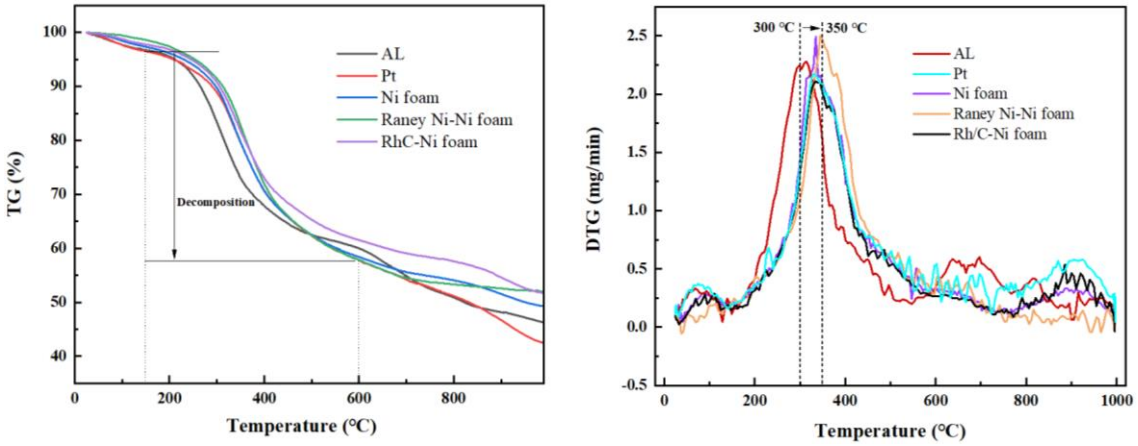

(a) (b)

Fig. 5- 14 Thermogravimetric analysis (TGA) for AL and HAL samples treated with different catalysts.

The main compounds in the oil-phase compounds after ECH of lignin were determined by GC-MS. The chromatogram of the different oil products with various electrodes is shown in Fig. 5-15. According to Table 5-6, the main compounds in the oil phase after electrochemical hydrogenation was phenolic aldehydes, like vanillin, and 4-hydroxy-benzaldehyde, which is also consistent with the results from Chen's work[38][39]. And other phenolic compounds, like 2-methoxy-phenol, 4-hydroxy-3-methoxy-benzenepropanol, 3-Allyl-6-methoxyphenol, and etc., were found in the bio-oil phase due to the occurrence of partial degradation and subsequent hydrogenation on lignin polymers[40]. Moreover, trace amounts of phenolic acids, such

as apocynin, vanillic acid, and homovanillic acid, were also discovered in the oil phase as high hydroxide concentration from 1 M NaOH electrolyte and the electrolysis of water. It is a fact that the reduction reaction of the water in the cathodic electrolyte occurs simultaneously with the electrochemical hydrogenation of lignin, forming H radicals and OH^- ions in base media[41]. Thus, both H and OH^- reacted with the lignin intermediates chemisorbed on the surface of the cathode, providing the hydrogen and hydroxyl groups along with lignin molecules. This is also the reason that the oxygen content of the hydrogenated lignin after ECH was reduced but not as low as that of the hydrogenated lignin after thermal catalytic hydrogenation (TCH)[15]. Moreover, H radicals chemisorbed on the electrode surface would suffer from desorption and form H_2 (by Tafel reaction) as a by-product with the negative overpotential, which would significantly affect the hydrogenation reaction of lignin. In truth, the acidic electrolyte is preferable for ECH applications due to the requirement of high proton concentration as the donor of hydrogen radicals[42]. But the most types of lignins can only dissolve in alkaline solutions or some organic solutions. Therefore, it is more important how to choose the electrolyte and how to provide a hydrogen source effectively in the study of lignin electrochemical hydrogenation.

According to the distribution of the main products in the oil phase, it can be seen that when Pt and bare Ni foam are used as working electrodes, the major product is vanillin, followed by small amounts of apocynin and vanillic acid. When Raney Ni was loaded on the electrode as a catalyst, the product distribution changed; Raney Ni-CP promoted more vanillic acid production, while the presence of Raney Ni-NF led to an increase in the proportion of apocynin. However, the saturated cyclic hydrocarbons were not found in the present oil-phase products, which proves that the hydrogenation reaction still has not occurred efficiently on the aromatic structure of lignin; instead mainly occurred on the free radicals after the internal bonds cleavage of lignin. This part of the oil-phase products, especially vanillin, can be used as a flavouring, or chemical

intermediate in producing pharmaceuticals, cosmetics, and other fine chemicals[43], when isolated and purified properly from the oil mixture[39]. Otherwise, this oil-phase product can be used as bio-oil energy, which is the purpose of the most lignin degradation research.

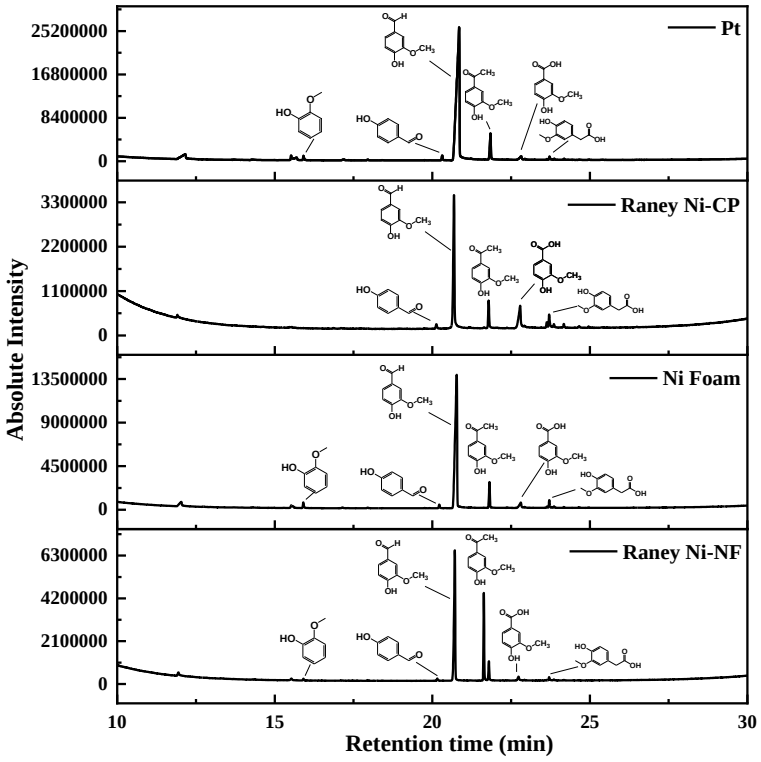

Fig. 5- 15 The GC-MS chromatogram of oil-phase compounds with different electrodes: Pt, Raney Ni-CP, Ni foam, Raney Ni-NF.

Table 5- 6 The main compounds in the oil-phase compounds after electrochemical hydrogenation pretreatment with different electrodes were detected by GC-MS.

Compounds (area-%)	Chemical formula	Retention time	Pt	Raney Ni-CP	Ni foam	Raney Ni-NF

Propanoic acid, 2-hydroxy-, ethyl ester	$C_5H_{10}O_3$	11.94	4.16	1.24	3.6	2.29
3-Pentanol	$C_5H_{12}O$	13.71	0.14	-	-	-
2-Hydroxy-gamma-butyrolactone	$C_4H_6O_3$	14.28	0.29	-	0.19	-
Diethyl carbitol	$C_8H_{18}O_3$	15.53	1.12	-	0.91	0.94
2-Furancarboxylic acid	$C_5H_4O_3$	15.58	1.47	-	0.69	-
Phenol, 2-methoxy-	$C_7H_8O_2$	15.91	0.92	-	2.81	0.54
Benzoic acid	$C_7H_6O_2$	17.11	0.35	-	0.34	0.13
Ethane, 1,1'-oxybis, 2-methoxy-	$C_6H_{14}O_3$	17.94	0.17	-	0.27	0.22
2-Isobutoxyethyl acetate	$C_8H_{16}O_3$	19.76	0.06	0.15	-	-
Benzaldehyde, 4-hydroxy-	$C_7H_6O_2$	20.16	0.95	1.72	1.85	0.88
Vanillin	$C_8H_8O_3$	20.72	78.99	58.23	67.22	58.37
Acetophenone, 4'-hydroxy-	$C_8H_8O_2$	21.20	0.08	0.43	0.25	0.28
Tetraglyme	$C_{10}H_{22}O_5$	21.64	0.08	0.31	-	23.88
Apocynin	$C_9H_{10}O_3$	21.80	7.03	8.99	13.03	6.48
Phenol, 2-methoxy-4-(methoxymethyl)-	$C_9H_{12}O_3$	22.38	0.44	0.21	0.29	0.16
Vanillic acid	$C_8H_8O_4$	22.74	1.75	16.08	2.68	2.35
1-Propanone, 1-(4-hydroxy-3-methoxyphenyl)-	$C_{10}H_{12}O_3$	22.93	0.35	1.22	0.44	0.27
Homovanillic acid	$C_9H_{10}O_4$	23.63	0.88	1.89	0.61	0.23
Benzenepropanol, 4-hydroxy-3-methoxy-	$C_{10}H_{14}O_3$	23.71	0.29	5	3.88	1.28
Benzaldehyde,	$C_9H_{10}O_4$	23.86	0.2	1.63	0.78	0.35

4-hydroxy-3,5-dimethoxy-Phenylacetylformic acid, 4-hydroxy-3-methoxy-	$C_{10}H_{10}O_5$	24.18	0.16	1.02	0.43	0.15
Ethanone, 1-(4-hydroxy-3,5-dimethoxyphenyl)-	$C_{10}H_{12}O_4$	24.66	0.44	0.67	0.31	0.12
3-Allyl-6-methoxyphenol	$C_{10}H_{12}O_2$	24.96	1.75	0.35	0.08	-

After characterizing the solid and oil-phase products, the authors suggested possible reaction pathways in the cathodic electrolyzer (in Fig. 5-16), which has been scarcely mentioned in the literature. Importantly, the water reduction and hydrogen evolution reactions proceed in base solutions for the formation of adsorbed hydrogen radicals and H_2 evolution[44], continuously occurring in the cathodic electrolyte, simultaneously with the ECH of lignin. The dimer compounds illustrated in Fig. 5-16 represent the most typical lignin structures, including phenylpropane uint, which are linked with common ether bonds (β-O-4, α-O-4). The R here represents -H or methoxyl group. First, the lignin polymers were adsorbed on the electrode, and then the electrolysis reaction occurred on the ether bonds and was cleaved into the lower-weight intermediates. And the hydrogenation of lignin intermediates happened with absorbed H radicals to form guaiacol or guaiacyl oligomers and apocynin. The hydroxide in the electrolyte further reacted with the lignin oligomers or monomers, so that the vanillic acid, vanillin, 4-hydroxy-benzaldehyde, as well as homovanillic acid generated. For solid hydrogenated lignin, in addition to depolymerization and hydrogenation reactions of lignin, there is also the addition of the hydroxyl group, which is consistent with the findings in FTIR.

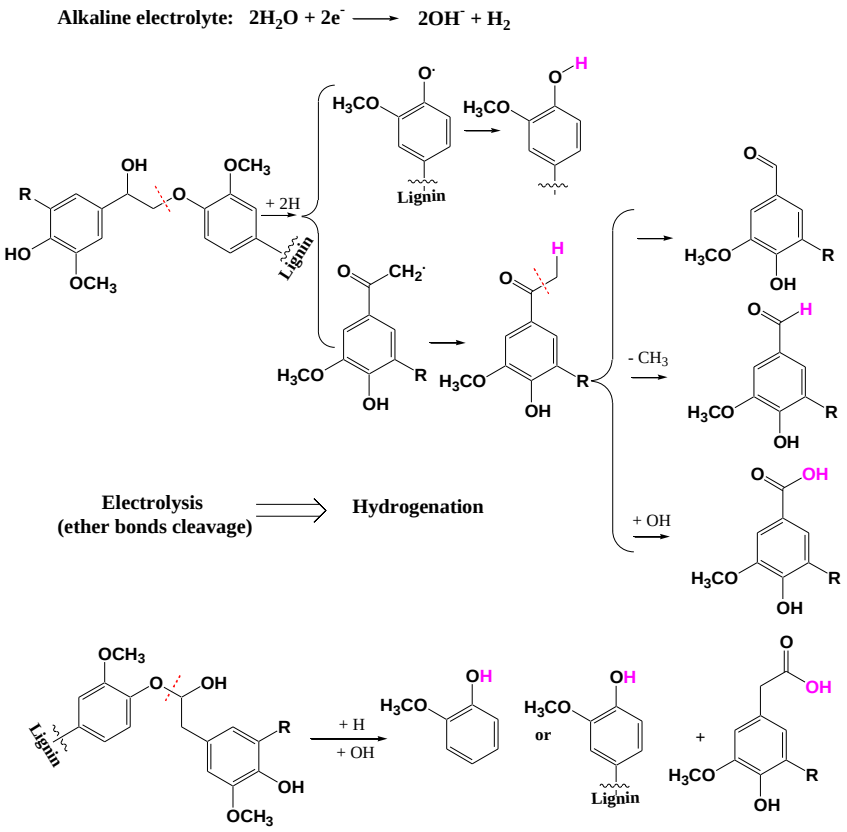

Fig. 5- 16 The proposed reaction pathways for the electrochemical cathodic reaction of lignin.

5.5 Conclusions

In the present study, we investigate the effect of electrochemical hydrogenation on alkaline lignin structure and the pyrolysis characteristic of hydrogenated lignin. The various parameters (such as lignin concentrations, reaction time, temperature, input current/potential, and electrode materials) affect hydrogenated products, which were examined and rationalized through analyzing product structure. The electrode material is one of the important factors to affect the redox properties of the electrochemical reaction, in which an obvious reduction peak (in CV curve) was shown when Ni foam was used as the WE substrate. And a better reduction effect was obtained when Ni foam was loaded with common commercial hydrogenation catalysts (Raney Ni, Ru/C, and

Rh/C). The electrochemical conversion under mild conditions effectively prevented the depolymerization of lignin and allowed the recovery of more HAL (64-82 wt.%). According to the characterizations (FTIR, TGA, and elemental analysis), the HAL samples have shown intensive C=O functional stretching, relatively higher thermal reactivity, and higher H/C_{eff} ratio, especially treated with Raney Ni-NF as WE. So, electrochemical hydrogenation is regarded as an effective pretreatment for lignin to produce more light olefins. Fast pyrolysis of HAL samples has been performed by TS-TR coupled with GC-TCD/FID with different columns. The light hydrocarbons and aromatic compounds released from the lignin samples can be detected, showing a noticeable increase after ECH. Compared to 0.75 wt.% of olefins yield from AL, the highest olefins yield of HAL obtained from Raney Ni-NF catalyst for 2 hours reaction was 2.22 wt.%. Moreover, the aromatics yield also significantly increased from 1.23 wt.% of AL to 4.07 wt.% of HAL (Raney Ni-NF, 2 hours, RT). For the oil products after ECH, not only phenolic monomers but the phenolic aldehydes and acids were generated by lignin electrochemical reaction due to the high hydroxide concentration in the cathodic cell. Vanillin is the major product after the ECH of lignin, and can also be used for other fine chemicals or cosmetics in manufacturing production after proper purification. Milder electrochemical hydrogenation technology can avoid the thermal depolymerization of lignin at high temperatures. Furthermore, ECH has offered several advantages in terms of safety, operability, and economics. Thus, the insights gained from this work will benefit the future technology on electrochemical hydrogenation and the fast pyrolysis process on lignin.

5.6 Reference

[1] M. Yang, J. Shao, Z. Yang, H. Yang, X. Wang, Z. Wu, H. Chen, Conversion of lignin into light olefins and aromatics over Fe/ZSM-5 catalytic fast pyrolysis: Significance of Fe contents and temperature, J. Anal. Appl. Pyrolysis. 137 (2019) 259–265. https://doi.org/10.1016/j.jaap.2018.12.003.

[2] J.A. Caballero, R. Font, A. Marcilla, Pyrolysis of Kraft lignin: Yields and correlations, J. Anal. Appl. Pyrolysis. 39 (1997) 161.

[3] E.T. Liakakou, B.J. Vreugdenhil, N. Cerone, F. Zimbardi, F. Pinto, R. André, P. Marques, R. Mata, F. Girio, Gasification of lignin-rich residues for the production of biofuels via syngas fermentation: Comparison of gasification technologies, Fuel. 251 (2019) 580–592. https://doi.org/https://doi.org/10.1016/j.fuel.2019.04.081.

[4] S.C. Qi, J.I. Hayashi, S. Kudo, L. Zhang, Catalytic hydrogenolysis of kraft lignin to monomers at high yield in alkaline water, Green Chem. 19 (2017) 2636–2645. https://doi.org/10.1039/c7gc01121k.

[5] J. Jeong, W.S. Kim, M.W. Lee, M. Goh, Liquefaction of Lignin Using Chemical Decomposition and Its Application to Polyurethane Foam, ACS Omega. 6 (2021) 10745–10751. https://doi.org/10.1021/acsomega.1c00285.

[6] L. Das, S. Xu, J. Shi, Catalytic Oxidation and Depolymerization of Lignin in Aqueous Ionic Liquid, Front. Energy Res. 5 (2017) 21. https://doi.org/10.3389/fenrg.2017.00021.

[7] G. Jiang, D.J. Nowakowski, A. V. Bridgwater, Effect of the temperature on the composition of lignin pyrolysis products, Energy and Fuels. 24 (2010) 4470–4475. https://doi.org/10.1021/ef100363c.

[8] J. Cao, G. Xiao, X. Xu, D. Shen, B. Jin, Study on carbonization of lignin by TG-FTIR and high-temperature carbonization reactor, Fuel Process. Technol. 106

(2013) 41–47. https://doi.org/10.1016/j.fuproc.2012.06.016.

[9] A. Bjelić, M. Grilc, M. Huš, B. Likozar, Hydrogenation and hydrodeoxygenation of aromatic lignin monomers over Cu/C, Ni/C, Pd/C, Pt/C, Rh/C and Ru/C catalysts: Mechanisms, reaction micro-kinetic modelling and quantitative structure-activity relationships, Chem. Eng. J. 359 (2019) 305–320. https://doi.org/10.1016/j.cej.2018.11.107.

[10] S. Tang, C. Zhang, X. Xue, Z. Pan, D. Wang, R. Zhang, Catalytic pyrolysis of lignin over hierarchical HZSM-5 zeolites prepared by post-treatment with alkaline solutions, J. Anal. Appl. Pyrolysis. 137 (2019) 86–95. https://doi.org/10.1016/j.jaap.2018.11.013.

[11] X. Cui, A.E. Surkus, K. Junge, C. Topf, J. Radnik, C. Kreyenschulte, M. Beller, Highly selective hydrogenation of arenes using nanostructured ruthenium catalysts modified with a carbon-nitrogen matrix, Nat. Commun. 7 (2016). https://doi.org/10.1038/ncomms11326.

[12] M. Yang, J. Shao, Z. Yang, H. Yang, X. Wang, Z. Wu, H. Chen, Conversion of lignin into light olefins and aromatics over Fe/ZSM-5 catalytic fast pyrolysis: Significance of Fe contents and temperature, J. Anal. Appl. Pyrolysis. 137 (2019) 259–265. https://doi.org/10.1016/j.jaap.2018.12.003.

[13] J. Long, Q. Zhang, T. Wang, X. Zhang, Y. Xu, L. Ma, An efficient and economical process for lignin depolymerization in biomass-derived solvent tetrahydrofuran, Bioresour. Technol. 154 (2014) 10–17. https://doi.org/https://doi.org/10.1016/j.biortech.2013.12.020.

[14] L. Zhang, C. Choi, H. Machida, K. Norinaga, Production of light hydrocarbons from organosolv lignin through catalytic hydrogenation and subsequent fast pyrolysis, J. Anal. Appl. Pyrolysis. 156 (2021) 105096. https://doi.org/https://doi.org/10.1016/j.jaap.2021.105096.

[15] L. Zhang, C. Choi, H. Machida, Z. Huo, K. Norinaga, Catalytic hydrotreatment

of alkaline lignin and its consequent influences on fast pyrolysis, Carbon Resour. Convers. 4 (2021) 219–229. https://doi.org/https://doi.org/10.1016/j.crcon.2021.09.001.

[16] P. Zuman, E.B. Rupp, Electrochemical investigations of alkaline cleavage of lignin under mild conditions, Collect. Czechoslov. Chem. Commun. 66 (2001) 1125–1139. https://doi.org/10.1135/cccc20011125.

[17] C. Lan, H. Fan, Y. Shang, D. Shen, G. Li, Electrochemically catalyzed conversion of cornstalk lignin to aromatic compounds: An integrated process of anodic oxidation of a Pb/PbO2 electrode and hydrogenation of a nickel cathode in sodium hydroxide solution, Sustain. Energy Fuels. 4 (2020) 1828–1836. https://doi.org/10.1039/c9se00942f.

[18] Z. Fang, M.G. Flynn, J.E. Jackson, E.L. Hegg, Thio-assisted reductive electrolytic cleavage of lignin β-O-4 models and authentic lignin, Green Chem. 23 (2021) 412–421. https://doi.org/10.1039/d0gc03597a.

[19] J. Zhang, X. Zhang, D. Xie, D. Liu, Z. Li, Effect of technological factors on electrochemical hydrogenation of lignin, Can. J. Chem. Eng. 80 (2002) 1–5. https://doi.org/10.1002/cjce.5450800402.

[20] M. Garedew, C.H. Lam, L. Petitjean, S. Huang, B. Song, F. Lin, J.E. Jackson, C.M. Saffron, P.T. Anastas, Electrochemical upgrading of depolymerized lignin: a review of model compound studies, Green Chem. 23 (2021) 2868–2899. https://doi.org/10.1039/d0gc04127k.

[21] K. Norinaga, O. Deutschmann, Detailed kinetic modeling of gas-phase reactions in the chemical vapor deposition of carbon from light hydrocarbons, Ind. Eng. Chem. Res. 46 (2007) 3547–3557. https://doi.org/10.1021/ie061207p.

[22] H.-M. Yang, S. Appari, S. Kudo, J. Hayashi, K. Norinaga, Detailed Chemical Kinetic Modeling of Vapor-Phase Reactions of Volatiles Derived from Fast Pyrolysis of Lignin, Ind. Eng. Chem. Res. 54 (2015) 6855–6864.

https://doi.org/10.1021/acs.iecr.5b01289.

[23] T.-Q. Yuan, S.-N. Sun, F. Xu, R.-C. Sun, Characterization of Lignin Structures and Lignin–Carbohydrate Complex (LCC) Linkages by Quantitative 13C and 2D HSQC NMR Spectroscopy, J. Agric. Food Chem. 59 (2011) 10604–10614. https://doi.org/10.1021/jf2031549.

[24] J.C. del Río, P. Prinsen, J. Rencoret, L. Nieto, J. Jiménez-Barbero, J. Ralph, Á.T. Martínez, A. Gutiérrez, Structural Characterization of the Lignin in the Cortex and Pith of Elephant Grass (Pennisetum purpureum) Stems, J. Agric. Food Chem. 60 (2012) 3619–3634. https://doi.org/10.1021/jf300099g.

[25] M. Liu, Y. Wen, J. Qi, S. Zhang, G. Li, Fine Chemicals Prepared by Bamboo Lignin Degradation through Electrocatalytic Redox between Cu Cathode and Pb/PbO2 Anode in Alkali Solution, ChemistrySelect. 2 (2017) 4956–4962. https://doi.org/https://doi.org/10.1002/slct.201700881.

[26] W. Xu, S.J. Miller, P.K. Agrawal, C.W. Jones, Depolymerization and hydrodeoxygenation of switchgrass lignin with formic acid, ChemSusChem. 5 (2012) 667–675. https://doi.org/10.1002/cssc.201100695.

[27] R. Shu, Y. Xu, P. Chen, L. Ma, Q. Zhang, L. Zhou, C. Wang, Mild Hydrogenation of Lignin Depolymerization Products over Ni/SiO2 Catalyst, Energy and Fuels. 31 (2017) 7208–7213. https://doi.org/10.1021/acs.energyfuels.7b00934.

[28] J. van Drunen, B.K. Pilapil, Y. Makonnen, D. Beauchemin, B.D. Gates, G. Jerkiewicz, Electrochemically Active Nickel Foams as Support Materials for Nanoscopic Platinum Electrocatalysts, ACS Appl. Mater. Interfaces. 6 (2014) 12046–12061. https://doi.org/10.1021/am501097t.

[29] A. Cyr, F. Chiltz, P. Jeanson, A. Martel, L. Brossard, J. Lessard, H. Ménard, Electrocatalytic hydrogenation of lignin models at Raney nickel and palladium-based electrodes, Can. J. Chem. 78 (2000) 307–315.

https://doi.org/10.1139/v00-009.

[30] R. Fonocho, C.L. Gardner, M. Ternan, A study of the electrochemical hydrogenation of o-xylene in a PEM hydrogenation reactor, Electrochim. Acta. 75 (2012) 171–178. https://doi.org/10.1016/j.electacta.2012.04.116.

[31] K. Yan, Y. Zhang, M. Tu, Y. Sun, Electrocatalytic Valorization of Organosolv Lignin Utilizing a Nickel-Based Electrocatalyst, Energy and Fuels. 34 (2020) 12703–12709. https://doi.org/10.1021/acs.energyfuels.0c02284.

[32] C. Yang, H. Chen, T. Peng, B. Liang, Y. Zhang, W. Zhao, Lignin valorization toward value-added chemicals and fuels via electrocatalysis: A perspective, Chinese J. Catal. 42 (2021) 1831–1842. https://doi.org/https://doi.org/10.1016/S1872-2067(21)63839-1.

[33] Y. Jia, Y. Wen, X. Han, J. Qi, Z. Liu, S. Zhang, G. Li, Electrocatalytic degradation of rice straw lignin in alkaline solution through oxidation on a Ti/SnO2-Sb2O3/α-PbO2/β-PbO2 anode and reduction on an iron or tin doped titanium cathode, Catal. Sci. Technol. 8 (2018) 4665–4677. https://doi.org/10.1039/c8cy00307f.

[34] T.P. Vispute, H. Zhang, A. Sanna, R. Xiao, G.W. Huber, Renewable chemical commodity feedstocks from integrated catalytic processing of pyrolysis oils, Science (80-.). 330 (2010) 1222–1227. https://doi.org/10.1126/science.1194218.

[35] C.G. Boeriu, D. Bravo, R.J.A. Gosselink, J.E.G. Van Dam, Characterisation of structure-dependent functional properties of lignin with infrared spectroscopy, Ind. Crops Prod. 20 (2004) 205–218. https://doi.org/10.1016/j.indcrop.2004.04.022.

[36] J.J. Villaverde, J. Li, M. Ek, P. Ligero, A. de Vega, Native Lignin Structure of Miscanthus x giganteus and Its Changes during Acetic and Formic Acid Fractionation, J. Agric. Food Chem. 57 (2009) 6262–6270. https://doi.org/10.1021/jf900483t.

[37] T.-Q. Yuan, S. Sun, F. Xu, R. Sun, Isolation and physico-chemical characterization of lignins from ultrasound irradiated fast-growing poplar wood, BioResources. 6 (2011) 414–433.

[38] A. Chen, Y. Wen, X. Han, J. Qi, Z.-H. Liu, S. Zhang, G. Li, Electrochemical Decomposition of Wheat Straw Lignin into Guaiacyl-, Syringyl-, and Phenol-Type Compounds Using Pb/PbO2 Anode and Alloyed Steel Cathode in Alkaline Solution, Environ. Prog. Sustain. Energy. 38 (2019) 13117. https://doi.org/https://doi.org/10.1002/ep.13117.

[39] D. Schmitt, C. Regenbrecht, M. Hartmer, F. Stecker, S.R. Waldvogel, Highly selective generation of vanillin by anodic degradation of lignin: A combined approach of electrochemistry and product isolation by adsorption, Beilstein J. Org. Chem. 11 (2015) 473–480. https://doi.org/10.3762/bjoc.11.53.

[40] V.L. Pardini, C.Z. Smith, J.H.P. Utley, R.R. Vargas, H. Viertler, Electroorganic Reactions. 38. Mechanism of Electrooxidative Cleavage of Lignin Model Dimers, J. Org. Chem. 56 (1991) 7305–7313. https://doi.org/10.1021/jo00026a022.

[41] Y.P. Wijaya, K.J. Smith, C.S. Kim, E.L. Gyenge, Electrocatalytic hydrogenation and depolymerization pathways for lignin valorization: Toward mild synthesis of chemicals and fuels from biomass, Green Chem. 22 (2020) 7233–7264. https://doi.org/10.1039/d0gc02782k.

[42] Y.P. Wijaya, T. Grossmann-Neuhaeusler, R.D. Dhewangga Putra, K.J. Smith, C.S. Kim, E.L. Gyenge, Electrocatalytic Hydrogenation of Guaiacol in Diverse Electrolytes Using a Stirred Slurry Reactor, ChemSusChem. 13 (2020) 629–639. https://doi.org/10.1002/cssc.201902611.

[43] A.K. Sinha, U.K. Sharma, N. Sharma, A comprehensive review on vanilla flavor: Extraction, isolation and quantification of vanillin and others constituents, Int. J. Food Sci. Nutr. 59 (2008) 299–326. https://doi.org/10.1080/09687630701539350.

[44] Y.P. Wijaya, K.J. Smith, C.S. Kim, E.L. Gyenge, Synergistic effects between electrocatalyst and electrolyte in the electrocatalytic reduction of lignin model compounds in a stirred slurry reactor, J. Appl. Electrochem. 51 (2021) 51–63. https://doi.org/10.1007/s10800-020-01429-w.

Chapter 6 Economic evaluation of the two-stage processes

6.1 Abstract

Appropriately utilizing lignin is a promising direction for improving the exploitation of biomass sources. In addition to experimental scale demonstration, the techno-economic of the processes should also be verified at the demonstration plant-scale. Aspen Plus was used to represent this two-stage on process simulation for converting lignin into valuable products in this chapter. Based on previous experimental data, the process was evaluated based by modelling a 1000 kg-feedstock/h. For the overall hydrogenation process coupled with pyrolysis reactions, process simulation buildup and optimization, heat exchange network creation, and economic evaluation were performed. The impact of different lignin feedstock (organosolv lignin and alkaline lignin) and hydrogenation technologies (thermal catalytic hydrogenation and electrochemical hydrogenation) on the overall economics was calculated and compared as different Scenarios. Simulations revealed that the annual profit of the whole process was mainly influenced by the product's value and the reaction materials, especially hydrogen and the solvent of the hydrogenation reaction. Economic analysis determines the feasibility of the process and is therefore necessary to provide some data support for the industrialization of lignin utilization.

6.2 Setup of process simulation in aspen plus

6.2.1 Process design

According to the process design, the overall process can be simplified separated into these five sections, hydrogenation process, product separation, fast pyrolysis

process, aimed product purification and heat supply. The process setup is shown like Fig. 6-1. The parameter setup was all based on the experiment data. Aspen Plus V12.1 was used to develop the process model and simulation setup. PR-BM method was used to describe the global properties.

In the hydrogenation process, the reactor used a RYield module, while 1000 kg/h lignin feedstock was set in the simulation. The condition was set to 250 ℃, and 3 MPa H_2 atmosphere according to the previous experimental data. The hydrogenation reaction was performed in the presence of 5% Ru/C as a catalyst. After the hydrogenation reaction, hydrogenated lignin was separated by flash modules and then go to the subsequent pyrolysis section. The product distribution was input in the ASPEN model as the data reported in Chapter 4.4.1 (hydrogenated lignin treated under the condition of 3 MPa H_2 at 250 ℃ with Ru/C). The phenolic products were separated from two-stage flash modules. Moreover, around 90% of hydrogen gas and 97% of THF can be recycled to reduce material costs.

When the stream moves to the pyrolysis reaction step, 20 kg/h of hydrogen is used as the carrier gas to pass the hydrogenated lignin into the reactor at 850 ℃. The pyrolysis reactor was also used with the RYield module, so that the pyrolyzed products yield, including C1-C4 olefins and alkanes, inorganic gases and major aromatic hydrocarbons (BTXN: benzene, toluene, xylenes, naphthalene) were input into the process with reference to the experimental data (Chapter 4.4.3).

After that, the products from fast pyrolysis were sent to the product separation section. The flash module was used to separate the char residue and bio-oil products from the volatile mixture at 100 ℃. And then, the volatiles was fed into two distillation columns (RadFrac), in which the gaseous products were separated from the top of the column, and the light aromatics (benzene, toluene, xylenes and naphthalene) were delivered to the bottom column for distillation. Moreover, the distillation solvent (THF) was going to the top column and recovered for recycling. Finally, the char residue was

put into the combustion section for heating supply.

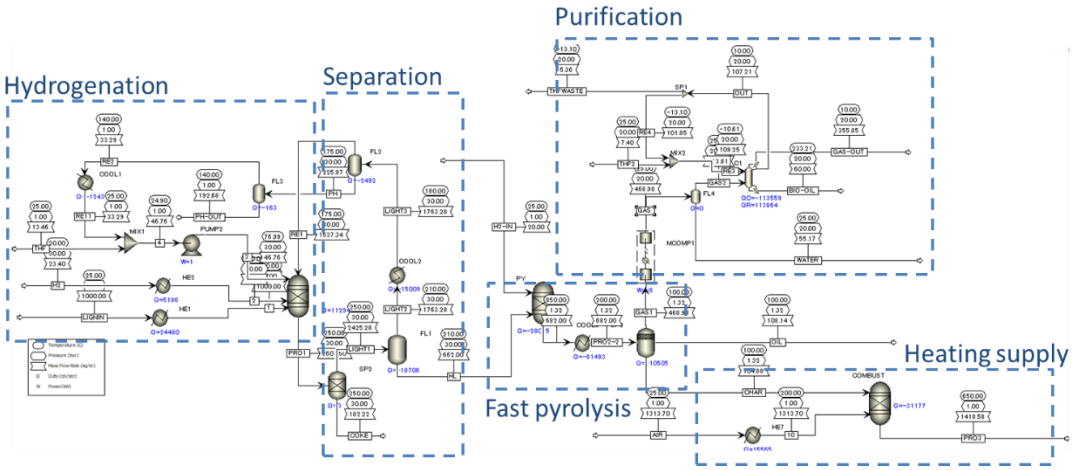

Fig. 6- 1 The simulation flow sheet for the whole process combined hydrogenation with fast pyrolysis.

The economic assumptions of the process were determined based on the parameters provided in Table 6-1. In this study, the basic information of plant, equipment, and its operating consumption, and raw material prices are referenced to Yang's work[1] with some adjustments. The price of the feedstock is highly dependent on the type of lignin used, which is assumed that organosolv lignin as technical lignin with a price of $120/MT in this work.

Table 6- 1 Description of parameters assumption for economic estimation.

Parameters	**Assumptions**
Plant	
Plant life	15 years
Start-up time	0.25 years
Construction period	3 years
Depreciation	7 years

On-stream percentage after start-up	91.3% (8000 operating hours each year)
Finance	
Construction costs	32% Y1; 60% Y2; 8% Y3
Equity	40%
Working capital	5% of FCI
Plant salvage value	No
Internal rate of return (IRR)	10%
Revenue	50% of normal
Variable and fixed costs	75% and 100% of normal
Interest rate of financing	8% annually
Income tax rate	35%
Feedstock and chemicals	
Feedstock price	$120 /MT
H_2	$3.3 /kg
THF	$2740/ MT
5% Ru/C	$14.2/g (Sigma-Aldrich)
Products	
Olefins	$697/MT
Alkanes	$1350/tons [2]
Benzene	$883/ MT
Char	$42.5/MT
Syngas	$1041/tons
Phenolics	$750 /tons[a]

Bio-oil	$0.94/gal[3]
Utility	
Electricity price	$0.06 /kWh
Cooling water	$0.002 /kWh
H_2O	$0.2 /MT
Cooling tower chemicals	$33.8 /ton-cool/year
Wastewater treatment	$1.36 /MT
Solid disposal	$33 /MT
Operation cost	
Plant manager	$140000 annual
Maintenance	3% of FCI
Total salaries	$5.958*10^4 per position annual
Insurance and taxes	0.7% of FCI

[a] : Value is taken from the blog of Forest2Market (https://www.forest2market.com/blog), which varies from $650-1000/ton.

6.2.2 Process optimization

And after the process set up, the heating network was built for energy saving, as seen in Fig. 6-2. The heat exchange network consists of two main parts, one is the hydrogenation process, and another is the pyrolysis part. A part of the heat from the hydrogenated products was used to preheat the lignin, and another part was used to supply to EX4. And the heating exchange of the pyrolysis process is very important for energy saving of the whole process because the pyrolysis reaction takes place at a higher temperature (850 °C), so utilizing the extra heating energy is essential. Here, five

heat exchange modules (EX1-EX5) were added after the pyrolysis reaction to utilize the heat energy after the pyrolysis in a hierarchical way. One part is used for the preheating of the hydrogenated lignin (EX1). Another part acts on the char combustion part for preheating the char and air by EX2 and EX3, respectively. EX4 and EX5 exchanged part of the heat from the hydrogenation process and the heat of the column module (C1), respectively.

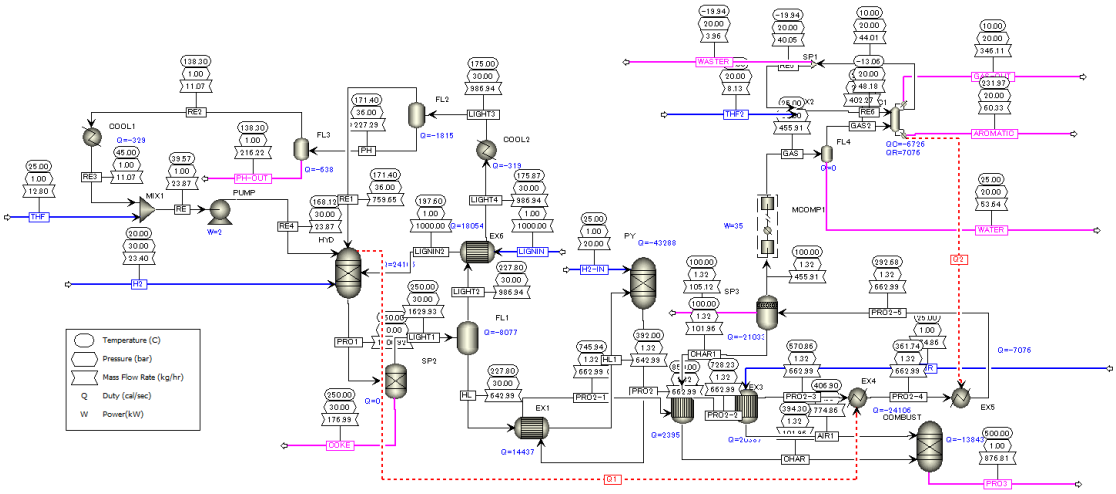

Fig. 6- 2 The main flow sheet of the optimized process with data (heat duties, flow rate and operating conditions) on streams.

The establishment of the heat exchange network significantly reduces the energy consumption of the whole process. The whole process after optimization has a net heat value of 0, consumes 235.4 kW of electrical energy, and consumes a net cooling value of $5.4967*10^4$ cal/sec. Figure 6-3 shows the energy savings after building the heat exchange network, which is enabled directly by Aspen Energy Analyzer (AEA) module. It can be seen that due to the heat exchange network, there is a substantial reduction in the energy consumption of the entire process, especially the heating utilities. Because the heat energy after pyrolysis is used for heat exchange, it can meet the heat energy supply needs of other equipment. And carbon emission derived from AEA shows a large

decrease after being optimized with the heating exchange network (seen in Table 6-2). Although the cost of heat exchange equipment rises as the number of exchange units grows, energy conservation is the primary requirement of modern industry.

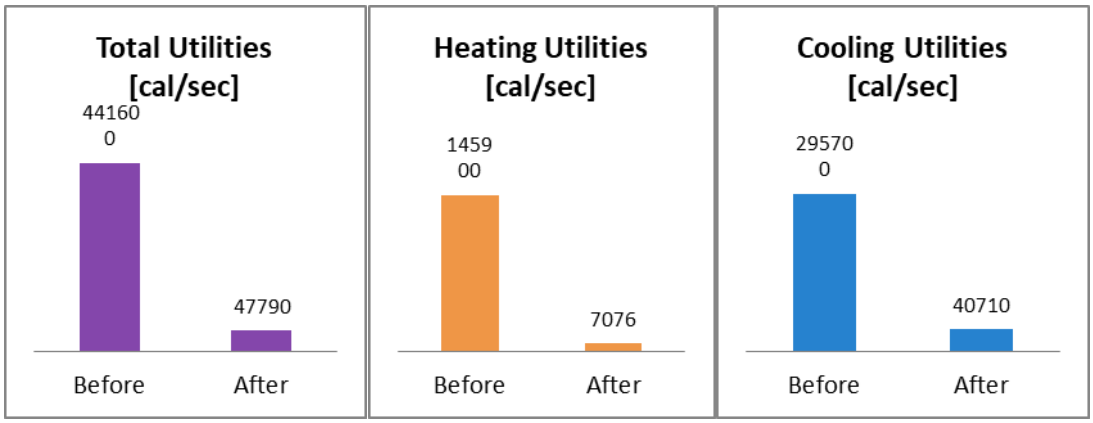

Fig. 6- 3 Energy analysis of the utilities before and after heating exchange network setup.

Table 6- 2 Summary of the energy saving before and after heating exchange network setup.

Property	Before	After
Total Utilities [cal/sec]	441600	47790
Heating Utilities [cal/sec]	145900	7076
Cooling Utilities [cal/sec]	295700	40710
Carbon Emissions [kg/hr]	240.3	12.84

After that, the author also optimized the process using MATLAB software. In order to optimize the process, an economic assessment of the processes was introduced. The total annualized profit was defined as the value of products (V_{Pro}) minus the total operating cost (TOC), expressed in eq. (6-1).

$$\text{Profit} = V_{Pro} - \text{TOC} \quad (6\text{-}1)$$

Where the V_{Pro} includes the annualized value of olefins, syngas, aromatics,

bio-oils (in pyrolysis), and phenolics (PH in hydrogenation); TOC is the sum of variable operating costs (e.g., feedstock cost, consumable cost, and fixed capital investment (FCI)) and fixed operating costs (e.g., operating labour cost and maintenance cost, and insurance costs).

To achieve the maximum profits of the process, the parameters, including the operating specifications of the distillation column, the temperature and pressure of flashes, and the temperature of the exchangers, have been optimized as discrete variables or continuous variables. Therefore, the maximum profit can be formulated as an MINLP problem and is mathematically demonstrated as follows.

$$\max_{x} \text{Profit} = f(x) \tag{6-2}$$

$$s.t. h(x) = 0 \tag{6-3}$$

$$g(x) \leq 0 \tag{6-4}$$

$$x_{\min} \leq x \leq x_{\max} \tag{6-5}$$

Where $f(x)$ represents the objective function in Eq. 6-2, which is the maximum profit of the process, $h(x)$ represents the black-box model of the process in Aspen Plus; $g(x)$ represents the nonlinear inequality constraints of the optimization problem, x is the vector of decision variables that contain both discrete and continuous variables, which are bounded by Eq. 6-5 and expressed by Eq. 6-6 for the optimization of the combine plant process.

$$\begin{aligned} x = [&T_{EX1}, T_{EX2}, T_{EX3}, ST_{RE6}, ST_{GAS2}, RR_{C1}, T_{FL1}, T_{FL2}, T_{FL3}, \\ &P_{FL2}, T_{Cool2}, T_{EX6}]^T \end{aligned} \tag{6-6}$$

$$g(x) = \begin{bmatrix} g(1) \\ g(2) \end{bmatrix} = \begin{bmatrix} 0.70 - p_{C6H6} \\ 0.92 - p_{PH} \end{bmatrix} \tag{6-7}$$

Where $T_{EX1, EX2, EX3, EX6}$ and $T_{FL1, FL2, FL3}$ are the temperature of the exchangers and flashes; P_{FL2} is the pressure of the Flash 2; $ST_{RE6}, ST_{RE6} + ST_{GAS2}, RR_{C1}$ are the feed trays of RE6, the total number of feed trays, and reflux ratio of distillation columns, respectively. In this study, the constraints ($g(x)$) for the optimization of the process can

be expressed as follow Eq. (6-7). g(1) and g(2) represent the purity of the benzene and phenolic compounds in the product stream, respectively.

Figure 6-2 shows the optimal process and stream data, like temperature, pressure, flow rate, and heat duties. The multi-tube reactors for hydrogenation and pyrolysis were designed to consist of 5 and 10 tubes with 6 m lengths and 0.04 m diameters, respectively. The gaseous products and aromatic products separation column has a total of 16 stages, and the reflux ratio became 0.05 moles. Moreover, the condenser pressure and temperature are 20 bar and 10 ℃, and the flow rate from the bottom of the column is 60.33 kg/h. The spacing of each tray is 0.6096 meters with diameters of 0.135 m.

The calculation formulas of the total profit, and the total operating costs (TOC) consisting of the materials cost, fixed capital investment (FCI), and fixed operating cost are based on Douglas' book[4]. The annual profit of this the two-stage process is calculated $\$1.86\times10^6$, in which total V_{Pro} is $\$5.20\times10^6$, TOC is $\$3.34\times10^6$, and FCI is $\$7.24\times10^5$.

6.3 Results and discussion

6.3.1 Economic evaluation

The economic analysis was investigated and estimated in the different scenarios, named Scenario 1-3. The descriptions are listed in Table 6-3. The effect of feedstock and hydrogenation techniques on the economic evaluation of the whole process was compared in this section. Two types of lignin, organosolv lignin and alkaline lignin, were selected as feedstock to compare in this two-stage process (scenario1 and scenario2). Base on the experimental findings[5][6], these two types of technical lignins had different performances in the hydrogenation process and the fast pyrolysis process for product distribution. The differences generated by thermal catalytic hydrogenation

and electrochemical hydrogenation were compared in Scenarios 2 and 3.

The economic calculations are all based on the process in Figure 6-3, changing the price of the feedstock and the corresponding product distribution to calculate the total profit. And for different hydrogenation technologies, although the conditions are different, they all consume electrical energy. It is possible to use part of the thermal energy of pyrolysis for the thermal catalytic hydrogenation reaction by thermal integration, while electrochemical hydrogenation is performed at room temperature consuming only electrical energy. With thermal integration, it's assumed that both processes consume the same amount of energy.

Table 6- 3 Description of different Scenarios.

Scenarios	**Descriptions**
Scenario 1	Thermal catalytic hydrogenation + fast pyrolysis on organosolv lignin
Scenario 2	Thermal catalytic hydrogenation + fast pyrolysis on alkaline lignin
Scenario 3	Electrochemical hydrogenation + fast pyrolysis on alkaline lignin

First, the comparison of economic analysis on two processes which are using organosolv lignin (Scenario1, left charts) and alkaline lignin (Scenario2, right charts) as the feedstock separately. As can be seen from Figures 6-4, the difference in feedstock causes a significant difference in the overall benefit, with the total annual profit of Scenario 1 being $\$1.86*10^6$ and that of Scenario 2 increasing to $\$2.78*10^6$. This is due to the difference in the price of raw materials on the one hand, and the difference in the product yields on the other hand, which also leads to a difference in the revenue. From the comparison of Fig. 6-4(a) and (b), it can be seen that the difference in the feedstock leads to different product distribution in the hydrogenation and pyrolysis processes, respectively. For Scenario1, the alkane products from pyrolysis accounted for the largest ratio of V_{pro}. Whereas, olefins and aromatic hydrocarbons have the lowest ratio of the overall V_{pro}, because they had the lowest yield relative to the raw feedstock. Here, the

syngas mainly includes inorganic gaseous products, like CO and CO_2, which can also be used as fuel with further separation from the major gas phase. Therefore, this part of the product was calculated separately with the price of $1.041/kg, which is lower than syngas. For Scenario 2, due to the hydrogenation process, the liquefaction ratio was higher, so the value of phenolic compounds (PH) accounts for more than half of the total product value. The other pyrolyzed products do not account for much value because the amount is too low, especially olefins and aromatics. The difference in product values between the two scenarios is not significant, at around 2.5%.

Then, Figure 6-4(c) and (d) shows the annual total operating costs (TOC), including major raw feedstock and chemicals (THF, H_2, and catalyst), fixed capital investment (FCI), labour costs (col cost), waste costs (total cwt cost), and cut (heating/cooling cost and electricity). The feedstock, hydrogen gas, and pure THF account for a large percentage of the total operating cost, as both hydrogen and THF are pure chemicals with a high price. Scenario 2 employed THF as the solvent in the hydrogenation reaction to dissolve alkaline lignin instead of NaOH solution. So, the solution cost was greatly reduced. And the cost of the feedstock was also reduced from $120/MT to $58.5/MT in Scenario 2. So, when comparing Scenario 1 and 2, alkaline lignin as raw material would effectively reduce the value of TOC.

In addition to that, Figures 6-4(c) and (d) show the distribution of fixed capital investment (FCI), which includes the utility investment and the operating costs. The utility investment includes the exchangers (EXs), condensers, reboilers, columns, flashes, cooler, and MCOMP, while the operating costs mainly include the hydrogenation and pyrolysis reaction. Since more HL flows into the pyrolysis process in Scenario 1, the consumption of the pyrolysis reaction (Reaction-Py) accounts for a higher percentage of FCI in Scenario 1, resulting in a higher value of the fixed capital investment. In fact, the consumption of utilities was calculated proportionally to the volume of the flow of materials.

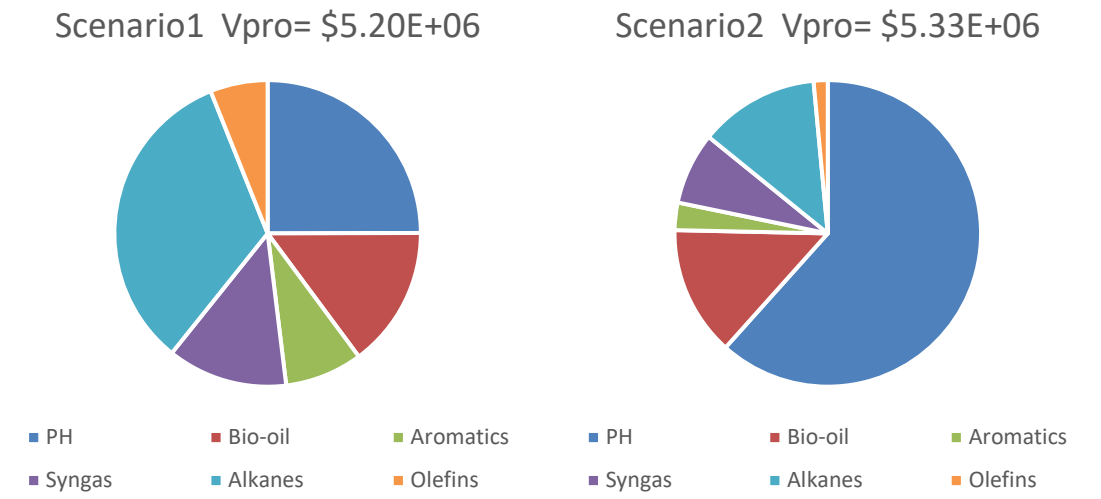
Scenario1 Vpro= $5.20E+06
PH
Bio-oil
Aromatics
Syngas
Alkanes
Olefins

(a)

Scenario2 Vpro= $5.33E+06
PH
Bio-oil
Aromatics
Syngas
Alkanes
Olefins

(b)

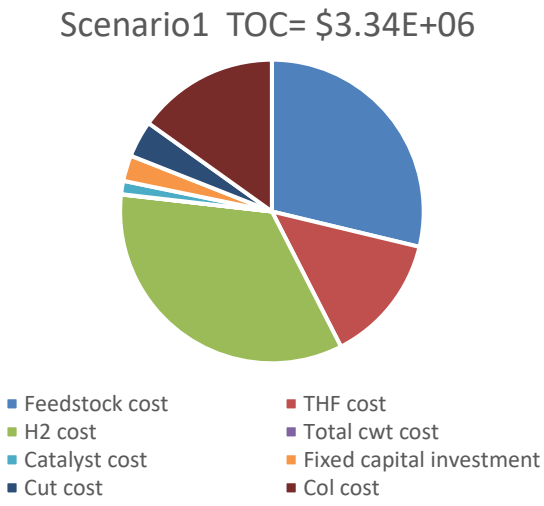
Scenario1 TOC= $3.34E+06
Feedstock cost
THF cost
H2 cost
Total cwt cost
Catalyst cost
Fixed capital investment
Cut cost
Col cost

(c)

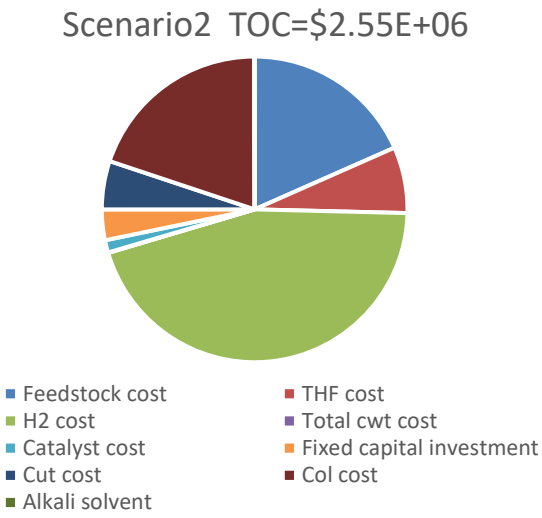
Scenario2 TOC=$2.55E+06
Feedstock cost
THF cost
H2 cost
Total cwt cost
Catalyst cost
Fixed capital investment
Cut cost
Col cost
Alkali solvent

(d)

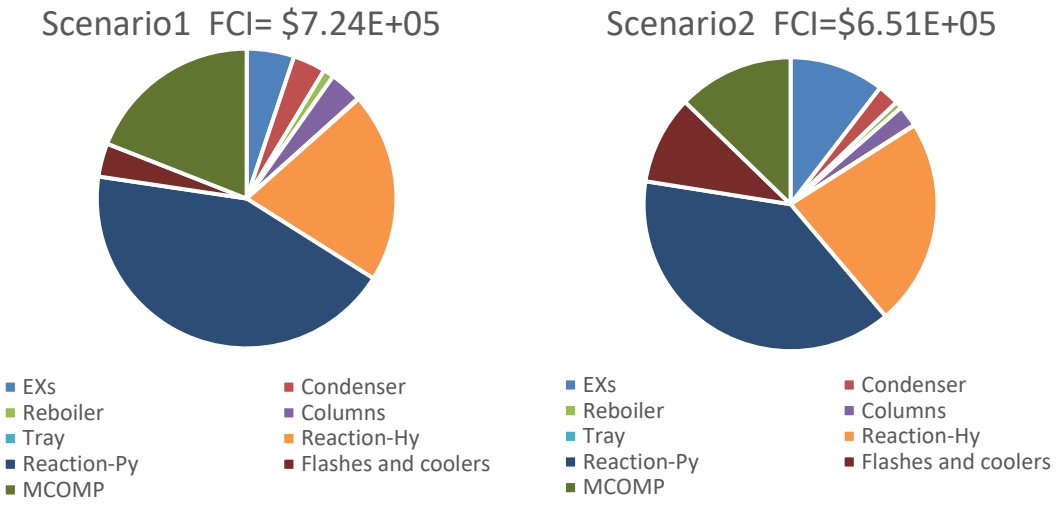

(e) (f)

Fig. 6- 4 The cost contribution and economic evaluation of Scenario 1 and Scenario 2 with the different feedstock.

The comparison of economic analysis on two technologies, thermal catalytic hydrogenation (Scenario2, left charts) and electrochemical hydrogenation (Scenario3, right charts) was shown below (Fig. 6-5). The settings for the electrochemical hydrogenation process were entered based on the experimental data in Chapter 5.4. The comparison of hydrogenation technologies was also determined by the same calculation, comparing the annual profit and total operating costs of thermal catalytic hydrogenation and electrochemical hydrogenation with alkaline lignin as feedstock. In the electrochemical hydrogenation process (Scenario3), the hydrogenated lignin retains more due to performing on the milder reaction conditions, and therefore the phenolic compounds account for a smaller V_{pro}. The overall product value of Scenario3 was reduced to $\$4.84*10^6$ per year, because the alkaline lignin itself produced fewer valuable products (like alkanes, olefins, and aromatics) by fast pyrolysis. The main difference for TOC is that electrochemical hydrogenation does not use hydrogen gas, so this part of the consumption is reduced. The reduction of hydrogen consumption leads

to a 23.5% reduction in TOC. And the overall Profit of Scenario3 is thus slightly increased from $\$2.78*10^6$ of Scenario2 to $\$2.89*10^6$ each year. For the fixed capital investment of both processes, the consumption of the hydrogenation reaction caused the main influence. Electrochemical hydrogenation was carried out under mild conditions, so this part of the consumption accounts for less, while the larger amount of hydrogenated lignin leads to an increase in the consumption of the pyrolysis reaction, which in turn increases the overall FCI. So, this is the main reason for the higher FCI of Scenario3 compared to Scenario2.

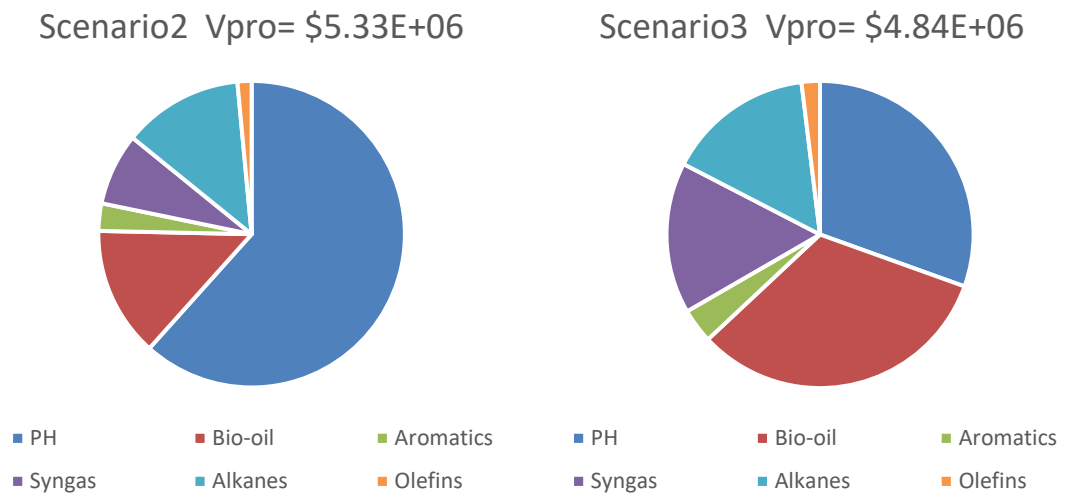

(a) (b)

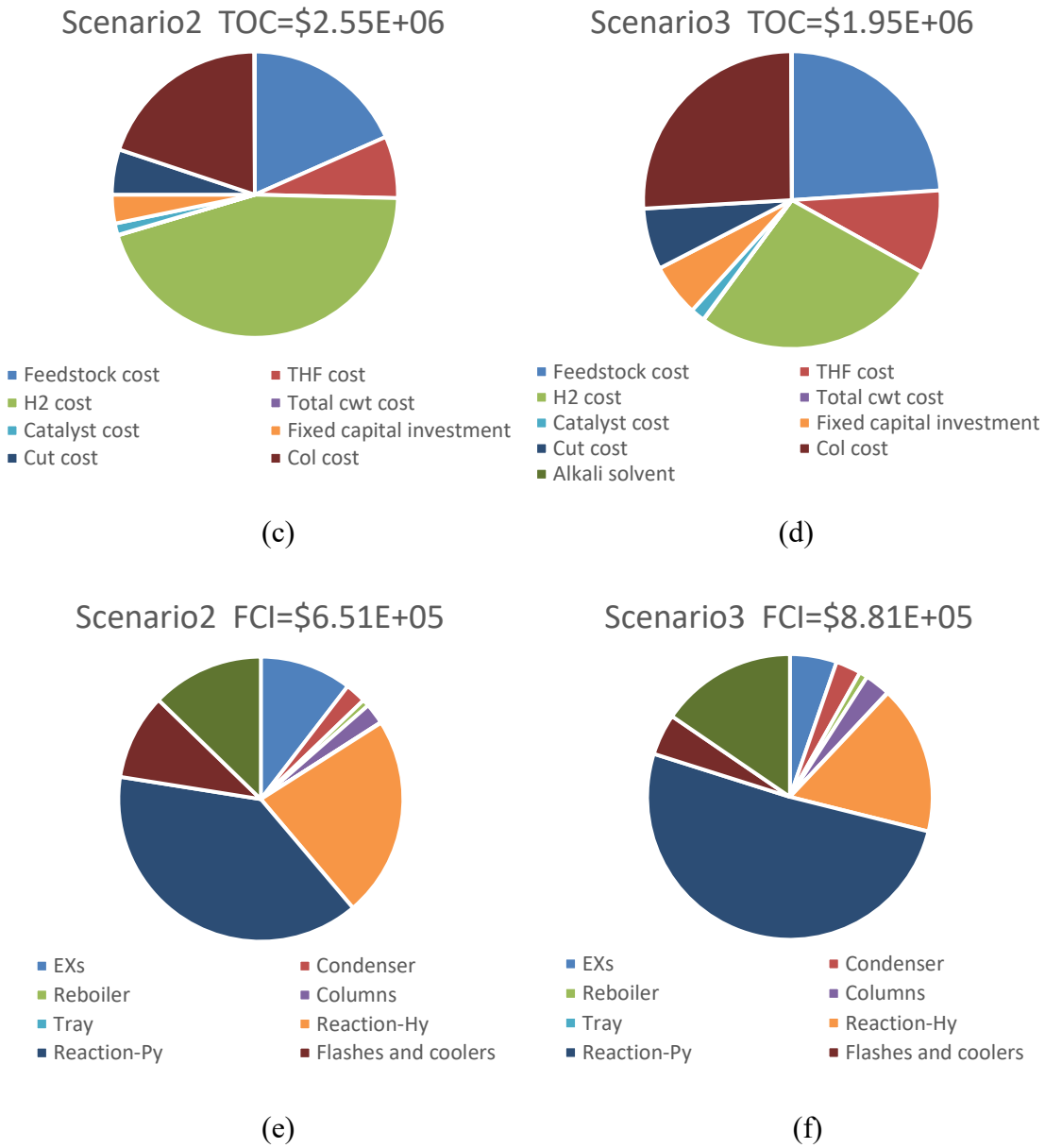

Fig. 6- 5 The comparison of Scenario2 and Scenario3 on economic analysis and cost contribution for different hydrogenation techniques.

6.3.2 Sensitivity analysis

To investigate the economic feasibility, the minimum selling price (MSP) for the products (olefins, aromatics and alkanes) was calculated based on Scenario1 (Fig. 6-6). The product's MSP is the price at which the overall value of the products equals the total

operating cost of the process, expressed in US dollars per kilogram. Therefore, sensitivity analysis was conducted to check that the price of feedstock and the cost of hydrogen gas contributed the largest percentage of the total operating costs. The influence of the price of the materials (feedstock and H_2) on the MSP of the main products in decreasing order is aromatic > olefins > alkanes.

The price of feedstock has a relatively large impact on the MSP of olefins and aromatics, and the slope is similar (slightly larger for aromatics), which is partly related to the price of the product and partly due to the product yield. It can be concluded that the higher the product value accounted in the total product value, the smaller the influence of material price on its MSP. H_2 cost contributed a large proportion of the MSP of the products. Fig. 6-6 (b) lists sensitivity analysis conducted on H_2 obtained from the typical sources[7]. The price of hydrogen gas fluctuates between \$2/kg and \$18.9/kg because of the different technologies and sources of hydrogen production. So here are the MSP values of the products obtained from different prices of hydrogen.

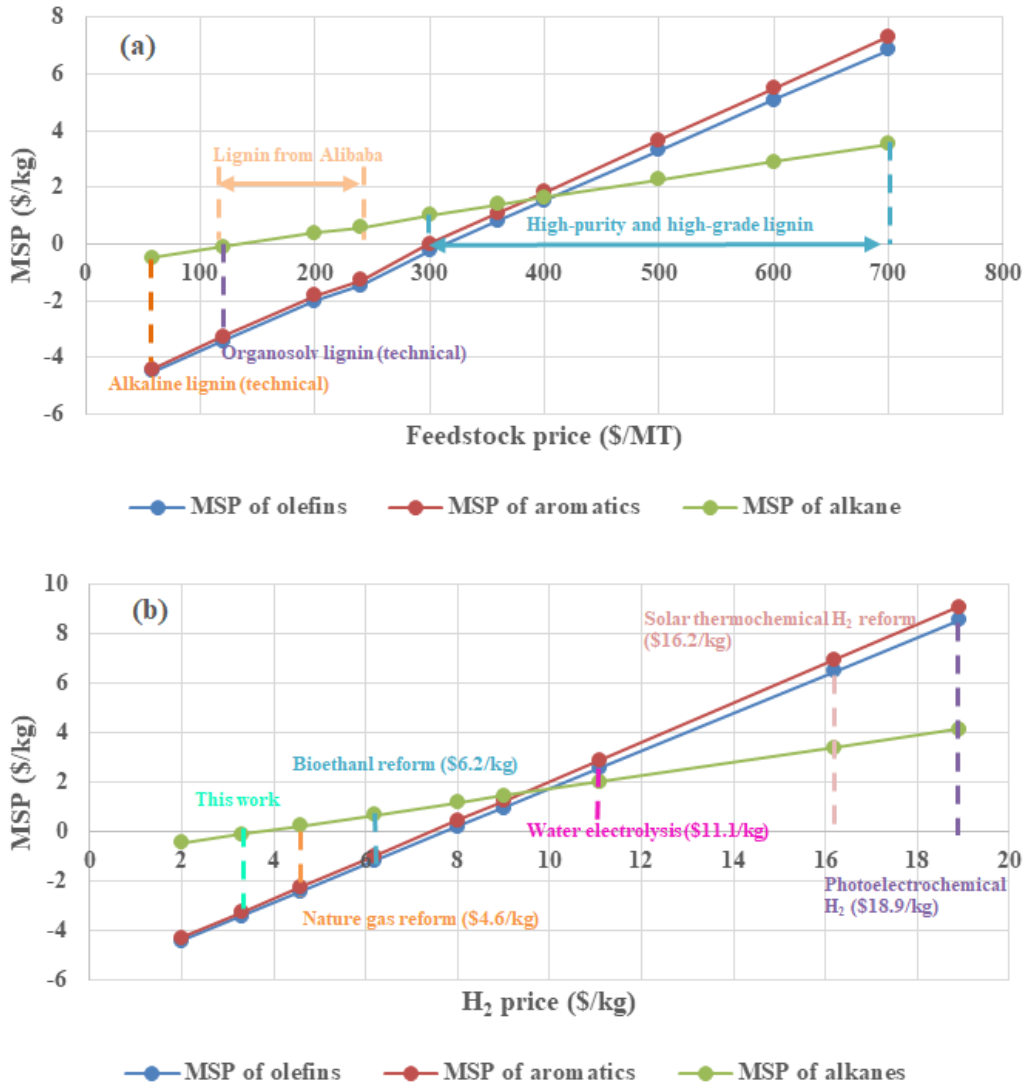

Fig. 6- 6 The MSPs of the products (olefins, aromatics, and alkanes) with the different feedstock (a) and various H_2 prices (b).

In truth, market fluctuations, exchange rate variations, and numerous elements such as the purity of the substance all affect the product's price, and the product's value is the factor that has the most impact on profitability. So, the effect of the products (alkanes and phenolic compounds) price on the total annual profit was shown in Fig. 6-7. Alkanes, as the most important pyrolyzed products were identified as C1-C3 alkanes. As can be shown, the price of alkanes has a significant impact on the entire product's

annual return. When the price of alkane rises from \$0.5/kg to \$1.5/kg, the annual profit increases from $\$7.7*10^5$ to $\$2.05*10^6$ proportionally. In addition, as the major product of the hydrogenation reaction, the phenolic products were also considered in the profits of products. There is no specific ratio of phenolic products, after the thermochemical hydrogenation process, such oil-phase products mainly consisted of guaiacol and its derivatives, while after the electrochemical hydrogenation mainly phenolic aldehyde，especially vanillin, were produced as PH. And since they are blended compounds, the price would vary substantially. \$0.2-0.75/kg was chosen for the range of phenolics price, and the overall yield will range from $\$9.06 *10^5$ to $\$1.86*10^6$. It can be shown that phenolics' price has a greater impact on overall profit, which is mostly owing to phenolics' higher yield and higher percentage of the products value. In sum, although olefins, alkanes, and aromatics have very high prices, the overall yield is low, making it difficult to have a significant impact on overall revenue.

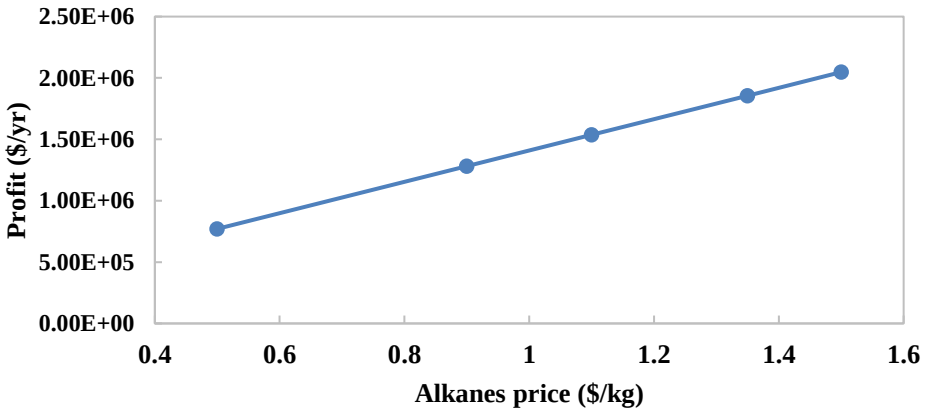

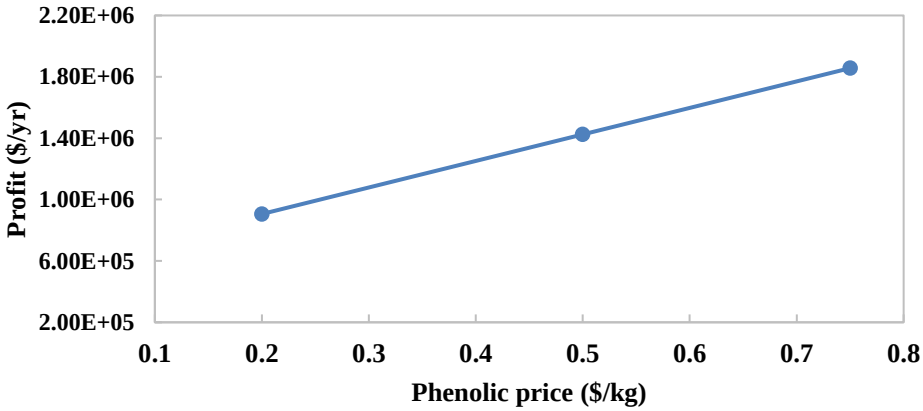

Fig. 6- 7 The effect of the products (alkanes and phenolic compounds) price on the total annual profit.

6.4 Conclusions

This chapter utilizes ASPEN plus to perform a process simulation of the proposed process, which evaluates the feasibility of the processes in terms of a large scale. A heat transfer network was constructed to efficiently reduce overall process energy consumption. MATLAB software is also employed to further optimize the process primarily through the purity of the phenolic and aromatic products. The impact of different lignin feedstocks on the economics of the process was analyzed, as well as the impact of different hydrogenation technologies on the economics of the overall process. From this part of the process simulation work, it can be concluded that.

(1) The thermal energy of the pyrolysis section can be utilized via thermal integration techniques to lower the energy consumption of the overall process.

(2) The use of different lignins can have a significant impact on the process' profitability. The feedstock cost is cheaper when alkaline lignin is used instead of organosolv lignin, and alkali water is replaced with THF as the solvent, which are the main reasons for the TOC value being reduced. Despite the fact that the amount of

aimed pyrolyzed product is lower for alkaline lignin, the profit value can be increased by selling phenolic compounds. As a result of the whole analysis, alkaline lignin has a greater profit and feasibility value.

(3) The contribution of hydrogenation technologies to total profit is minor. The advantage of electrochemical hydrogenation over thermochemical hydrogenation technology in terms of lower energy consumption is not fully shown because this process involves thermal integration technology. The electrochemical hydrogenation process decreases a major amount of the TOC due to a lack of H_2 consumption; however, the overall product value is lower in Scenario3, bringing the total net profit of the two hydrogenation technologies closer to each other.

(4) Moreover, involving in hydrogenation technology makes this process impossible to avoid lignin partial liquefaction during the hydrogenation process, which leads to PH products stated above. The focus of improving the feasibility of this process is on how to use this part of phenolic products and how to raise the value of those phenolic products.

The framework of this part of the work is extensively applicable to the utilization technologies for lignin. However, the environmental analysis was not involved in this work, but analyzed in terms of heat transfer optimization and economy. But this process use utilization of renewable energy so that the environmental impact needs to take into account, which is the purpose of using lignin or biomass. Therefore, in further lignin studies, the environmental impact needs to be taken into account in terms of products, process operation, and material transportation.

6.5 Reference

[1] Z. Yang, K. Qian, X. Zhang, H. Lei, C. Xin, Y. Zhang, M. Qian, E. Villota, Process design and economics for the conversion of lignocellulosic biomass into jet fuel range cycloalkanes, Energy. 154 (2018) 289–297. https://doi.org/10.1016/j.energy.2018.04.126.

[2] A. Saraeian, A. Aui, Y. Gao, M.M. Wright, M. Foston, B.H. Shanks, Evaluating lignin valorization: Via pyrolysis and vapor-phase hydrodeoxygenation for production of aromatics and alkenes, Green Chem. 22 (2020) 2513–2525. https://doi.org/10.1039/c9gc04245h.

[3] P. Badger, S. Badger, M. Puettmann, P. Steele, J. Cooper, Techno-economic analysis: Preliminary assessment of pyrolysis oil production costs and material energy balance associated with a transportable fast pyrolysis system, BioResources. 6 (2011) 34–47. https://doi.org/10.15376/biores.6.1.34-47.

[4] J.M. Douglas, Conceptual Design of Chemical, (1988) 455–456.

[5] L. Zhang, C. Choi, H. Machida, K. Norinaga, Production of light hydrocarbons from organosolv lignin through catalytic hydrogenation and subsequent fast pyrolysis, J. Anal. Appl. Pyrolysis. 156 (2021) 105096. https://doi.org/10.1016/j.jaap.2021.105096.

[6] L. Zhang, C. Choi, H. Machida, Z. Huo, K. Norinaga, Catalytic hydrotreatment of alkaline lignin and its consequent influences on fast pyrolysis, 2021. https://doi.org/10.1016/j.crcon.2021.09.001.

[7] D. Kim, J. Han, Comprehensive analysis of two catalytic processes to produce formic acid from carbon dioxide, Appl. Energy. 264 (2020) 114711. https://doi.org/https://doi.org/10.1016/j.apenergy.2020.114711.

Chapter 7 Conclusions and comparison

7.1 Comparison of two hydrogenation technologies

7.1.1 Products yield

This research does not only conduct lignin conversion via thermochemical hydrogenation coupled with fast pyrolysis, but also via green electrochemical technology with fast pyrolysis. The comparison of these two technology processes on alkaline lignin was reported in Table 7-1. The hydrogenated lignin treated by electrochemical hydrogenation (ECH) is called “ECH-HAL”, and the hydrogenated lignin treated by thermal catalytic hydrogenation (TCH) is called “TCH-HAL”. Electrochemical conversion has been increasingly explored as a more environmentally friendly alternative method due to its properties like low cost, reagent free, environmentally friendly, and mild conditions[1]. According to the experimental results of ECH on lignin, more hydrogenated lignin was recovered because of the gentle conditions, which avoid the decomposition of lignin macromolecules. In contrast, TCH requires high temperature and high-pressure hydrogen conditions to prompt the hydrogenation reaction, which leads to the breaking of internal bonds[2].

Through the exploration of experiments, these two processes boosted the generation of olefins, benzene, and toluene from pyrolysis of hydrogenated lignin after being modified with hydrogenation. TCH-HAL appears to have a greater ability to generate olefins and aromatics (benzene and toluene). However, the olefins and aromatics yield of ECH-HAL is not as much high as that of TCH-HAL, which accounted for 2.05 wt.% and 2.2 wt.%, respectively. This is attributed to (1) the high OH^- concentration of the electrolyte, which causes the hydroxide group to react with lignin molecules; (2) the occurrence of water electrolysis limited chemisorption of lignin. So more efficient

lignin electrochemical approaches and catalytic electrodes should be utilized to further hydrogenate lignin while limiting the water reduction and hydroxide reaction with lignin, which is a further research direction for this technology.

When the product calculation was based on raw lignin due to the higher yield of hydrogenated lignin, the high olefin yield was found via ECH-HAL. The olefins yield of ECH-HAL based on raw lignin even has twice as much as that of AL. Because the electrochemical hydrogenation process is simple and mild to operate, a higher yield of hydrogenated lignin allows for the production of relative more olefins and benzene. In summary, the goal of this procedure is to achieve improved hydrogenation selectivity under mild conditions, which should confirm not only the yield of olefins and aromatics, but also the yield of hydrogenated lignin. At the same time, the yield of char produced from hydrogenated lignin was reduced, and the char yield obtained from TCH-HAL was even lower. This is due to the effect of high temperature and high pressure, lower molecular weight and higher pyrolytic activity was obtained after thermal catalytic hydrogenation.

Table 7- 1 Comparison of electrochemical hydrogenation and thermal catalytic hydrogenation in terms of the yield of major pyrolyzed products.

Lignin type	**HAL yield (wt. %)**	**Products yield of fast pyrolysis (wt.%)**				**Products yield based on raw lignin (wt.%)**		
		Olefins	**Benzene**	**Toluene**	**Char**	**Olefins**	**Benzene**	**Toluene**
AL	-	0.75	0.88	0.12	45.21	0.75	0.88	0.12
ECH-HAL[a]	81.95	2.05	1.85	0.35	41.55	1.68	1.52	0.29
TCH-HAL[2]	45.94	3.09	2.85	0.95	36.46	1.42	1.31	0.44

Note: ECH-HAL was alkaline lignin treated with electrochemical hydrogenation under

the conditions (Constant potential: -0.25 V, reaction time: 2 h, room temperature, H-cell.); TCH-HAL was alkaline lignin treated with thermal catalytic hydrogenation under the conditions (Raney Ni, reaction time: 7 h, 250 ℃, 0.9 MPa H_2, Parr reactor), according to Chapter 3. [a]: work based on Chapter 5.

Based on the experimental results, the author also compared the oil-phase products from thermal catalytic hydrogenation and electrochemical hydrogenation. It found that after the thermal catalytic hydrogenation reaction, high-temperature and high-pressure conditions mainly caused the breaking of C-O bonds, and then hydrogenation reaction was carried out to produce stable low-molecule compounds or monomer compounds in the presence of a catalyst. As shown in Figure 7-1(a), the oil phase consists mainly of guaiacol, creosol, 4-ethyl-2-methoxy-phenol, 3-Allyl-6-methoxyphenol as well a small number of phenolic aldehydes. However, for electrochemical hydrogenation, the main oil-phase products were determined to be phenolic aldehydes like vanillin, which is also consistent with the results from Chen's work[3]. This is due to the fact that the reduction reaction of the water in the cathode electrolyte occurs simultaneously with the electrochemical hydrogenation of lignin, producing H_2 and $^{\bullet}OH$ radicals. Thus, both H_2 and $^{\bullet}OH$ reacted with the lignin intermediates, providing the hydroxyl groups along with saturating lignin molecules. This is why the oxygen content of the hydrogenated lignin after TCH is reduced but not as low as that of the hydrogenated lignin after ECH.

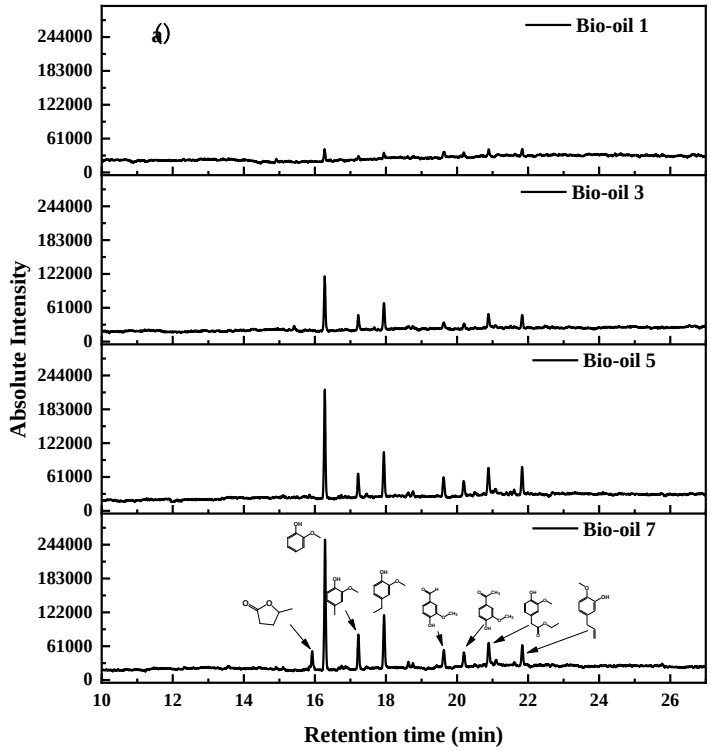
a)
Bio-oil 1
Bio-oil 3
Bio-oil 5
Bio-oil 7
Absolute Intensity
Retention time (min)

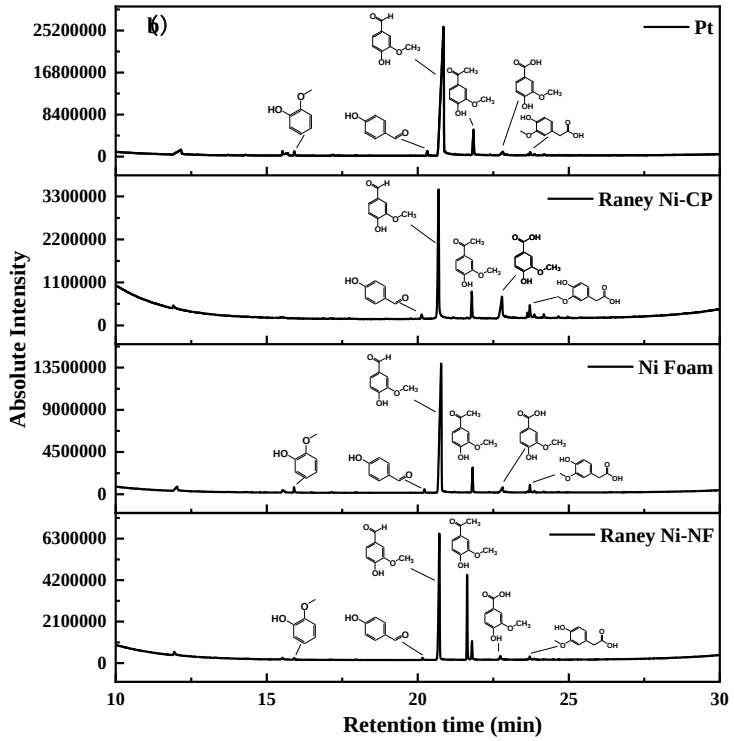
b)
Pt
Raney Ni-CP
Ni Foam
Raney Ni-NF
Absolute Intensity
Retention time (min)

Fig. 7- 1 GC-MS of the bio-oil samples after being treated with thermal catalytic hydrogenation (a) and electrochemical hydrogenation (b). (a) Bio-oil samples with different reaction times. Bio-oil 1: reaction time: 1 h; Bio-oil 3: reaction time: 3 h; Bio-oil 5: reaction time: 5 h; Bio-oil 7: reaction time: 7 h. (b) Bio-oil samples with different electrodes, Pt: being treated with Pt as working electrode; Raney Ni -CP: being treated with Raney Ni on carbon paper as a working electrode; Ni foam: being treated with bare Ni foam as a working electrode; Raney Ni-NF: being treated with Raney Ni on Ni foam as a working electrode.

In fact, it can be found that the content of olefins and aromatic hydrocarbons obtained from the lignin here is significantly increased after the hydrogenation pretreatment, while the content is still relatively low. This is partly due to the effect of the lignin species, which the alkaline lignin has a lower purity and activity due to its over-modified isolation. The further exploration of the effect of this technology on other types of lignin is required in the future. On the other hand, the selectivity and effectiveness of the electrochemical hydrogenation reaction can have further improvement, either by catalysts optimization or by the choice of reaction conditions. This technique effectively verified that the electrochemical hydrotreating can improve the pyrolytic properties of hydrogenated lignin to obtain more olefins and aromatic products, and it was also found that the oil-phase products in ECH are composed of phenolics and phenolic aldehyde monomers (including mainly vanillin) when the oil phase was qualified. Therefore, the oil phase products can also be utilized to improve the feasibility of this whole technology, either as a bio-oil source for petroleum alternatives or via further purification and refinement to obtain high-value chemicals.

7.1.2 Economic and energy consumption

Process simulation was conducted by ASPEN plus software, which analyzes the feasibility of the processes in terms of a large scale. After setting up the overall process, not only is a heat transfer network constructed to efficiently reduce the energy consumption of the overall process, but MATLAB software is also used to further optimize the process based on the purity of the phenolic and aromatic products. From the process simulation of this two-stage process, the impact of different hydrogenation technologies (TCH and ECH) and different feedstock on the economics of the overall process was compared.

Firstly, the thermal energy of the pyrolysis section can be utilized on thermal hydrogenation via thermal integration to lower the overall process energy consumption. Therefore, the advantage of ECH over TCH in terms of lower energy consumption is not fully shown. Electrochemical hydrogenation has a lower amount of the total operating cost (TOC) due to a lack of gaseous hydrogen. At the same time, the overall product value is lower than that of the process consisting of TCH and pyrolysis. Thus, the total annual net profit of the processes contained in these two different hydrogenation technologies is closer. For different feedstock, the difference in price and the difference in solvent are the main factors affecting the value of TOC. When alkaline lignin was used as feedstock, it is cheaper and can be solved with a low-cost sodium hydroxide solution, so TOC is lower, and the revenue is higher.

This process employs a hydrogenation reaction for pretreatment of lignin, so it is difficult to avoid partial liquefaction of lignin during the hydrogenation process, which leads to phenolic products (like guaiacol, vanillin and etc.). The focus of improving the feasibility of this process is on how to use this part of the phenolic products. However, the environmental analysis was not involved in this work, but analyzed in terms of heat transfer optimization and economy. The environmental impact needs to be considered when lignin is used as a feedstock, which is the purpose of utilizing a renewable energy source. And the environmental impact needs to be taken into account in terms of

products, process operation, and material transportation in further lignin studies.

7.2 Conclusions

To sum up, the use of lignin as a raw material for the production of high-value chemicals is a promising research direction, but it is still in a preliminary stage for lab-scale research. Because of the intrinsic stubborn overlapping structure and irregular composition of lignin polymers, the effectiveness and feasibility of its chemical conversion are limited. Therefore, an effective process is expected to modify the structure and chemical characteristics of lignin, for example, hydrogenation. This work explored the thermal pyrolyzed features of hydrogenated lignin and checked its characterization under various hydrogenation conditions. The influence of both thermal catalytic hydrogenation (TCH) and electrochemical hydrogenation (ECH) techniques on lignin was investigated in depth in this study. Because of the harsh conditions in TCH, thermal depolymerization is more likely to occur so that the yield of hydrogenated lignin is lower. As a result, the electrochemical process performed on lignin hydrogenation was investigated under gentler conditions. The performance of thermal catalytic hydrogenation and electrochemical hydrogenation on lignin was compared and investigated in this work at a preliminary stage, which was mainly examining the structure of hydrogenated lignin and the effect on pyrolysis properties before and after two different hydrogenation processes. For the overall two-stage procedure, ASPEN Plus software was used to simulate the process, and the economic analysis of the process in large-scale operation was also evaluated in this work. The following results are concluded.

(1) Compared with raw lignin, the H/C_{eff} ratio[4] of hydrogenated lignin samples has an increase. The content of oxygen and sulfur both decreased significantly after pretreatment due to the thermal decomposition of ether bonds and side-chain groups.

The vibrational stretching of O-H groups C-O, and C=O of H-EOL becomes weaker, while the aliphatic group is the only functional group increased after thermal catalytic hydrogenation of organosolv lignin. This phenomenon can be more pronounced in response to a higher temperature and longer reaction time. Hydrogenolysis of ether bonds, hydrodeoxygenation of hydroxyl groups, demethoxylation and alkylation happened in the hydrogenation process successively

(2) Organosolv lignin has a lower molecular weight, and can decompose to more volatiles in fast pyrolysis than that of alkaline lignin. And both lignin samples can produce more light hydrocarbons through the fast pyrolysis in the hydrogen atmosphere. An activated atmosphere can promote thermochemical decomposition. Almost all compounds except CO_2 detected by GC-TCD/FID were intensively yielded. Less char was remained after pyrolysis under the hydrogen atmosphere, since the hydrogen can react with the intermediates and suppress the repolymerization.

(3) The TGA results signify that hydrogenated lignin samples have higher reactivity which can be easily decomposed at relatively low temperatures. At the same time, fast pyrolysis of H-EOL samples has been checked, in which the maximum yield of light olefins is 9.94 wt.% from hydrogenated organosolv lignin. Besides, the yield of alkanes, benzene, and toluene also has a marked increase after hydrogenation pretreatment. More than 85 wt.% of hydrogenated organosolv lignin can be converted into volatiles in fast pyrolysis. Moreover, 3.1 wt.% of total olefins were obtained for pyrolysis of hydrogenated alkaline lignin (HAL), which was treated with Raney Ni for 7 hours at 250 ℃. HAL's olefins yield is almost three times that of the raw alkaline lignin.

(4) Milder electrochemical hydrogenation technology can avoid the thermal depolymerization of lignin under severe conditions. Furthermore, ECH has offered several advantages in terms of safety, operability, and economics. In addition, operating under mild conditions provides high catalytic efficiency and selectivity toward the target products.

(5) The oil-phase products in the hydrogenation process are mainly phenolic monomers, resulting from the liquefaction of the lignin macromolecules. After thermochemical hydrogenation, the major compounds are guaiacol and its derivatives in the oil phase. After electrochemical hydrogenation, it contains mainly vanillin. This is due to the fact that the electrochemical conversion process provided ·OH in addition to hydrogen from the electrolyte. This part of the oil product can also be utilized as an available product, which can improve the utilization of lignin sources and the feasibility of the process. But more exploration is required in future work.

7.3 Future outlook

The author has conducted a more thorough evaluation of this proposed process combining the two steps of hydrogenation and pyrolysis reactions to convert lignin into valuable chemicals throughout this part of the research. For this process, some modifications and enhancements have been offered, which the author plans to investigate more in future work.

First of all, the hydrogenation catalysts must be more selective; only commercially hydrogenation catalysts were utilized in this study, and more efficient catalysts can be developed later to improve the selectivity of the aromatic ring hydrogenation reaction. Then, this work also can be combined with the existing technology for hydrogenolysis lignin, which only focuses on generating liquefied phenolic chemicals and ignores solid products. This work offers the possibility of utilizing hydrogenated lignin that has higher pyrolytic activity and the capacity for producing olefins and aromatic hydrocarbons. What's more, additional olefins and aromatic products can be produced by catalytically pyrolyzing the phenolic compounds formed in hydrogenation, which is aimed for resulting in more target olefins and aromatic compounds from the lignin source. Yang's group performed catalytic pyrolysis of phenolic model compounds like

cresol, phenol, guaiacol, and syringol, and C1-C5 hydrocarbons as well as aromatics were successfully obtained with zeolite catalyst[5]. These are the conclusions based on current experimental and calculations results, which should have more extension and improvement in these directions in the future.

7.4 Reference

[1] X. Du, H. Zhang, K.P. Sullivan, P. Gogoi, Y. Deng, Electrochemical Lignin Conversion, ChemSusChem. 13 (2020) 4318–4343. https://doi.org/https://doi.org/10.1002/cssc.202001187.

[2] L. Zhang, C. Choi, H. Machida, Z. Huo, K. Norinaga, Catalytic hydrotreatment of alkaline lignin and its consequent influences on fast pyrolysis, Carbon Resour. Convers. 4 (2021) 219–229. https://doi.org/https://doi.org/10.1016/j.crcon.2021.09.001.

[3] A. Chen, Y. Wen, X. Han, J. Qi, Z.-H. Liu, S. Zhang, G. Li, Electrochemical Decomposition of Wheat Straw Lignin into Guaiacyl-, Syringyl-, and Phenol-Type Compounds Using Pb/PbO2 Anode and Alloyed Steel Cathode in Alkaline Solution, Environ. Prog. Sustain. Energy. 38 (2019) 13117. https://doi.org/https://doi.org/10.1002/ep.13117.

[4] T.P. Vispute, H. Zhang, A. Sanna, R. Xiao, G.W. Huber, Renewable chemical commodity feedstocks from integrated catalytic processing of pyrolysis oils, Science (80-.). 330 (2010) 1222–1227. https://doi.org/10.1126/science.1194218.

[5] H. Yang, K. Norinaga, J. Li, W. Zhu, H. Wang, Effects of HZSM-5 on volatile products obtained from the fast pyrolysis of lignin and model compounds, Fuel Process. Technol. 181 (2018) 207–214. https://doi.org/10.1016/j.fuproc.2018.09.022.